INFORMATION TO USERS

While the most advanced technology has been used to photograph and reproduce this manuscript, the quality of the reproduction is heavily dependent upon the quality of the material submitted. For example:

- Manuscript pages may have indistinct print. In such cases, the best available copy has been filmed.
- Manuscripts may not always be complete. In such cases, a note will indicate that it is not possible to obtain missing pages.
- Copyrighted material may have been removed from the manuscript. In such cases, a note will indicate the deletion.

Oversize materials (e.g., maps, drawings, and charts) are photographed by sectioning the original, beginning at the upper left-hand corner and continuing from left to right in equal sections with small overlaps. Each oversize page is also filmed as one exposure and is available, for an additional charge, as a standard 35mm slide or as a 17"x 23" black and white photographic print.

Most photographs reproduce acceptably on positive microfilm or microfiche but lack the clarity on xerographic copies made from the microfilm. For an additional charge, 35mm slides of 6"x 9" black and white photographic prints are available for any photographs or illustrations that cannot be reproduced satisfactorily by xerography.

Ding, Zheng Ming

SYSTEMATIC STUDY OF BREMSSTRAHLUNG AMPLITUDE AND A NEW MODEL FOR BREMSSTRAHLUNG CALCULATION

City University of New York PH.D. 1987

PLEASE NOTE:

In all cases this material has been filmed in the best possible way from the available copy. Problems encountered with this document have been identified here with a check mark ✓.

1. Glossy photographs or pages _____
2. Colored illustrations, paper or print _____
3. Photographs with dark background _____
4. Illustrations are poor copy _____
5. Pages with black marks, not original copy ✓
6. Print shows through as there is text on both sides of page _____
7. Indistinct, broken or small print on several pages _____
8. Print exceeds margin requirements _____
9. Tightly bound copy with print lost in spine _____
10. Computer printout pages with indistinct print _____
11. Page(s) _____ lacking when material received, and not available from school or author.
12. Page(s) _____ seem to be missing in numbering only as text follows.
13. Two pages numbered _____. Text follows.
14. Curling and wrinkled pages _____
15. Dissertation contains pages with print at a slant, filmed as received ✓
16. Other _____

_____

_____

SYSTEMATIC STUDY OF BREMSSTRAHLUNG AMPLITUDE AND A NEW MODEL FOR BREMSSTRAHLUNG CALCULATION

Zheng-Ming Ding

A dissertation submitted to the Graduate Faculty in Physics in partial fulfillment of the requirements for the degree of Doctor of Philosophy, the City University of New York.

1987

This manuscript has been read and accepted for the Graduate Faculty in Physics in satisfaction of the dissertation requirement for the degree of Doctor of Philosophy.

Sept. 1, 1986
Date

Ying-Kung Lim
Chair of Examining Committee

Sept. 1, 1986
Date

Executive Officer

Professor L. S. Celenza

Professor M. I. Sobel

Professor M. Mittleman

Professor B. F. Gibson
Supervisory Committee

The City University of New York

Abstract

SYSTEMATIC STUDY OF BREMSSTRAHLUNG AMPLITUDE AND

A NEW MODEL FOR BREMSSTRAHLUNG CALCULATION

by

Zheng Ming Ding

Adviser: Professor Ming Kung Liou

A general parametrization which enables us to construct all possible approximations to the bremsstrahlung amplitude is applied to explore generalizations of existing soft-photon approximations. We establish the existence of theoretical ambiguity in defining the soft-photon approximations and we show how the bremsstrahlung cross section calculated from a soft-photon amplitude depends on the parameters. We also show that if bremsstrahlung spectrum exhibits resonant structure, then the position of this structure K_γ and its width Γ_γ can be predicted by either performing the detailed bremsstrahlung calculation or using two simple formulas which relate K_γ and Γ_γ directly to the resonant energy E_R and the width Γ_{el} of the resonant structure observed in the elastic scattering cross sections. This new information about K_γ and Γ_γ can be used to study the validity of any bremsstrahlung amplitude.

All approximations have been divided into classes and the following approximations have been systematically studied: (i) The one-energy one-angle approximation (OEOA), which is the generalized Low's approximation, (ii) the one-energy two-angle approximation (OETA), which is another version of the generalized Low's approximation, (iii) the two-energy one-angle approximation (TEOA), which is the generalized Feshbach-Yennie approximation, and (iv) the two-energy two-angle

approximation (TETA), which is essentially a new approximation for bremsstrahlung calculations. We find that all soft-photon amplitudes in the OEOA or OETA fail to adequately describe the proton-carbon bremsstrahlung ($p^{12}C\gamma$) data near the 1.7-MeV or 0.5-MeV resonance. These amplitudes predict the values of K_γ and Γ_γ which do not agree with the experimental ones. Although the problem comes from both the leading term (A_μ/K) and the second term (B_μ) of the amplitudes (M_μ^{AB}), the major difficulty lies in the derivatives of the elastic scattering amplitudes in the second term B_μ. Our study also shows that the limited existing data (which is available only in the soft photon region, $K< 200$ keV) can be described by many (infinite) soft-photon amplitudes in the TEOA. Since these amplitudes in the TEOA can be differentiated at higher photon energies (200 keV<K<600 keV), a new $p^{12}C\gamma$ experiment is suggested to test these amplitudes so that the best one can be selected. Finally, we develop and test a new two-energy two-angle approximation for describing bremsstrahlung processes. The natural choice of kinematic variables (determined by the four external emission diagrams) leads to the situation in which the second term of the amplitude vanishes, $B_\mu=0$. This approximation provides an excellent description of all the available $\pi^{\pm}p\gamma$ and the $p^{12}C\gamma$ data by means of a single soft-photon approximation.

ACKNOWLEDGEMENTS

To Professor Ming-Kung Liou, my thesis advisor, I wish to express my deepest gratitude for his valuable guidance and constant encouragement throughout this thesis work.

I would also like to express my sincere thanks to Prof. C.C. Trail and Prof. P. Lesser for their help in my early research activities.

I wish to acknowledge with gratitude the Department of Physics, Brooklyn College and the Research Foundation of the CUNY for the financial support during my graduate work.

CONTENTS

LIST OF FIGURES

Figure 10
The relative $p^{12}C\gamma$ cross section σ_{rel} as a function of photon energy K at an incident proton energy of 1.594 MeV.

Figure 11
The relative $p^{12}C\gamma$ cross section σ_{rel} as a function of photon energy K at an incident proton energy of 1.810 MeV.

Figure 12
The relative $p^{12}C\gamma$ cross section σ_{rel} as a function of photon energy K at an incident proton energy of 0.591 MeV.

Figure 13
The $\pi^+p\gamma$ cross section as a function of photon energy K at 269 MeV for the photon counter G1.

Figure 14
Same as Fig.13 but for the photon counter G11.

Figure 15
Same as Fig.13 but for the photon counter G12.

Figure 16
Same as Fig.13 but for the photon counter G13.

Figure 17
Same as Fig.13 but for the photon counter G14.

Figure 18
Same as Fig.13 but for the photon counter G15.

Figure 19
Same as Fig.13 but for the photon counter G17.

Figure 20
Same as Fig.13 but for the photon counter G18.

Figure 21
Same as Fig.13 but for the photon counter G19.

Figure 22
Same as Fig.13 but at 298 MeV for the photon counter G10.

Figure 23
Same as Fig.13 but at 298 MeV for the photon counter G11.

Figure 24
Same as Fig.13 but at 298 MeV for the photon counter G12.

Figure 25
Same as Fig.13 but at 298 MeV for the photon counter G13.

Figure 26
Same as Fig.13 but at 298 MeV for the photon counter G14.

Figure 27
Same as Fig.13 but at 298 MeV for the photon counter G15.

Figure 28
Same as Fig.13 but at 298 MeV for the photon counter G17.

Figure 29
Same as Fig.13 but at 298 MeV for the photon counter G18.

Figure 30
Same as Fig.13 but at 298 MeV for the photon counter G19.

Figure 31
Same as Fig.13 but at 324 MeV for the photon counter G11.

Figure 32
Same as Fig.13 but at 324 MeV for the photon counter G12.

Figure 33
Same as Fig.13 but at 324 MeV for the photon counter G14.

Figure 34
Same as Fig.13 but at 324 MeV for the photon counter G15.

Figure 35
Same as Fig.13 but at 324 MeV for the photon counter G17.

Figure 36
Same as Fig.13 but at 324 MeV for the photon counter G19.

Figure 37
The $\pi^- p\gamma$ cross section as a function of photon energy K at 263 MeV for the photon counter G1-G10(averaged).

Figure 38
Same as Fig.38 but for the photon counter G12.

Figure 39
Same as Fig.38 but for the photon counter G14.

Figure 40
Same as Fig.38 but at 298 MeV for the photon counter G1-G10(average).

Figure 41
Same as Fig.38 but at 298 MeV for the photon counter G14.

Figure 42
Same as Fig.38 but at 298 MeV for the photon counter G15.

Figure 43

Same as Fig.41 but at 298 MeV for the photon counter G18.

I Introduction

Historically, the most important reason for studying the radiation accompanying a scattering process has been to investigate the off-shell behavior of the process, information which is not available in the elastic scattering process itself. For example, in studying nucleon-nucleon bremsstrahlung, one hopes that from among the many different phenomenological potentials one can distinguish, by its off-energy-shell behavior, the best two-nucleon potential.[1] In addition to this important goal in the study of bremsstralung, there are several areas in which one hopes to use the radiation accompanying certain processes to obtain specific information about these processes. The study of pion-proton bremsstrahlung ($\pi^{\pm}p\gamma$) was originally suggested for the study of electromagnetic properties of the Δ-resonance,[2] and the nucleon-nucleus and nucleus-nucleus bremsstrahlung in the resonance region were motivated by the hope that this process could be used as a tool for investigating nuclear reactions.[3,4,5]

The idea of using bremsstrahlung emission as a tool for investigating nuclear reactions was first proposed by Eisberg, Yennie and Wilkinson in 1960.[3] Their classical treatment was extended later to a quantum mechanical treatment by Feshbach and Yennie.[4] Briefly, the amplitude which represents the photon emission before nuclear scattering and the amplitude which represents the photon emission after scattering add coherently. Since these two amplitudes differ in phase by $\omega\tau$ (ω=radiation frequency, τ=time delay), the bremsstrahlung cross section evaluated from these two amplitudes (and an internal amplitude obtained

through the gauge invariant condition) will contain an interference term which depends upon the time delay τ. For small values of $\omega\tau$, one obtains a typical, smooth bremsstrahlung spectrum with 1/K dependence (K = photon energy). As $\omega\tau$ increases, the interference between the two amplitudes is altered, causing a change in the bremsstrahlungg spectrum. For example, when a long-lived resonant state is formed, the bremsstrahlung spectrum will show structure. A quantitative measurement of the bremsstrahlung cross section can then provide a measure of the time delay. This information about the time delay can be used to distinguish unambiguously between a direct nuclear reaction and a compound nuclear reaction. A serious attempt to measure the proton-carbon bremsstrahlung ($p^{12}C\gamma$) cross sections near the 1.7-MeV and 0.5-MeV resonances and to extract important information about the time delay was made by the Bologna group[6] and the Brooklyn Group[7,8] and these results have been confirmed by a group from Tokyo.[9] Each group has clearly observed the resonance structure in the measured $p^{12}C\gamma$ spectra and used these spectra to extract a delay time of the order of 10^{-20} second. In addition to the $\pi^{\pm}p\gamma$ and the $p^{12}C\gamma$ processes which have already been measured systematically, the proton-oxygen bremsstrahlung ($p^{16}O\gamma$) has also been studied recently by our Brooklyn group.[10,11]

Most of the bremsstrahlung calculations performed in the past were either model independent calculations or potential model calculations. The model independent calculations are based upon a fundamental theorem, known as the soft-photon theorem or the low-energy theorem for photons. It was first derived by Low[12] and was extended by Adler and Dothan.[13] This theorem states that the first two terms in the series expansion of the differential bremsstrahlung cross section (or the bremsstrahlung

amplitude) in powers of the photon energy may be calculated exactly in terms of the corresponding elastic amplitude and the electromagnetic constants of the participating particles. Thus, the theorem provides a method to construct an approximate bremsstrahlung amplitude, which can be used to calculate the bremsstrahlung cross section in terms of the corresponding elastic amplitude.

However, the soft-photon theorem states nothing about the energy and the scattering angle at which the elastic amplitude should be evaluated. Since there are two different energies (s_i and s_f) and two different scattering angles (t_p and t_q) which can be defined for any bremsstrahlung process, the elastic amplitude can be evaluated at any linear combination of s_i and s_f ($s_{\alpha\beta} = (\alpha s_i+\beta s_f)/(\alpha+\beta)$) and any linear combination of t_p and t_q ($t_{\alpha'\beta'} = (\alpha' t_p+\beta' t_q)/(\alpha'+\beta')$). This is the theoretical ambiguity involved in using this theorem, and this ambiguity implies that the prescription used to construct an approximate bremsstrahlung amplitude is by no means unique. This can be seen from the fact that several approximations to the bremsstrahlung amplitude have been proposed by many other authors since Low first put forward his famous soft-photon theorem in 1958. These approximations, called soft-photon approximations (SPA) or on-shell approximations, have played an important role in the study of bremsstrahlung processes. Among the approximations proposed so far, Low's original SPA (LSPA), the EED (external emission dominance) approximation of Nefkens and Sober (EED),[14] the modified SPA of Nutt, Liu and Liou (MSPA),[15] the Feshbach-Yennie approximation (FYA),[16] and many other approximations[17] have been applied to predict either the $\pi^{\pm}p\gamma$ or the $p^{12}C\gamma$ cross sections.

An important connection between the ambiguity problem of the soft-photon theorem and the validity problem of the soft-photon approximations was not fully understood in the past and the ambiguity problem was completely ignored. Realizing the importance of this problem, we have proposed a special parametrization which enable us to generate all possible linear combinations of energies and angles so that the most general bremsstrahlung amplitude can be constructed. We then used this general bremsstrahlung amplitude to study the range of validity of various bremsstrahlung approximations and the nature of the resonant structure predicted by these approximations in the resonance region. To study all approximations systematically, we have divided them into several classes. Four classes have been carefully studied. A comparison with all the experimental $\pi^{\pm}p\gamma$ and the $p^{12}C\gamma$ data shows that the best approximation is a <u>new</u> two-energy two-angle approximation which has never before been studied.

The main purpose of this thesis is to report some important results of our study, especially to introduce the new two-energy two-angle approximation which can be used to describe almost all of the $\pi^{\pm}p\gamma$ and the $p^{12}C\gamma$ data.

II Bremsstrahlung Amplitude

We consider photon emission accompanying the scattering of two particles A and B:

$$A(q_i^\mu) + B(p_i^\mu) \rightarrow A(q_f^\mu) + B(p_f^\mu) + \gamma(K^\mu)$$

Here $q_i^\mu(q_f^\mu)$ and $p_i^\mu(p_f^\mu)$ are the initial (final) four-momenta for particles A and B, respectively, and K^μ is the four-momentum for the emitted photon. These five momenta are defined in the laboratory frame as

$$\begin{aligned}
q_i^\mu &= (m+E_i, 0, 0, q_i) \\
p_i^\mu &= (M, 0, 0, 0) \\
q_f^\mu &= (m+E_q,\ q_f\sin\theta_q\cos\phi_q,\ q_f\sin\theta_q\sin\phi_q,\ q_f\cos\theta_q) \\
p_f^\mu &= (M+E_p,\ p_f\sin\theta_p\cos\phi_p,\ p_f\sin\theta_p\sin\phi_p,\ p_f\cos\theta_p) \qquad (1) \\
K^\mu &= (K,\ K\sin\theta_\gamma\cos\phi_\gamma,\ K\sin\theta_\gamma\sin\phi_\gamma,\ K\cos\theta_\gamma),
\end{aligned}$$

where

$$\begin{aligned}
E_i &= (m^2+q_i^2)^{\frac{1}{2}} - m \\
E_q &= (m^2+q_f^2)^{\frac{1}{2}} - m \\
E_p &= (M^2+p_f^2)^{\frac{1}{2}} - M,
\end{aligned}$$

and m and M are the masses of particles A and B, respectively. These four-momenta satisfy energy-momentum conservation:

$$q_i^\mu + p_i^\mu = q_f^\mu + p_f^\mu + K^\mu \ . \qquad (2)$$

As we shall see later, our main purpose is to study how a given amplitude (or the bremsstrahlung cross section calculated from a given amplitude) depends on the choice of the total energy squared and the momentum transfer squared. The answer to this question does not depend on whether the particles (A and B) have spin or not. Therefore, for the sake of simplicity, we shall discuss only the spinless case and assume

that particles A and B have charges $Z_A e$ and $Z_B e$, respectively, but they have no spin. In our actual calculations of the $p^{12}C\gamma$ and the $\pi^{\pm}p\gamma$ cross sections, however, the spin of the proton has been taken into consideration.

It is well-known that the total bremsstrahlung amplitude, M_μ^T, consists of the external scattering amplitude, M_μ^E, and the internal scattering amplitude, M_μ^I, :

$$M_\mu^T = M_\mu^E + M_\mu^I. \tag{3}$$

M_μ^E can be determined exactly from four external emission diagrams (see Fig.1(a)-(d)). In these diagrams, T_x (x=a,b,c,d) represent the half-off-shell T-matrices which depend upon three Lorentz invariants. Choosing these three invariants to be the total energy squared s, the momentum transfer squared t, and the square of the invariant mass Δ of the off-mass-shell leg on which the photon emission occurs, we can define four T-matrices as

$$\begin{aligned} T_a &= T(s_a, t_a, \Delta_a) \\ T_b &= T(s_b, t_b, \Delta_b) \\ T_c &= T(s_c, t_c, \Delta_c) \\ T_d &= T(s_d, t_d, \Delta_d), \end{aligned} \tag{4}$$

where

$$\begin{aligned} s_a &= s_c = s_i \\ s_b &= s_d = s_f \\ t_c &= t_d = t_q \\ t_a &= t_b = t_p \\ \Delta_a &= (q_f + K)^2 \\ \Delta_b &= (q_i - K)^2 \\ \Delta_c &= (p_f + K)^2 \end{aligned}$$

$$\Delta_d=(p_i-K)^2 \tag{5}$$

$$s_i=(q_i+p_i)^2=(m+M)^2+2ME_i$$

$$s_f=(q_f+p_f)^2=(q_i+p_i-K)^2$$

$$=s_i-2(q_i+p_i)\cdot K=(m+M)^2+2M(E_i-K/N)$$

$$N=M/[(m+M+E_i)-(E_i^2+2mE_i)^{\frac{1}{2}}\cos\theta_\gamma]$$

$$t_p=(p_f-p_i)^2=[q_i-(q_f+K)]^2$$

$$=t_q-2(q_i-q_f)\cdot K$$

$$t_q=(q_f-q_i)^2=[p_i-(p_f+K)]^2$$

$$=t_p-2(p_i-p_f)\cdot K.$$

In terms of these four half-off-shell T-matrices, M_μ^E can be written in the form:

$$M_\mu^E = Z_A\frac{q_{f\mu}}{q_f\cdot K}T_a - Z_A\frac{q_{i\mu}}{q_i\cdot K}T_b + Z_B\frac{p_{f\mu}}{p_f\cdot K}T_c - Z_B\frac{p_{i\mu}}{p_i\cdot K}T_d. \tag{6}$$

M_μ^E must be expanded in powers of K in order to obtain the leading term of M_μ^I (the internal emission diagram is shown in Fig.1(e)) from the gauge invariant condition. Such an expansion is not unique because $T_x(x=a,b,c,d)$ can be expanded, in general, about $(s_{\alpha_x\beta_x}(K),\ t_{\alpha_x'\beta_x'}(K))$, where,

$$s_{\alpha_x\beta_x}=(\alpha_x s_i+\beta_x s_f)/(\alpha_x+\beta_x),$$

$$t_{\alpha_x'\beta_x'}=(\alpha_x' t_p+\beta_x' t_q)/(\alpha_x'+\beta_x'), \tag{7}$$

and α_x, β_x, α_x' and $\beta_x'(x=a,b,c,d)$ are any arbitrary real numbers. Using the following expressions,

$$s_i-s_{\alpha_x\beta_x} = 2\frac{\beta_x}{\alpha_x+\beta_x}(q_i+p_i)\cdot K$$

$$s_f-s_{\alpha_x\beta_x} =-2\frac{\alpha_x}{\alpha_x+\beta_x}(q_i+p_i)\cdot K \tag{8}$$

$$t_p-t_{\alpha_x'\beta_x'} =-2\frac{\beta_x}{\alpha_x'+\beta_x'}(q_i-q_f)\cdot K$$

$$t_q - t_{\alpha'_x \beta'_x} = 2\frac{\alpha_x}{\alpha'_x+\beta'_x}(q_i-q_f)\cdot K$$

we obtain:

$$T_a = T_a^{el} + 2\frac{\beta_a}{\alpha_a+\beta_a}(q_i+p_i)\cdot K T_a^s - 2\frac{\beta_a}{\alpha'_a+\beta'_a}(q_i-q_f)\cdot K T_a^t + 2q_f\cdot K T_a^\Delta + \ldots \quad (9a)$$

$$T_b = T_b^{el} - 2\frac{\alpha_b}{\alpha_b+\beta_b}(q_i+p_i)\cdot K T_b^s - 2\frac{\beta_b}{\alpha'_b+\beta'_b}(q_i-q_f)\cdot K T_b^t - 2q_i\cdot K T_b^\Delta + \ldots \quad (9b)$$

$$T_c = T_c^{el} + 2\frac{\beta_c}{\alpha_c+\beta_c}(q_i+p_i)\cdot K T_c^s + 2\frac{\alpha_c}{\alpha'_c+\beta'_c}(q_i-q_f)\cdot K T_c^t + 2p_f\cdot K T_c^\Delta + \ldots \quad (9c)$$

$$T_d = T_d^{el} - 2\frac{\alpha_d}{\alpha_d+\beta_d}(q_i+p_i)\cdot K T_d^s + 2\frac{\alpha_d}{\alpha'_d+\beta'_d}(q_i-q_f)\cdot K T_d^t - 2p_i\cdot K T_d^\Delta + \ldots \quad (9d)$$

and

$$\begin{aligned} M_\mu^E = {} & Z_A\frac{q_{f\mu}}{q_f\cdot K}T_a^{el} - Z_A\frac{q_{i\mu}}{q_i\cdot K}T_b^{el} + Z_B\frac{p_{f\mu}}{p_f\cdot K}T_c^{el} - Z_B\frac{p_{i\mu}}{p_i\cdot K}T_d^{el} \\ & + (q_i+p_i)\cdot K\{2Z_A\frac{\beta_a}{\alpha_a+\beta_a}\cdot\frac{q_{f\mu}}{q_f\cdot K}T_a^s + 2Z_A\frac{\alpha_b}{\alpha_b+\beta_b}\cdot\frac{q_{i\mu}}{q_i\cdot K}T_b^s \\ & \quad + 2Z_B\frac{\beta_c}{\alpha_c+\beta_c}\cdot\frac{p_{f\mu}}{p_f\cdot K}T_c^s + 2Z_B\frac{\alpha_d}{\alpha_d+\beta_d}\cdot\frac{p_{i\mu}}{p_i\cdot K}T_d^s\} \\ & + (q_i-q_f)\cdot K\{-2Z_A\frac{\beta_a}{\alpha'_a+\beta'_a}\cdot\frac{q_{f\mu}}{q_f\cdot K}T_a^t + 2Z_A\frac{\beta_b}{\alpha'_b+\beta'_b}\cdot\frac{q_{i\mu}}{q_i\cdot K}T_b^t \\ & \quad + 2Z_B\frac{\alpha_c}{\alpha'_c+\beta'_c}\cdot\frac{p_{f\mu}}{p_f\cdot K}T_c^t - 2Z_B\frac{\alpha_d}{\alpha'_d+\beta'_d}\cdot\frac{p_{i\mu}}{p_i\cdot K}T_d^t\} \\ & + 2[Z_A q_{f\mu}T_a^\Delta + Z_A q_{i\mu}T_b^\Delta + Z_B p_{f\mu}T_c^\Delta + Z_B p_{i\mu}T_d^\Delta] + \ldots\ldots, \end{aligned} \quad (9e)$$

where

$$T_x^s = \partial T_x^{el}/\partial s_{\alpha_x\beta_x}$$

$$T_x^t = \partial T_x^{el}/\partial t_{\alpha'_x\beta'_x} \quad (9f)$$

$$T_x^\Delta = \partial T(s_{\alpha_x\beta_x}, t_{\alpha'_x\beta'_x}, \Delta_x)/\partial\Delta_x \qquad (x=a,b,c,d)$$

and $T_x^{el} = T(s_{\alpha_x\beta_x}, t_{\alpha_x'\beta_x'})$ represents the T-matrix evaluated at $s_{\alpha_x\beta_x}$ and $t_{\alpha_x'\beta_x}$, for the corresponding elastic (nonradiative) process (i.e. the A-B elastic scattering process).

To obtain the leading term of M_μ^I, we follow Low's prescription to impose the gauge invariant condition:

$$\begin{aligned}
K^\mu M_\mu^I &= -K^\mu M_\mu^E \\
&= -[Z_A T_a^{el} - Z_A T_b^{el} + Z_B T_c^{el} - Z_B T_d^{el}] \\
&\quad -2(q_i+p_i)\cdot K\{Z_A \frac{\beta_a}{\alpha_a+\beta_a} T_a^s + Z_A \frac{\alpha_b}{\alpha_b+\beta_b} T_b^s \\
&\qquad + Z_B \frac{\beta_c}{\alpha_c+\beta_c} T_c^s + Z_B \frac{\alpha_d}{\alpha_d+\beta_d} T_d^s\} \\
&\quad -2(q_i-q_f)\cdot K\{-Z_A \frac{\beta_a}{\alpha_a'+\beta_a'} T_a^t + Z_A \frac{\beta_b}{\alpha_b'+\beta_b'} T_b^t \\
&\qquad + Z_B \frac{\alpha_c}{\alpha_c'+\beta_c'} T_c^t - Z_B \frac{\alpha_d}{\alpha_d'+\beta_d'} T_d^t\} \\
&\quad -2[Z_A q_f\cdot K T_a^\Delta + Z_A q_i\cdot K T_b^\Delta + Z_B p_f\cdot K T_c^\Delta + Z_B p_i\cdot K T_d^\Delta] \\
&\quad +..... \qquad (10)
\end{aligned}$$

From Eq.(10), we obtain

$$\begin{aligned}
M_\mu^I &= -Z_A \frac{(q_f+p_f)_\mu}{(q_f+p_f)\cdot K} T_a^{el} + Z_A \frac{(q_i+p_i)_\mu}{(q_i+p_i)\cdot K} T_b^{el} \\
&\quad - Z_B \frac{(q_f+p_f)_\mu}{(q_f+p_f)\cdot K} T_c^{el} + Z_B \frac{(q_i+p_i)_\mu}{(q_i+p_i)\cdot K} T_d^{el} \\
&\quad - 2(q_i+p_i)_\mu\{Z_A \frac{\beta_a}{\alpha_a+\beta_a} T_a^s + Z_A \frac{\alpha_b}{\alpha_b+\beta_b} T_b^s \\
&\qquad + Z_B \frac{\beta_c}{\alpha_c+\beta_c} T_c^s + Z_B \frac{\alpha_d}{\alpha_d+\beta_d} T_d^s]\} \\
&\quad - 2(q_i-q_f)_\mu\{-Z_A \frac{\beta_a}{\alpha_a'+\beta_a'} T_a^t + Z_A \frac{\beta_b}{\alpha_b'+\beta_b'} T_b^t \\
&\qquad + Z_B \frac{\alpha_c}{\alpha_c'+\beta_c'} T_c^t - Z_B \frac{\alpha_d}{\alpha_d'+\beta_d'} T_d^t\} \\
&\quad - 2[Z_A q_{f\mu} T_a^\Delta + Z_A q_{i\mu} T_b^\Delta + Z_B p_{f\mu} T_c^\Delta + Z_B p_{i\mu} T_d^\Delta] \\
&\quad + ... \qquad (11)
\end{aligned}$$

The total bremsstrahlung amplitude M_μ^T is then obtained from the sum of M_μ^E and M_μ^I (i.e., to combine Eq.(9e) with Eq.(11)) which can be written as

$$M_\mu^T = A_\mu(K)/K + B_\mu(K) + C_\mu(K)K + \ldots\ldots, \qquad (12)$$

where

$$\begin{aligned} A_\mu(K)/K = &+ Z_A\left[\frac{q_{f\mu}}{q_f\cdot K} - \frac{(q_f+p_f)_\mu}{(q_f+p_f)\cdot K}\right]T_a^{el} \\ &- Z_A\left[\frac{q_{i\mu}}{q_i\cdot K} - \frac{(q_i+p_i)_\mu}{(q_i+p_i)\cdot K}\right]T_b^{el} \\ &+ Z_B\left[\frac{p_{f\mu}}{p_f\cdot K} - \frac{(q_f+p_f)_\mu}{(q_f+p_f)\cdot K}\right]T_c^{el} \\ &- Z_B\left[\frac{q_{i\mu}}{q_i\cdot K} - \frac{(q_i+p_i)_\mu}{(q_i+p_i)\cdot K}\right]T_d^{el} \end{aligned} \qquad (13a)$$

and

$$\begin{aligned} B_\mu(K) = &+ 2Z_A\frac{\beta_a}{\alpha_a+\beta_a}\left[\frac{q_{f\mu}}{q_f\cdot K} - \frac{(q_i+p_i)_\mu}{(q_i+p_i)\cdot K}\right](q_i+p_i)\cdot K T_a^s \\ &+ 2Z_A\frac{\alpha_b}{\alpha_b+\beta_b}\left[\frac{q_{i\mu}}{q_i\cdot K} - \frac{(q_i+p_i)_\mu}{(q_i+p_i)\cdot K}\right](q_i+p_i)\cdot K T_a^s T_b^s \\ &+ 2Z_B\frac{\beta_c}{\alpha_c+\beta_c}\left[\frac{p_{f\mu}}{p_f\cdot K} - \frac{(q_i+p_i)_\mu}{(q_i+p_i)\cdot K}\right](q_i+p_i)\cdot K T_a^s T_c^s \\ &+ 2Z_B\frac{\alpha_d}{\alpha_d+\beta_d}\left[\frac{p_{i\mu}}{p_i\cdot K} - \frac{(q_i+p_i)_\mu}{(q_i+p_i)\cdot K}\right](q_i+p_i)\cdot K T_a^s T_d^s \\ &- 2Z_A\frac{\beta_a}{\alpha_a'+\beta_a'}\left[\frac{q_{f\mu}}{q_f\cdot K} - \frac{(q_i-q_f)_\mu}{(q_i-q_f)\cdot K}\right](q_i-q_f)\cdot K T_a^t \\ &+ 2Z_A\frac{\beta_b}{\alpha_b'+\beta_b'}\left[\frac{q_{i\mu}}{q_i\cdot K} - \frac{(q_i-q_f)_\mu}{(q_i-q_f)\cdot K}\right](q_i-q_f)\cdot K T_b^t \\ &+ 2Z_B\frac{\alpha_c}{\alpha_c'+\beta_c'}\left[\frac{p_{f\mu}}{p_f\cdot K} - \frac{(q_i-q_f)_\mu}{(q_i-q_f)\cdot K}\right](q_i-q_f)\cdot K T_c^t \\ &- 2Z_B\frac{\alpha_d}{\alpha_d'+\beta_d'}\left[\frac{p_{i\mu}}{p_i\cdot K} - \frac{(q_i-q_f)_\mu}{(q_i-q_f)\cdot K}\right](q_i-q_f)\cdot K T_d^t \,. \end{aligned} \qquad (13b)$$

We can see from Eqs.(13a) and (13b) that $A_\mu(K)$ depends only on T_x^{el}, (x=a,b,c,d), while $B_\mu(K)$ depends on T_x^s and T_x^t. Both $A_\mu(K)$ and $B_\mu(K)$ are independent of the off-shell derivatives T_x^Δ, but they are still functions of K. (Since, in general, $\beta_x \neq 0$ and $q_{f\mu}$ and/or $p_{f\mu}$ depend on K implicitly.) As for $C_\mu(K)$ and the coefficients of other higher powers in K, they involve the off-shell derivatives which cannot be determined from the corresponding elastic amplitude. Therefore, only the first two terms of the expansion given by Eq.(12) can be used to calculate the bremsstrahlung cross section from a given elastic scattering amplitude. The bremsstrahlung amplitude used in soft-photon approximations can be written in the form

$$M_\mu^{AB} = A_\mu(K)/K + B_\mu(K) \ . \qquad (14)$$

In some calculations, such as the EED approximation of Nefkens and Sober[14] for example, only the leading term of Eq.(12) has been used. In that case, the amplitude becomes

$$M_\mu^{A} = A_\mu(K)/K \ . \qquad (15)$$

The amplitude M_μ^{AB} (or M_μ^{A}) depends on sixteen parameters, $\alpha_x, \beta_x, \alpha_x'$ and β_x'(x=a,b,c,d), and is therefore very general. By varying these parameters, it can be used to study all possible soft-photon approximations.

III Soft-photon Approximations

To study M_μ^{AB} and M_μ^{A} systematically, we have divided them into the following classes:

(i) One-energy One-angle approximation (OEOA): This approximation is defined by choosing $\alpha_a=\alpha_b=\alpha_c=\alpha_d=\alpha$, $\beta_a=\beta_b=\beta_c=\beta_d=\beta$, $\alpha_a'=\alpha_b'=\alpha_c'=\alpha_d'=\alpha'$, $\beta_a'=\beta_b'=\beta_c'=\beta_d'=\beta'$. The amplitude in this approximation which depends only on $s_{\alpha\beta}$ and $t_{\alpha'\beta'}$ can be written as

$$M_\mu^{AB}(s_{\alpha\beta},t_{\alpha'\beta'})= M_\mu^{A}(s_{\alpha\beta},t_{\alpha'\beta'}) + B_\mu(s_{\alpha\beta},t_{\alpha'\beta'}) \ , \tag{16a}$$

where

$$M_\mu^{A}(s_{\alpha\beta},t_{\alpha'\beta'}) =$$
$$[Z_A(\frac{q_{f\mu}}{q_f\cdot K} - \frac{q_{i\mu}}{q_i\cdot K}) + Z_B(\frac{p_{f\mu}}{p_f\cdot K} - \frac{p_{i\mu}}{p_i\cdot K})]T(s_{\alpha\beta},t_{\alpha'\beta'}) \tag{16b}$$

and

$$\begin{aligned} B_\mu(s_{\alpha\beta},t_{\alpha'\beta'}) = & \\ & 2\{Z_A\frac{\beta}{\alpha+\beta}(\frac{q_{f\mu}}{q_f\cdot K}p_f\cdot K - p_{f\mu}) \\ & +Z_A\frac{\alpha}{\alpha+\beta}(\frac{q_{i\mu}}{q_i\cdot K}p_i\cdot K - p_{i\mu}) \\ & +Z_B\frac{\beta}{\alpha+\beta}(\frac{p_{f\mu}}{p_f\cdot K}q_f\cdot K - q_{f\mu}) \\ & +Z_B\frac{\alpha}{\alpha+\beta}(\frac{p_{i\mu}}{p_i\cdot K}q_i\cdot K - q_{i\mu})\}\partial T(s_{\alpha\beta},t_{\alpha'\beta'})/\partial s_{\alpha\beta} \\ & +2\{Z_A\frac{\beta'}{\alpha'+\beta'}(\frac{q_{i\mu}}{q_i\cdot K} - \frac{q_{f\mu}}{q_f\cdot K}) \\ & -Z_B\frac{\alpha'}{\alpha'+\beta'}(\frac{p_{i\mu}}{p_i\cdot K} - \frac{p_{f\mu}}{p_f\cdot K})\}(q_i-q_f)\cdot K\partial T(s_{\alpha\beta},t_{\alpha'\beta'})/\partial t_{\alpha'\beta'} \ . \end{aligned} \tag{16c}$$

In deriving Eqs.(16b) and (16c), we have used the fact that $K^\mu K_\mu=0$ and we have ignored those terms which are proportional to K_μ since $\varepsilon^\mu K_\mu=0$. Here ε^μ is the photon polarization.

The OEOA approximation is a generalization of Low's original SPA. To obtain Low's original result from Eq.(16a), we assume that particle A has charge e and particle B is neutral, i.e., we have $Z_A=1$ and $Z_B=0$. By choosing $\alpha=\beta=1$, $\beta'=0$ and $\alpha'=1$, we obtain, using $\bar{s}=(s_i+s_f)/2$,

$$M_\mu^{AB}(\bar{s},t_p) = \left(\frac{q_{f\mu}}{q_f\cdot K} - \frac{q_{i\mu}}{q_i\cdot K}\right)T(\bar{s},t_p) + \left(\frac{q_{f\mu}}{q_f\cdot K}p_f\cdot K - p_{f\mu} + \frac{q_{i\mu}}{q_i\cdot K}p_i\cdot K - p_{i\mu}\right)\partial T(\bar{s},t_p)/\partial\bar{s} \ , \tag{17}$$

which is precisely the Eq.(1.7) of Ref. 12. Low's original SPA has been extended and applied to calculate cross sections for various bremsstrahlung processes.

The EED approximation used by Nefkens and Sober is also a good example of the OEOA. This approximation uses the amplitude M_μ^A given by Eq.(16b) and it is evaluated at $(\bar{s},\bar{t})$ or (s_o,t_o). That is, $M_\mu^A(\bar{s},\bar{t})$ or $M_\mu^A(s_o,t_o)$ is used. Here, $\bar{s}=(s_i+s_f)/2$ and $\bar{t}=(t_q+t_p)/2$ are obtained by choosing $\alpha=\beta=\alpha'=\beta'=1$, but s_o and t_o, which are defined by

$$s_o = \lim_{k\to o} s_{\alpha\beta} = s_i$$

and

$$t_o = \lim_{k\to o} t_{\alpha'\beta'} \tag{18}$$

are independent of α, β, α' and β'.

Another interesting example of the OEOA is the modified SPA used by Nutt, Liu and Liou[15]. This approximation uses the amplitude given by Eq.(16a) with the parameters chosen to be $\alpha=1$, $\beta=0$, $\alpha'/\beta' = -(q_f-q_i-\frac{1}{2}R_q)\cdot R_q/(p_f-p_i-\frac{1}{2}R_p)\cdot R_p$, where R_q and R_p are defined by

$$q_{f\mu} = \lim_{k\to o} q_{f\mu} + R_{q\mu}$$

$$p_{f\mu} = \lim_{k\to o} p_{f\mu} + R_{p\mu}$$

$$R_{q\mu} + R_{p\mu} + K_{\mu} = 0. \qquad (19)$$

If Eq.(19) is used to expand the amplitude further in powers of K, Eqs.(41) and (42) of the Ref. 18 can be obtained. (In Ref. 18, both A and B are assumed to have charge e, i.e., $Z_A=Z_B=1$.) The amplitude obtained in Ref. 18 is evaluated at (s_o,t_o).

(ii) One-energy two-angle approximation (OETA):

The amplitude in the OETA approximation is evaluated at one energy but two different angles. For example, we can choose

$\alpha_a=\alpha_b=\alpha_c=\alpha_d=\alpha$, $\beta_a=\beta_b=\beta_c=\beta_d=\beta$, $\alpha_a'=\alpha_b'=\alpha_1'$, $\alpha_c'=\alpha_d'=\alpha_2'$, $\beta_a'=\beta_b'=\beta_1'$ and $\beta_c'=\beta_d'=\beta_2'$ and obtain the following amplitude:

$$M_{\mu}^{AB}(s_{\alpha\beta},t_{\alpha_1'\beta_1'},t_{\alpha_2'\beta_2'}) = M_{\mu}^{A}(s_{\alpha\beta},t_{\alpha_1'\beta_1'},t_{\alpha_2'\beta_2'}) + B_{\mu}(s_{\alpha\beta},t_{\alpha_1'\beta_1'},t_{\alpha_2'\beta_2'}), \qquad (20a)$$

where

$$M_{\mu}^{A}(s_{\alpha\beta},t_{\alpha_1'\beta_1'},t_{\alpha_2'\beta_2'}) = + Z_A\left(\frac{q_{f\mu}}{q_f\cdot K} - \frac{q_{i\mu}}{q_i\cdot K}\right)T(s_{\alpha\beta},t_{\alpha_1'\beta_1'}) + Z_B\left(\frac{p_{f\mu}}{p_f\cdot K} - \frac{p_{i\mu}}{p_i\cdot K}\right)T(s_{\alpha\beta},t_{\alpha_2'\beta_2'}) \qquad (20b)$$

and

$$B_{\mu}(s_{\alpha\beta},t_{\alpha_1'\beta_1'},t_{\alpha_2'\beta_2'}) =$$

$$2Z_A\frac{\beta}{\alpha+\beta}\left(\frac{q_{f\mu}}{q_f\cdot K}p_f\cdot K - p_{f\mu}\right)\partial T(s_{\alpha\beta},t_{\alpha_1'\beta_1'})/\partial s_{\alpha\beta}$$

$$+2Z_A\frac{\alpha}{\alpha+\beta}\left(\frac{q_{i\mu}}{q_i\cdot K}p_i\cdot K - p_{i\mu}\right)\partial T(s_{\alpha\beta},t_{\alpha_1'\beta_1'})/\partial s_{\alpha\beta}$$

$$+2Z_B\frac{\beta}{\alpha+\beta}\left(\frac{p_{f\mu}}{p_f\cdot K}q_f\cdot K - q_{f\mu}\right)\partial T(s_{\alpha\beta},t_{\alpha_2'\beta_2'})/\partial s_{\alpha\beta}$$

$$+2Z_B\frac{\alpha}{\alpha+\beta}\left(\frac{p_{i\mu}}{p_i\cdot K}q_i\cdot K - q_{i\mu}\right)\partial T(s_{\alpha\beta},t_{\alpha_2'\beta_2'})/\partial s_{\alpha\beta}$$

$$+2Z_A\frac{\beta_1}{\alpha_1'+\beta_1'}\left(\frac{q_{i\mu}}{q_i\cdot K} - \frac{q_{f\mu}}{q_f\cdot K}\right)(q_i-q_f)\cdot K\partial T(s_{\alpha\beta},t_{\alpha_1'\beta_1'})/\partial t_{\alpha_1'\beta_1'}$$

$$-2Z_B\frac{\alpha_2}{\alpha_2'+\beta_2'}\left(\frac{p_{i\mu}}{p_i\cdot K} - \frac{p_{f\mu}}{p_f\cdot K}\right)(q_i-q_f)\cdot K\partial T(s_{\alpha\beta},t_{\alpha_2'\beta_2'})/\partial t_{\alpha_2'\beta_2'}\ . \tag{20c}$$

An amplitude used by the UCLA group (Ref. 19) in the calculation of the $\pi^{\pm}p\gamma$ cross section is a good axample of this approximation. That amplitude, which is obtained by choosing $\alpha=\beta=1$, $\alpha_1'=\beta_2'=1$ and $\alpha_2'=\beta_1'=0$, is evaluated at $(\bar{s},t_p)$ and $(\bar{s},t_q)$.

(iii) Two-energy one-angle approximation (TEOA):

The amplitude in the TEOA approximation is evaluated at a common momentum-transfer-squared $t_{\alpha'\beta'}$ (i.e., we choose $\alpha_a'=\alpha_b'=\alpha_c'=\alpha_d'=\alpha'$ and $\beta_a'=\beta_b'=\beta_c'=\beta_d'=\beta'$) and two different energies which can be chosen from $s_{\alpha_x\beta_x}$ (x=a,b,c,d). An important example of this approximation can be obtained by choosing $\alpha_a=\alpha_c=\alpha_1$, $\alpha_b=\alpha_d=\alpha_2$, $\beta_a=\beta_c=\beta_1$ and $\beta_b=\beta_d=\beta_2$ leading to the following amplitude:

$$M_\mu^{AB}(s_{\alpha_1\beta_1},s_{\alpha_2\beta_2},t_{\alpha'\beta'}) = M_\mu^{A}(s_{\alpha_1\beta_1},s_{\alpha_2\beta_2},t_{\alpha'\beta'}) + B_\mu(s_{\alpha_1\beta_1},s_{\alpha_2\beta_2},t_{\alpha'\beta'}), \tag{21a}$$

where

$$M_\mu^{A}(s_{\alpha_1\beta_1},s_{\alpha_2\beta_2},t_{\alpha'\beta'}) =$$

$$\left[Z_A\frac{q_{f\mu}}{q_f\cdot K} + Z_B\frac{p_{f\mu}}{p_f\cdot K} - (Z_A+Z_B)\frac{(q_f+p_f)_\mu}{(q_f+p_f)\cdot K}\right]T(s_{\alpha_1\beta_1},t_{\alpha'\beta'})$$

$$-\left[Z_A\frac{q_{i\mu}}{q_i\cdot K} + Z_B\frac{p_{i\mu}}{p_i\cdot K} - (Z_A+Z_B)\frac{(q_i+p_i)_\mu}{(q_i+p_i)\cdot K}\right]T(s_{\alpha_2\beta_2},t_{\alpha'\beta'}) \tag{21b}$$

and

$$
\begin{aligned}
B_\mu(s_{\alpha_1\beta_1}, s_{\alpha_2\beta_2}, t_{\alpha'\beta'}) = \\
& 2\frac{\beta_1}{\alpha_1+\beta_1}\left[Z_A\frac{q_{f\mu}}{q_f\cdot K} + Z_B\frac{p_{f\mu}}{p_f\cdot K} - (Z_A+Z_B)\frac{(q_i+p_i)_\mu}{(q_i+p_i)\cdot K}\right] \\
& \quad x(q_i+p_i)\cdot K\partial T(s_{\alpha_1\beta_1}, t_{\alpha'\beta'})/\partial s_{\alpha_1\beta_1} \\
& +2\frac{\alpha_2}{\alpha_2+\beta_2}\left[Z_A\frac{q_{i\mu}}{q_i\cdot K} + Z_B\frac{p_{i\mu}}{p_i\cdot K} - (Z_A+Z_B)\frac{(q_i+p_i)_\mu}{(q_i+p_i)\cdot K}\right] \\
& \quad x(q_i+p_i)\cdot K\partial T(s_{\alpha_2\beta_2}, t_{\alpha'\beta'})/\partial s_{\alpha_2\beta_2} \\
& -2Z_A\frac{\beta'}{\alpha'+\beta'}\left[\frac{q_{f\mu}}{q_f\cdot K} - \frac{(q_i-q_f)_\mu}{(q_i-q_f)\cdot K}\right](q_i-q_f)\cdot K \\
& \quad x\partial T(s_{\alpha_1\beta_1}, t_{\alpha'\beta'})/\partial t_{\alpha'\beta'} \\
& +2Z_A\frac{\beta'}{\alpha'+\beta'}\left[\frac{q_{i\mu}}{q_i\cdot K} - \frac{(q_i-q_f)_\mu}{(q_i-q_f)\cdot K}\right](q_i-q_f)\cdot K \\
& \quad x\partial T(s_{\alpha_2\beta_2}, t_{\alpha'\beta'})/\partial t_{\alpha'\beta'} \\
& +2Z_B\frac{\alpha'}{\alpha'+\beta'}\left[\frac{p_{f\mu}}{p_f\cdot K} - \frac{(q_i-q_f)_\mu}{(q_i-q_f)\cdot K}\right](q_i-q_f)\cdot K \\
& \quad x\partial T(s_{\alpha_1\beta_1}, t_{\alpha'\beta'})/\partial t_{\alpha'\beta'} \\
& -2Z_B\frac{\alpha'}{\alpha'+\beta'}\left[\frac{p_{i\mu}}{p_i\cdot K} - \frac{(q_i-q_f)_\mu}{(q_i-q_f)\cdot K}\right](q_i-q_f)\cdot K \\
& \quad x\partial T(s_{\alpha_2\beta_2}, t_{\alpha'\beta'})/\partial t_{\alpha'\beta'} \ .
\end{aligned}
\tag{21c}
$$

The approximation defined by this particular amplitude is a generalization of the original FYA,[16] which corresponds to $\alpha_1=\beta_2=1$ and $\beta_1=\alpha_2=0$. If $Z_A=1$, $Z_B=Z$ and $\alpha'/\beta'=-(q_f-q_i-\frac{1}{2}R_q)\cdot R_q/(p_f-p_i-\frac{1}{2}R_p)\cdot R_p$ are used, then we obtain an amplitude which is very similar to the Eq.(15) of Ref.16. (The Eq.(15) of Ref.16 can be precisely reproduced if $q_{f\mu}$ and $p_{f\mu}$ are also expanded in powers of K (using Eq.(19)) before we impose the gauge invariant condition to obtain the leading term of M^I_μ.)

(iv) Two-energy two-angle approximation (TETA):

The amplitude in this approximation is evaluated at two different angles, which can be chosen from $t_{\alpha_x\beta_x}$, (x=a,b,c,d) and two different energies, which can be chosen from $s_{\alpha_x\beta_x}$ (x=a,b,c,d). For example, an amplitude can be obtained by choosing $\alpha_a=\alpha_c=\alpha_1$, $\alpha_b=\alpha_d=\alpha_2$, $\beta_a=\beta_c=\beta_1$, $\beta_b=\beta_d=\beta_2$, $\alpha'_a=\alpha'_b=\alpha'_1$, $\alpha'_c=\alpha'_d=\alpha'_2$, $\beta'_a=\beta'_b=\beta'_1$, and $\beta'_c=\beta'_d=\beta'_2$. We have

$$M^{AB}_\mu(s_{\alpha_1\beta_1},t_{\alpha'_1\beta'_1},s_{\alpha_2\beta_2},t_{\alpha'_2\beta'_2}) = M^A_\mu(s_{\alpha_1\beta_1},t_{\alpha'_1\beta'_1},s_{\alpha_2\beta_2},t_{\alpha'_2\beta'_2}) + B_\mu(s_{\alpha_1\beta_1},t_{\alpha'_1\beta'_1},s_{\alpha_2\beta_2},t_{\alpha'_2\beta'_2}) , \qquad (22a)$$

where

$$\begin{aligned} M^A_\mu(s_{\alpha_1\beta_1},t_{\alpha'_1\beta'_1},s_{\alpha_2\beta_2},t_{\alpha'_2\beta'_2})= & \\ & +Z_A\left[\frac{q_{f\mu}}{q_f\cdot K}-\frac{(q_f+p_f)_\mu}{(q_f+p_f)\cdot K}\right]T(s_{\alpha_1\beta_1},t_{\alpha'_1\beta'_1}) \\ & -Z_A\left[\frac{q_{i\mu}}{q_i\cdot K}-\frac{(q_i+p_i)_\mu}{(q_i+p_i)\cdot K}\right]T(s_{\alpha_2\beta_2},t_{\alpha'_1\beta'_1}) \\ & +Z_B\left[\frac{p_{f\mu}}{p_f\cdot K}-\frac{(q_f+p_f)_\mu}{(q_f+p_f)\cdot K}\right]T(s_{\alpha_1\beta_1},t_{\alpha'_2\beta'_2}) \\ & -Z_B\left[\frac{p_{i\mu}}{p_i\cdot K}-\frac{(q_i+p_i)_\mu}{(q_i+p_i)\cdot K}\right]T(s_{\alpha_2\beta_2},t_{\alpha'_2\beta'_2}) \qquad (22b) \end{aligned}$$

and

$$B_\mu(s_{\alpha_1\beta_1}, t_{\alpha_1'\beta_1'}, s_{\alpha_2\beta_2}, t_{\alpha_2'\beta_2'}) =$$

$$+2Z_A \frac{\beta_1}{\alpha_1+\beta_1}\left[\frac{q_{f\mu}}{q_f\cdot K} - \frac{(q_i+p_i)_\mu}{(q_i+p_i)\cdot K}\right] \times (q_i+p_i)\cdot K\,\partial T(s_{\alpha_1\beta_1}, t_{\alpha_1'\beta_1'})/\partial s_{\alpha_1\beta_1}$$

$$+2Z_A \frac{\alpha_2}{\alpha_2+\beta_2}\left[\frac{q_{i\mu}}{q_i\cdot K} - \frac{(q_i+p_i)_\mu}{(q_i+p_i)\cdot K}\right] \times (q_i+p_i)\cdot K\,\partial T(s_{\alpha_2\beta_2}, t_{\alpha_1'\beta_1'})/\partial s_{\alpha_2\beta_2}$$

$$+2Z_B \frac{\beta_1}{\alpha_1+\beta_1}\left[\frac{p_{f\mu}}{p_f\cdot K} - \frac{(q_i+p_i)_\mu}{(q_i+p_i)\cdot K}\right] \times (q_i+p_i)\cdot K\,\partial T(s_{\alpha_1\beta_1}, t_{\alpha_2'\beta_2'})/\partial s_{\alpha_1\beta_1}$$

$$+2Z_B \frac{\alpha_2}{\alpha_2+\beta_2}\left[\frac{p_{i\mu}}{p_i\cdot K} - \frac{(q_i+p_i)_\mu}{(q_i+p_i)\cdot K}\right] \times (q_i+p_i)\cdot K\,\partial T(s_{\alpha_2\beta_2}, t_{\alpha_2'\beta_2'})/\partial s_{\alpha_2\beta_2}$$

$$-2Z_A \frac{\beta_1}{\alpha_1'+\beta_1'}\left[\frac{q_{f\mu}}{q_f\cdot K} - \frac{(q_i-q_f)_\mu}{(q_i-q_f)\cdot K}\right] \times (q_i-q_f)\cdot K\,\partial T(s_{\alpha_1\beta_1}, t_{\alpha_1'\beta_1'})/\partial t_{\alpha_1'\beta_1'}$$

$$+2Z_A \frac{\beta_1}{\alpha_1'+\beta_1'}\left[\frac{q_{i\mu}}{q_i\cdot K} - \frac{(q_i-q_f)_\mu}{(q_i-q_f)\cdot K}\right] \times (q_i-q_f)\cdot K\,\partial T(s_{\alpha_2\beta_2}, t_{\alpha_1'\beta_1'})/\partial t_{\alpha_1'\beta_1'}$$

$$+2Z_B \frac{\alpha_2}{\alpha_2'+\beta_2'}\left[\frac{p_{f\mu}}{p_f\cdot K} - \frac{(q_i-q_f)_\mu}{(q_i-q_f)\cdot K}\right] \times (q_i-q_f)\cdot K\,\partial T(s_{\alpha_1\beta_1}, t_{\alpha_2'\beta_2'})/\partial t_{\alpha_2'\beta_2'}$$

$$-2Z_B \frac{\alpha_2}{\alpha_2'+\beta_2'}\left[\frac{p_{i\mu}}{p_i\cdot K} - \frac{(q_i-q_f)_\mu}{(q_i-q_f)\cdot K}\right] \times (q_i-q_f)\cdot K\,\partial T(s_{\alpha_2\beta_2}, t_{\alpha_2'\beta_2'})/\partial t_{\alpha_2'\beta_2'}. \quad (22c)$$

Various TETA approximations can be obtained from Eq.(22a) by varying the parameters α_1, β_1, α_2, β_2, α_1', β_1', α_2' and β_2'. These new approximations have never been studied.

From Eqs.(22a), (22b) and (22c), an interesting amplitude can be obtained if we choose $\beta_1 = \alpha_2 = \beta_1' = \alpha_2' = 0$. Since $B_\mu = 0$, the total bremsstrahlung amplitude has the following expression:

$$
\begin{aligned}
M_\mu^{AB} = {} & Z_A\left[-\frac{q_{f\mu}}{q_f\cdot K} - \frac{(q_f+p_f)_\mu}{(q_f+p_f)\cdot K}\right]T(s_i,t_p) \\
& -Z_A\left[-\frac{q_{i\mu}}{q_i\cdot K} - \frac{(q_i+p_i)_\mu}{(q_i+p_i)\cdot K}\right]T(s_f,t_p) \\
& +Z_B\left[-\frac{p_{f\mu}}{p_f\cdot K} - \frac{(q_f+p_f)_\mu}{(q_f+p_f)\cdot K}\right]T(s_i,t_q) \\
& -Z_B\left[-\frac{p_{i\mu}}{p_i\cdot K} - \frac{(q_i+p_i)_\mu}{(q_i+p_i)\cdot K}\right]T(s_f,t_q) \ .
\end{aligned}
$$

This amplitude is the simplest amplitude we can construct since it depends only on the elastic T-matrix (without any other terms involving $-\frac{\partial T}{\partial s}$ or $-\frac{\partial T}{\partial t}$). We shall discuss this amplitude again in Chapter V when the spin of the proton is taken into consideration. The main reason this amplitude is so interesting is that it gives the best fit to both the $\pi^{\pm}p\gamma$ and the $p^{12}C\gamma$ data.

Obviously, many more approximations, such as three-energy one-angle, four-energy two-angle, etc., can be defined.

IV Bremsstrahlung Cross Section Near a Resonance

We have used the proton-carbon bremsstrahlung process, $p^{12}C\gamma$, near the 1.7-MeV resonance as an example to study the one-energy one-angle approximation and the two-energy one-angle approximation. If θ_q, ϕ_q, θ_γ, ϕ_γ and K are chosen to be independent, then the bremsstrahlung cross section in the laboratory system can be written as:

$$\sigma_\gamma = d^3\sigma/d\Omega_q d\Omega_\gamma dK = (2\pi)^{-5}\delta^4(q_i+p_i-q_f-p_f-K)\{\tfrac{1}{2}\Sigma_{pol,spin}(M_\mu\varepsilon^\mu)^+(M^\mu\varepsilon_\mu)\}$$
$$\times J(q_f^2 dq_f/2E_q)(d^3\vec{p}_f/2E_p)(K^2/2K), \qquad (23)$$

where

$$J=e^2m^2/[(p_i\cdot q_i)^2-m^2M^2]^{\frac{1}{2}}$$

$$M_\mu=\bar{u}(q_f,\upsilon_f)M_\mu^{AB}u(q_i,\upsilon_i)$$

or

$$M_\mu=\bar{u}(q_f,\upsilon_f)M_\mu^{A}u(q_i,\upsilon_i)$$

and M_μ^{AB}(or M_μ^A) is given by Eq.(16a) (or Eq.(16b)) for the OEOA approximation and by Eq.(21a) (or Eq.(21b)) for the TEOA approximation (with Z_A=1, Z_B=6). Here, we should point out that Eqs. (16a) and (21a) were derived originally for two (spin-zero) spinless particles. The main reason why they can also be used for the $p^{12}C\gamma$ process, which is a spin-½ spin-0 case, is because the incident proton energy is about 1.7 MeV and K < 500 keV (or $K/q_i<<1$ and $K/q_f<<1$) which allows us to make the following approximations:

$$\bar{u}(q_f,\upsilon_f)\Gamma_\mu[1/(\not{q}_f+\not{K}-m)] \simeq \bar{u}(q_f,\upsilon_f)\gamma_\mu[1/(\not{q}_f+\not{K}-m)]$$
$$= \bar{u}(q_f,\upsilon_f)(q_{f\mu}+\tfrac{1}{2}\gamma_\mu\not{K})/q_f\cdot K \simeq \bar{u}(q_f,\upsilon_f)\frac{q_{f\mu}}{q_f\cdot K}$$

$$[1/(\not{q}_i-\not{K}-m)]\Gamma_\mu u(q_i,\upsilon_i) \simeq$$
$$[(-q_{i\mu}+\tfrac{1}{2}\not{K}\gamma_\mu)/q_i\cdot K]u(q_i,\upsilon_i) \simeq -\frac{q_{i\mu}}{q_i\cdot K}u(q_i,\upsilon_i),$$

where

$$\Gamma_\mu = \gamma_\mu - i\tfrac{1}{2}\lambda\sigma_{\mu\upsilon}K^\upsilon/m$$

$$\sigma_{\mu\upsilon} = i[\gamma_\mu, \gamma_\upsilon]/2$$

and λ is the proton anomalous magnetic moment. (The contribution from those terms which involve λ is negligible in this case.) In this study, particular attention is paid to two energy regions, the energy region far from any resonance and the energy region of a resonance (in this case the 1.7-MeV resonance), and we shall concentrate mainly on how M_μ^{AB} and M_μ^{A} depend on $s_{\alpha_x\beta_x}$. This can be done by evaluating T_x^{el} at a fixed momentum-transfer-squared t (or at a fixed scattering angle) and varying only α_x and β_x (not α_x' and β_x').

We have obtained some interesting and important results which can be summarized as follows:

(i) OEOA: In the energy region far from any resonance, the calculated bremsstrahlung cross section, $\sigma_\gamma^{OEOA}(s_{\alpha\beta}, t_{\alpha'\beta'})$, for a given set of α, β, α' and β' decreases monotonically with increasing K. As α and β are varied, (keeping α' and β' unchanged) we obtain various spectra which form a band. All predictions within this band are equally valid. This theoretical ambiguity cannot be avoided. The ambiguity will be small if the width of this band is very narrow, and in this case any set of (α,β) can be used. A set which was most commonly used in the past was $(\alpha,\beta)=(1,1)$, i.e., $s_{\alpha\beta}=\bar{s}=\tfrac{1}{2}(s_i+s_f)$. On the other hand, if the width of the band is wide, then a set of parameters $(\alpha,\beta,\alpha',\beta')$ which give the best fit to the data can be determined from the experiment. In the case of $p^{12}C\gamma$, the width of the band is found to be very narrow, indicating that the calculated $p^{12}C\gamma$ cross sections are quite independent of α and β. Fig. 2 shows a narrow band for $0 < \beta/\alpha < 10$ and $t_{\alpha'\beta'}=t_o$. It also shows that the $p^{12}C\gamma$ cross sections predicted by the

amplitude $M_{\mu}^{AB}(s_{\alpha\beta},t_{o})$ are in good agreement with the experimental data in the energy region far away from any resonance.

In the energy region of a resonance, the bremsstrahlung spectrum calculated from $M_{\mu}^{AB}(s_{\alpha\beta},t_{\alpha'\beta'})$ or $M_{\mu}^{A}(s_{\alpha\beta},t_{\alpha'\beta'})$ will show resonant structure if $s_{\alpha\beta}\neq s_{i}$ (i.e., if $\beta\neq 0$). The predicted structure will be centered about a photon energy K_{γ} in the bremsstrahlung spectrum and it will have a width Γ_{γ}. Both K_{γ} and Γ_{γ} will depend on a factor of the form $(\alpha+\beta)/\beta$ when α and β are varied. Furthermore, we have found that K_{γ} and Γ_{γ} can be accurately given without actually performing a complicated bremsstrahlung calculation. As shown in the Appendix A, if we assume that the cross section σ_{el} of the corresponding elastic scattering process exhibits a resonance with the resonance energy E_{R} and the width Γ_{el}, then we obtain, based purely on kinematical arguments, the following expressions for K_{γ} and Γ_{γ}:

$$K_{\gamma}=K_{o}(\alpha+\beta)/\beta \quad , \quad \beta\neq 0 \tag{24}$$

$$\Gamma_{\gamma}=N\Gamma_{el}(\alpha+\beta)/\beta \ , \tag{25}$$

where

$$K_{o}=(E_{i}-E_{R})N$$

$$N=M/[(m+M+E_{i})-(E_{i}^{2}+2mE_{i})^{\frac{1}{2}}\cos\theta_{\gamma}] \ .$$

Eqs.(24) and (25) enable us to predict (within 10% error) the values of K_{γ} and Γ_{γ} in terms of the observed values of E_{R} and Γ_{el}. The dependence of K_{γ} and Γ_{γ} on α and β is very interesting. It implies that α and β can be determined experimentally, by comparing the predicted structure with the observed one, and selecting the best approximation for σ_{γ}^{OEOA} in the resonance region.

In order to compare with the Brooklyn data[7], we have calculated the $p^{12}C\gamma$ cross section relative to the $p^{12}C$ elastic cross section,

$\sigma_{rel}^{OEOA}=\sigma_{\gamma}^{OEOA}/\sigma_{el}$, as a function of K near the 1.7-MeV resonance. Some results of the calculated σ_{rel}^{OEOA} at E_i=1.88 MeV for $\theta_q=155^o$ are shown in Figs.3. As we have already mentioned, we have concentrated mainly on how σ_{rel}^{OEOA} depends upon $s_{\alpha\beta}$. Therefore, a fixed momentum-transfer squared $t_{\alpha'\beta'}$ has been used in all these calculations. We have chosen $t_{\alpha'\beta'}$ to be $\bar{t}=\frac{1}{2}(t_q+t_p)$ or $t_o=\lim_{k\to o} t_{\alpha'\beta'}$. The values of (α,β) for those spectra labeled I,II and III in Fig.3 are (1,0.5), (1,1), (1,2), respectively, and $t_{\alpha'\beta'}$ used in these calculations is t_o. These figures show clearly that every spectrum exhibits resonant structure in the form of a peak. In Fig.3(a), the spectra are calculated from $M_{\mu}^{A}(s_{\alpha\beta},t_o)$. As we know, the levels associated with the 1.7-MeV resonance are two closely spaced levels of $\frac{5^+}{2}$ and $\frac{3^-}{2}$ in the compound nucleus ^{13}N. Since the main resonant peak in every spectrum arises from the level of $\frac{5^+}{2}$, we can use E_R=1.734 keV to predict the position of the main resonant peak from Eq.(24). Using $N=\frac{12}{13}$, the values of K_{γ} calculated from Eq.(24) are 404 keV, 269.6 keV and 202 keV for the spectra I,II and III, respectively. These values are to be compared with the following exact values calculated from σ_{rel}^{OEOA}: 405 keV, 270 keV and 204 keV. The agreement is excellent. We have also found that the values of Γ_{γ} calculated from Eq.(25) are in very good agreement with those calculated from σ_{rel}^{OEOA}. In Fig.3b, the spectra are calculated from the amplitude $M_{\mu}^{AB}(s_{\alpha\beta},t_o)$. The giant peaks obtained in these calculations arise mainly from the term involving $\partial T^{el}/\partial s_{\alpha\beta}$ in $B_{\mu}(k)$. The values of K_{γ} calculated from Eq.(24) are still in good agreement with those calculated from σ_{rel}^{OEOA}. However, because σ_{γ}^{OEOA} is roughly proportional to $|(s_i-s_{\alpha\beta})\partial T^{el}/\partial s_{\alpha\beta}|^2$ rather than to σ_{el}/K, we have slightly modified Eq.(25) to take into account the variation of

$\partial T^{el}/\partial s_{\alpha\beta}$ in the resonance region.

Unfortunately, a comparison with the experimental data shows that the OEOA approximation can not be used to describe the $p^{12}C\gamma$ spectra near the 1.7-MeV resonance. The observed peak appears at $K_o=(E_i-E_R)N$ ~135 keV rather than at $K_\gamma=K_o(\alpha+\beta)/\beta$ as predicted by Eq.(24) or σ_{rel}^{OEOA}. If we choose $\beta>>\alpha$ such that $(\alpha+\beta)/\beta\to1$, then we can obtain a peak at K_o but the shape of the structure(the giant peak) will be in complete disagreement with the observed one. In order to show this point clearly, we have used $(\alpha,\beta)=(0,1)$ and $t_{\alpha'\beta'}=t_o$ to calculate σ_{rel}^{OEOA}. As shown in Fig.4, we have obtained a giant peak at K_o=135 keV which is not observed experimentally. We must point out here that this conclusion will remain unchanged even if t_o is replaced by any other $t_{\alpha'\beta'}$, mainly because $t_{\alpha'\beta'}$ (or the corresponding scattering angle) changes slightly with K in the energy region of the calculated spectrum, $0 < K < K'$~600 keV, and $K_{max}>>K'>K_\gamma$ in this case. (If $K'<K_\gamma$, then no structure would appear.) Here K_{max} is the maximum kinematically allowed photon energy. To demonstrate this point, we have applied the EED approximation, evaluated at $\bar{s}=(s_i+s_f)/2$ and $\bar{t}=(t_q+t_p)/2$, to predict the spectrum in the region 0<K<400 keV. As shown in Fig.3(a), we have obtained a spectrum with a resonant peak around 270 keV, which is very similar to the spectrum II as expected.

Eq.(24) can also be applied to resolve a mystery found in the pion-proton bremsstrahlung, $\pi^{\pm}p\gamma$, calculation. The $\pi^{\pm}p\gamma$ cross sections near the $\Delta(1232)$ resonance have been calculated by the group from UCLA using an amplitude in the OETA approximation, $M_\mu^{AB}(\bar{s},t_p,t_q)$, in order to describe the spectra measured by the group.[2] (Details of the

experimental arrangement are shown in Appendix B.) Instead of getting a resonant peak at the expected photon energy K_o=50-70 MeV, the calculated cross sections rise steeply with increasing K above 80 MeV[19]. This mysterious result can be explained as follows: Since $s_{\alpha\beta}$=s was used in M_μ^{AB}, a resonant peak would be predicted at $K_\gamma=2K_o$ since $(\alpha+\beta)/\beta=2$. If K_o is about 60 Mev, then a giant peak will be predicted at 120 MeV(not at 60 MeV as might be expected). Therefore the predicted spectrum exhibits a minimum around 60 MeV and tends to rise with increasing K above 60 MeV. Our study shows that the giant peak comes from the B_μ term of the amplitude M_μ^{AB}, especially the term which involves $\partial T^{el}/\partial s$. The predicted spectra will be in better agreement with the data if M_μ^A is used. In fact, the EED approximation evaluated at $\bar{s}$ and $\bar{t}$, which is inadequate to describe the $p^{12}C\gamma$ data, gives good results for the $\pi^{\pm}p\gamma$ case. As we explain in the Appendix C, the reasons that the EED approximation predicts a monotonically decreasing spectra in this case are that $\bar{t}$ (or the scattering angle) changes substantially with K in the region $0 < K < K' \sim 120$ MeV and that K_γ is very close to K_{max} and K', i.e., $K_{max} \sim K' \sim K_\gamma$.

(ii) TEOA : The generalized FYA defined by Eq.(21a) or Eq.(21b) is the most important example of the TEOA approximation. The amplitude used in this generalized FYA, which is evaluated at $S_{\alpha_1\beta_1}$ and $S_{\alpha_2\beta_2}$, depends on four parameters$(\alpha_1,\beta_1,\alpha_2,\beta_2)$. In the energy region far from the 1.7-MeV resonance, the calculated σ_{rel}^{TEOA} for the $p^{12}C\gamma$ process is very similar to the one obtained in the OEOA, because of the smooth energy dependence of the scattering amplitude. In the vicinity of the resonance, however, the generalized FYA predicts a quite different resonant structure from that predicted in the OEOA.

The prediction of the resonant structure is the most interesting and important test of the approximation. By varying four parameters, we obtain various spectra with one or two resonant peaks depending on the values of $S_{\alpha_1\beta_1}$ and $s_{\alpha_2\beta_2}$. If $s_{\alpha_1\beta_1} \neq S_i \neq s_{\alpha_2\beta_2}$ and $s_{\alpha_1\beta_1} \neq s_{\alpha_2\beta_2}$ (i.e., $\beta_1 \neq 0, \beta_2 \neq 0$ and $\beta_1 \neq \beta_2$), then two resonant peaks are predicted. Applying Eqs.(24) and (25) to this case, we have $K_\gamma^{(i)} = K_o(\alpha_i+\beta_i)/\beta_i$ and $\Gamma_\gamma^{(i)} = N\Gamma_{el}(\alpha_i+\beta_i)/\beta_i$, i=1,2. On the other hand, if $s_{\alpha_1\beta_1} = S_i$ and $s_{\alpha_2\beta_2} \neq S_i$ (i.e., $\beta_1 = 0, \beta_2 \neq 0$), then only one resonant peak is predicted at $K_\gamma^{(2)}$. A typical example is the original FYA which predicts a single peak at $K_\gamma^{(2)} = K_o$ with $\Gamma_\gamma^{(2)} = N\Gamma_{el}$.

Some results of the calculated σ_{rel}^{TEOA} are shown in Figs.5(a) and 5(b). The values of the parameters$(\alpha_1,\beta_1,\alpha_2,\beta_2)$ for those spectra labeled I,II,III and IV are (1,0,0,1), (1,1,0,1), (1,1/2,0,1) and (1,1/3,0,1), respectively. Again, t_o is used in these calculations. Four spectra shown in Fig.5(a) are calculated from the amplitude $M_\mu^A(s_{\alpha_1\beta_1}, s_{\alpha_2\beta_2}, t_o)$. All of these spectra exhibit a common resonant peak (the first peak) at $K_\gamma^{(2)} = K_o \sim 135$ keV since $(\alpha_2+\beta_2)/\beta_2 = 1$. The spectra II,III and IV show also a second resonant peak at $K_\gamma^{(1)} = K_o(\alpha_1+\beta_1)/\beta_1$. The existence of the first peak at 135 keV has been verified by the experiment but no data are available to verify the existence of any other resonant peaks. All four spectra calculated from $M_\mu^A(s_{\alpha_1\beta_1}, s_{\alpha_2\beta_2}, t_o)$ are in good agreement with the data in the energy region k<100 keV, but the observed peak can not be satisfactorily described by any of these calculations.

Four spectra shown in Fig.5(b) are calculated from the amplitude $M_\mu^{AB}(s_{\alpha_1\beta_1}, s_{\alpha_2\beta_2}, t_o)$. Like those shown in Fig.5(a), these four spectra

have a common peak at 135 keV and every spectrum, except the spectrum I, has a second peak at $K_\gamma^{(1)}=K_o(\alpha_1+\beta_1)/\beta_1$. The contribution from the $B_\mu(k)$ term of the amplitude M_μ^{AB} is not negligible in the resonance region. It increases the cross section substantially near the second peak (mainly due to the term involving $\partial T_x^{el}/\partial s_{\alpha_1\beta_1}$) and decreases the magnitude of the cross section slightly near the first peak (mainly due to the term involving $\partial T_x^{el}/\partial t_o$). As we can see from this figure, the existing data in the energy region K<200 keV can be described by all four calculations, but these four calculations give quite different results in the energy region K>200 keV. Thus a precise measurement of the cross sections in the region K>200 keV can be used to determine a set of the best parameters. Finally, it should be pointed out that any calculation with the parameters $(1,\varepsilon,0,1)$, where $\varepsilon<K_o/(K_{max}-K_o)$, will give a spectrum which is almost identical to the spectrum I.

V Two-energy Two-angle Approximation

In section III(iv), the two-energy two-angle approximation (TETA) for bremsstrahlung production from the scattering of two spin-zero particles was discussed. The most general expression for this approximation is given by Eqs.(22a),(22b) and (22c). From Eq.(22c), we can see that B_μ vanishes if β_1, α_2, β_1', α_2' are chosen to be zero. Since $\beta_1= \alpha_2= \beta_1'= \alpha_2'=0$ implies that

$$s_{\alpha_1\beta_1}=s_i$$
$$t_{\alpha_1'\beta_1'}=t_p$$
$$s_{\alpha_2\beta_2}=s_f$$
$$t_{\alpha_2'\beta_2'}=t_q \ ,$$

the amplitude M_μ^{AB} becomes

$$\begin{aligned} M_\mu^{AB}(s_i,t_p,s_f,t_q) = M_\mu^{A}(s_i,t_p,s_f,t_q) \\ +Z_A\left[\frac{q_{f\mu}}{q_f\cdot K} - \frac{(q_f+p_f)_\mu}{(q_f+p_f)\cdot K}\right]T(s_i,t_p) \\ -Z_A\left[\frac{q_{i\mu}}{q_i\cdot K} - \frac{(q_i+p_i)_\mu}{(q_i+p_i)\cdot K}\right]T(s_f,t_p) \\ +Z_B\left[\frac{p_{f\mu}}{p_f\cdot K} - \frac{(q_f+p_f)_\mu}{(q_f+p_f)\cdot K}\right]T(s_i,t_q) \\ -Z_B\left[\frac{p_{i\mu}}{p_i\cdot K} - \frac{(q_i+p_i)_\mu}{(q_i+p_i)\cdot K}\right]T(s_f,t_q) \ . \end{aligned} \qquad (26)$$

This particular TETA approximation is very interesting for it depends only on the elastic scattering T-matrix, evaluated at four sets of (s,t): (s_i,t_p), (s_f,t_p), (s_i,t_q) and (s_f,t_q), but it does not depend on any derivative of T with respect to s or t. In other words, M_μ^{AB} does not involve $-\frac{\partial T}{\partial s}-$ or $-\frac{\partial T}{\partial t}-$. Thus, the choice of the parameters $\beta_1= \alpha_2= \beta_1'= \alpha_2'=0$ gives us the simplest amplitude for bremsstrahlung which can be constructed. Note that this amplitude should not be confused

with the amplitude used in the EED approximation. There is a substantial difference between the two amplitudes. From Eq.(16a), we can see that the most general amplitude in the OEOA approximation has the form

$$M_\mu^{AB}(s_{\alpha\beta},t_{\alpha'\beta'}) = M_\mu^{A}(s_{\alpha\beta},t_{\alpha'\beta'}) + B_\mu(s_{\alpha\beta},t_{\alpha'\beta'}) ,$$

where B_μ which involves $\frac{\partial T}{\partial s}$ and $\frac{\partial T}{\partial t}$ does not vanish in general. Thus, the EED approximation which uses only the amplitude M_μ^A for the bremsstrahlung calculation has ignored an important contribution from the B_μ term without justification. In fact, our calculation (as well as the calculation of the UCLA group) shows that the B_μ term dominates the bremsstrahlung cross section in the vicinity of a resonance. The amplitude M_μ^{AB} given by Eq.(26), on the other hand, does include the B_μ term but its contribution is identically zero.

Simplicity is not the sole reason for choosing the amplitude given by Eq.(26) for bremsstrahlung calculations. Our study shows that it is also the best choice. Moreover, if the elastic T-matrix, which has been used as imput for our bremsstrahlung calculations, varies rapidly with s and/or t in the vicinity of a resonance, then the expansion of the four half-off-shell T-matrices (included in the external amplitude) in powers of s or t, which is the common technique used in the soft-photon expansion, is obviously not valid. In that case, the amplitude given by Eq.(26) is the only proper choice. The fact that the term which involves $\frac{\partial T}{\partial s}$ and/or $\frac{\partial T}{\partial t}$ in any bremsstrahlung amplitude causes some difficulty in describing the $\pi^{\pm}p\gamma$ and $p^{12}C\gamma$ data is just an example of the problem related to this invalid expansion.

This idea of constructing the simplest bremsstrahlung amplitude can

be extended to the scattering of two particles with non-zero spin. In order to compare with the $\pi^{\pm}p\gamma$ and $p^{12}C\gamma$ data, let us show how the simplest bremsstrahlung amplitude for the scattering of a spin-½ particle with a spin-0 particle can be constructed. As we shall see later, such extension is not trivial. For the spin non-zero case, the nonunique choice of the internal scattering amplitude from the gauge-invariance condition adds further complication in selecting the best bremsstrahlung amplitude.

For $\pi^{\pm}p\gamma$,

$$\pi^{\pm}(q_i^{\mu}) + P(p_i^{\mu}) \rightarrow \pi^{\pm}(q_f^{\mu}) + P(p_f^{\mu}) + \gamma(K^{\mu}),$$

the external scattering amplitude can be written as

$$\begin{aligned} M_{\mu}^{E} = u(p_f,\upsilon_f)\{&Z_{\pi}\frac{q_{f\mu}}{q_f\cdot K}T_a - T_bZ_{\pi}\frac{q_{i\mu}}{q_i\cdot K} \\ &+\Gamma_{\mu}\cdot[1/(\not{p}_f+\not{K}-m_p)]T_c \\ &+T_d[1/(\not{p}_i-\not{K}-m_p)]\Gamma_{\mu}\}u(p_i,\upsilon_i) \ . \end{aligned} \qquad (27)$$

Here, T_a, T_b, T_c and T_d are the half-off-mass-shell T matrices for πp scattering (corresponding to Fig.1(a), 1(b), 1(c) and 1(d), respectively), $m_{\pi}(m_p)$ is the pion (proton) mass, $Z_{\pi}=1$ for π^+ and -1 for π^-, and Γ_{μ} is given by

$$\Gamma_{\mu}=\gamma_{\mu}-i\lambda\sigma_{\mu\upsilon}K^{\upsilon}/2m_p \ , \qquad (28)$$

where $\sigma_{\mu\upsilon}=i[\gamma_{\mu},\gamma_{\upsilon}]/2$ and λ is the proton anomalous magnetic moment which is 1.79.

The four half-off-shell T-matrices have the following expressions:

$$\begin{aligned} T_a &= T(s_a,\ t_a,\ \Delta_a) \\ T_b &= T(s_b,\ t_b,\ \Delta_b) \\ T_c &= T(s_c,\ t_c,\ \Delta_c) \\ T_d &= T(s_d,\ t_d,\ \Delta_d) \ , \end{aligned} \qquad (29)$$

where

$$\Delta_a=(q_f+K)^2=m_\pi^2+2q_f\cdot K$$
$$\Delta_b=(q_i-K)^2=m_\pi^2-2q_i\cdot K$$
$$\Delta_c=(p_f+K)^2=m_p^2+2p_f\cdot K \qquad (30)$$
$$\Delta_d=(p_i-K)^2=m_p^2-2p_i\cdot K \quad .$$

The idea which we have used to obtain the simplest amplitude is to expand T_i (i=a,b,c,d) only about $\Delta_i(K=0)$. Since no further expansion about any s or t is imposed, the constructed amplitude will not involve $\frac{\partial T}{\partial s}$ or $\frac{\partial T}{\partial t}$. Expanding T_i about $\Delta_i(K=0)$ gives

$$T_a = T(s_i,t_p) + \frac{\partial T}{\partial \Delta_a}2q_f\cdot K + \ldots$$
$$T_b = T(s_f,t_p) - \frac{\partial T}{\partial \Delta_b}2q_i\cdot K + \ldots$$
$$T_c = T(s_i,t_q) + \frac{\partial T}{\partial \Delta_c}2p_f\cdot K + \ldots \qquad (31)$$
$$T_d = T(s_f,t_q) - \frac{\partial T}{\partial \Delta_d}2p_i\cdot K + \ldots \quad .$$

Inserting Eq.(31) into Eq.(27), we obtain

$$M_\mu^E = \bar{u}(p_f,v_f)\{Z_\pi\frac{q_{f\mu}}{q_f\cdot K}[T(s_i,t_p) + \frac{\partial T}{\partial \Delta_a}2q_f\cdot K]$$
$$-[T(s_f,t_p) - \frac{\partial T}{\partial \Delta_b}2q_i\cdot K]Z_\pi\frac{q_{i\mu}}{q_i\cdot K} \qquad (32)$$
$$+\Gamma_\mu\cdot[1/(\not{p}_f+\not{K}-m_p)][T(s_i,t_q) + \frac{\partial T}{\partial \Delta_c}2p_f\cdot K]$$
$$+[T(s_f,t_q) - \frac{\partial T}{\partial \Delta_d}2p_i\cdot K][1/(\not{p}_i-\not{K}-m_p)]\Gamma_\mu\}u(p_i,v_i) \quad .$$

Using the following identities

$$\varepsilon^\mu\bar{u}(p_f,v_f)\Gamma_\mu\cdot[1/(\not{p}_f+\not{K}-m_p)]=\varepsilon^\mu\bar{u}(p_f,v_f)\frac{p_{f\mu}+R_{f\mu}}{p_f\cdot K} \qquad (33)$$
$$\varepsilon^\mu[1/(\not{p}_i+\not{K}-m_p)]\Gamma_\mu u(p_i,v_i)=-\varepsilon^\mu\frac{p_{i\mu}-R_{i\mu}}{p_i\cdot K}u(p_i,v_i) \quad ,$$

where

$$R_{f\mu}=\gamma_\mu K[1+\lambda(\not{p}_f+m_p)/2m_p]/2$$

$$R_{i\mu}=[1+\lambda(\not{p}_i+m_p)/2m_p]K\gamma_\mu/2,$$

Eq.(32) becomes

$$\begin{aligned} M^E_\mu = \bar{u}(p_f,v_f)\{&Z_\pi \frac{q_{f\mu}}{q_f\cdot K}T(s_i,t_p) - T(s_f,t_p)Z_\pi \frac{q_{i\mu}}{q_i\cdot K} \\ &+\frac{p_{f\mu}+R_{f\mu}}{p_f\cdot K}T(s_i,t_q) - T(s_f,t_q)\frac{p_{i\mu}-R_{i\mu}}{p_i\cdot K} \\ &+2Z_\pi q_{f\mu}\frac{\partial T}{\partial \Delta_a} + 2Z_\pi q_{i\mu}\frac{\partial T}{\partial \Delta_b} \\ &+2p_{f\mu}\frac{\partial T}{\partial \Delta_c} + 2p_{i\mu}\frac{\partial T}{\partial \Delta_d} + \ldots\}u(p_i,v_i) . \end{aligned} \tag{34}$$

The leading term of the internal scattering amplitude M^I_μ can be obtained from M^E_μ by imposing the gauge-invariance condition:

$$M^T_\mu K^\mu = (M^E_\mu + M^I_\mu)K^\mu = 0 \tag{35}$$

which gives

$$\begin{aligned} M^I_\mu K^\mu = -\bar{u}(p_f,v_f)\{&Z_\pi T(s_i,t_p) - T(s_f,t_p)Z_\pi \\ &+T(s_i,t_q) - T(s_f,t_q) \\ &+2Z_\pi q_{f\mu}\frac{\partial T}{\partial \Delta_a} + 2Z_\pi q_{i\mu}\frac{\partial T}{\partial \Delta_b} \\ &+2p_{f\mu}\frac{\partial T}{\partial \Delta_c} + 2p_{i\mu}\frac{\partial T}{\partial \Delta_d} + \ldots\}u(p_i,v_i) . \end{aligned} \tag{36}$$

It is clear that there is no unique expression for M^I_μ which can be obtained from Eq.(36) even if we are interested only in the leading term. To the best of our knowledge, this gauge ambiguity has never before been carefully studied. It requires thorough study because we have found that the calculated cross sections depend very sensitively on the choice of M^I_μ. Many different expressions for M^I_μ, which all satisfy Eq.(36), have

been obtained and studied, and we have found that the following expression for M_μ^I gives the best fit to both the $\pi^\pm p\gamma$ and $p^{12}C\gamma$ data:

$$\begin{aligned} M_\mu^I = - u(p_f,v_f)\{ & Z_\pi \frac{(q_f+p_f+R_f)_\mu}{(q_f+p_f)\cdot K} T(s_i,t_p) \\ & - Z_\pi T(s_f,t_p)\frac{(q_i+p_i-R_i)_\mu}{(q_i+p_i)\cdot K} \\ & + \frac{(q_f+p_f+R_f)_\mu}{(q_f+p_f)\cdot K} T(s_i,t_q) \\ & - T(s_f,t_q)\frac{(q_i+p_i-R_i)_\mu}{(q_i+p_i)\cdot K} \\ & + 2Z_\pi q_{f\mu}\frac{\partial T}{\partial \Delta_a} + 2Z_\pi q_{i\mu}\frac{\partial T}{\partial \Delta_b} \qquad (37) \\ & + 2p_{f\mu}\frac{\partial T}{\partial \Delta_c} + 2p_{i\mu}\frac{\partial T}{\partial \Delta_d} + \ldots\} u(p_i,v_i) \ . \end{aligned}$$

Combining Eq.(34) and Eq.(37), we obtain the total bremsstrahlung amplitude M_μ^T:

$$\begin{aligned} M_\mu^T = u(p_f,v_f)\{ & Z_\pi [\frac{q_{f\mu}}{q_f\cdot K} - \frac{(q_f+p_f+R_f)_\mu}{(q_f+p_f)\cdot K}] T(s_i,t_p) \\ & - Z_\pi T(s_f,t_p)[\frac{q_{i\mu}}{q_i\cdot K} - \frac{(q_i+p_i-R_i)_\mu}{(q_i+p_i)\cdot K}] \\ & + [\frac{p_{f\mu}+R_{f\mu}}{p_f\cdot K} - \frac{(q_f+p_f+R_f)_\mu}{(q_f+p_f)\cdot K}] T(s_i,t_q) \qquad (38) \\ & - T(s_f,t_q)[\frac{p_{i\mu}-R_{i\mu}}{p_i\cdot K} - \frac{(q_i+p_i-R_i)_\mu}{(q_i+p_i)\cdot K}]\} u(p_i,v_i). \end{aligned}$$

It is easy to check that M_μ^T is gauge invariant,

$$M_\mu^T K^\mu = 0,$$

since $R_{i\mu}K^\mu = R_{f\mu}K^\mu = 0$. In the on-shell approximation, the T-matrices, $T(s_i,t_p)$, $T(s_f,t_p)$, $T(s_i,t_q)$ and $T(s_f,t_q)$, are treated as the elastic T-matrix evaluated at (s_i,t_p), (s_f,t_p), (s_i,t_q) and (s_f,t_q), respectively. Thus, if the elastic scattering T-matrix is given as a function of s and t, then M_μ^T can be used to calculate the bremsstrahlung cross section.

Furthermore, we are sure that M_μ^T will be valid for any bremsstrahlung process with or without a resonance since M_μ^T is independent of $\frac{\partial T}{\partial s}$ and $\frac{\partial T}{\partial t}$. It should be pointed out that the four sets of (s,t) used in this particular two-energy two-angle approximation are solely determined by the four external diagrams shown in Fig.1. For example, $T(s,t)=T(s_i,t_p)$ is used for Fig.1a simply because $s=(q_i+p_i)^2=(q_f+p_f+K)^2=s_i$ and $t=(p_f-p_i)^2=(q_i-q_f-K)^2=t_p$ for the diagram 1a. For this reason, the choice of the four sets of (s,t) is fixed and natural, not arbitrary, for this approximation.

The bremsstrahlung amplitude for the $p^{12}C\gamma$ process,

$$p(q_i^\mu) + {}^{12}C(p_i^\mu) \rightarrow p(q_f^\mu) + {}^{12}C(p_f^\mu) + \gamma(K^\mu),$$

is very similar to the amplitude M_μ^T given by Eq.(38) if carbon is treated as a single elementary particle of spin zero, mass m_C and charge Ze where Z is the atomic number of the carbon. Moreover, since the contribution from the proton anomalous magnetic moment is negligible in the low energy scattering (the incident bombarding energy is less than 2 MeV) and the momentum of the detected photon is much smaller than the momentum of the proton, i.e., $K/q_i<<1$ and $K/q_f<<1$, the terms which involve $R_{i\mu}$ and $R_{f\mu}$ in Eq.(38) can be neglected. Thus, the final expression for M_μ^T has the form:

$$\begin{aligned} M_\mu^T = u(q_f,v_f)\{&[\frac{q_{f\mu}}{q_f\cdot K} - \frac{(q_f+p_f)_\mu}{(q_f+p_f)\cdot K}]T(s_i,t_p) \\ &-[\frac{q_{i\mu}}{q_i\cdot K} - \frac{(q_i+p_i)_\mu}{(q_i+p_i)\cdot K}]T(s_f,t_p) \\ &+Z[\frac{p_{f\mu}}{p_f\cdot K} - \frac{(q_f+p_f)_\mu}{(q_f+p_f)\cdot K}]T(s_i,t_q) \\ &-Z[\frac{p_{i\mu}}{p_i\cdot K} - \frac{(q_i+p_i)_\mu}{(q_i+p_i)\cdot K}]T(s_f,t_q)\}u(q_i,v_i) \end{aligned} \qquad (39)$$

for the $p^{12}C\gamma$ process.

As we have already mentioned, two bremsstrahlung processes which have been systematically measured are the $\pi^{\pm}p\gamma$ near the $\Delta(1232)$-resonance and the $p^{12}C\gamma$ near both the 1.7-MeV resonance and the 0.5-MeV resonance. The combined $\pi^{\pm}p\gamma$ and $p^{12}C\gamma$ data can provide a very sensitive test of the validity of various theoretical approximations and models.

The fact that the combined data cannot be described by the one-energy one-angle (or the one-energy two-angle) approximation is almost well established in Section IV. Briefly, the one-energy one-angle approximation includes three well-known approximations: Low's original soft-photon approximation (LSPA)[12], the EED approximation of Nefkens and Sober (EED)[14], and the modified SPA of Nutt, Liu and Liou (MSPA).[15] LSPA was applied to predict the $\pi^{\pm}p\gamma$ spectra by the UCLA group in order to describe the spectra measured by the group. We have repeated the calculation and have obtained essentially the same result as that obtained by the UCLA group. Typically, the calculated spectra at 298 MeV rise steeply with increasing photon energy above K = 80 MeV in complete disagreement with experimental results. We have also applied the LSPA to calculate the $p^{12}C\gamma$ cross sections at 1.88 MeV for a scattering angle of 155^{o} and we have found that the calculated cross sections show a giant resonant peak around K = 270 keV which is quite different from the small observed peak appearing around K = 135 keV. The EED approximation, on the other hand, can be used to describe most of the $\pi^{\pm}p\gamma$ data, but it fails to describe the $p^{12}C\gamma$ data near the 1.7-MeV resonance or the 0.5-MeV resonance. Finally, the MSPA approximation does not predict any resonant structure in the resonance region; it always gives a typical smooth spectrum with 1/K dependence.

Therefore, it cannot be used to describe the structure observed in the $p^{12}C\gamma$ spectra even though the $\pi^{\pm}p\gamma$ data can be described by this approximation very successfully. In short, what we have established here is that the one-energy approximation (either one-angle or two-angle) is inadequate to describe the combined data. For this reason we will not compare the result calculated from the two-energy two-angle approximation with any result calculated from the one-energy approximation. Since the combined data can only be described by the two-energy approximation, we shall focus on the comparison between the Feshbach-Yennie approximation (a typical two-energy one-angle approximation, see Appendix D for the expression used in this calculation) and the simplest amplitude given by Eq.(38) for $\pi^{\pm}p\gamma$ and by Eq.(39) for $p^{12}C\gamma$ (the best two-energy two-angle approximation). The detailed comparison is shown in Fig.10-Fig.43.

The comparison between the predicted $p^{12}C\gamma$ cross sections and the experimental cross sections is shown in Figs. 10, 11 and 12 for the incident proton energies of 1.594 MeV, 1.81 MeV and 0.591 MeV, respectively. In the energy region far from any resonance, as shown in Fig. 10, all approximations give about the same prediction, and the result is in good agreement with the data. In the vicinity of the 0.5-MeV and the 1.7-MeV resonances, both the TETA approximation and the TEOA approximation predict resonant structure which is more or less the same as the observed one, but the amplitude M_{μ}^{AB} in the TEOA approximation, which predicts a cross section increasing with increasing photon energy K for the 0.591 MeV case, is not better than the amplitude M_{μ}^{A} in the TEOA approximation. Because of the finite size of the photon detector used in the experiment, the theoretical calculations should be

averaged over the solid angle of the photon detector. The effects of the finite size of the photon detector on our results are discussed in Appendix E. In general, the averaged cross sections are in much better agreement with the data than the unaveraged cross sections.

The comparison between the predicted $\pi^{\pm}p\gamma$ cross sections and the UCLA data is shown in Figs. 13-43. Except for the photon counter G18 (and G19 for some cases), the simplest amplitude in the TETA approximation, Eq. (38), predicts spectra which are consistently in excellent agreement with the UCLA data. As for the Feshbach-Yennie approximation in TEOA, the calculations based on the amplitude M_{μ}^{AB} are in excellent agreement with the data for the photon counters G11 - G17, but the agreement becomes very poor for the other counters. The predictions using the amplitude M_{μ}^{A}, on the contrary, are in poor agreement with the data for the counters G11 - G17, but the agreement is either good or excellent for the rest of the counters. In order to understand this peculiar change in the agreement between the Feshbach-Yennie approximation and the UCLA data, we have chosen three new locations for the photon counter between G1 and G11 and have calculated the $\pi^{\pm}p\gamma$ cross sections for them using both M_{μ}^{AB} and M_{μ}^{A} in the TEOA approximation. This is shown in the Appendix F.

From the over-all comparison between the simplest amplitude in the TETA approximation and the Feshbach-Yennie TEOA approximation, we conclude that the simplest amplitude in the TETA approximation is much better than the TEOA Feshbach-Yennie approximation. This fact supports our argument that the best bremsstrahlung amplitude to be used to describe the bremsstrahlung cross sections near a resonance is the amplitude which is free of terms involving $\partial T_x^{el}/\partial s_{\alpha_x\beta_x}$ or

$$\partial T_x^{el} / \partial t_{\alpha_x' \beta_x'} .$$

VI Conclusion

(i) We have constructed the most general bremsstrahlung amplitude which can be used to study the predictive power of all possible approximations or models, including those well-known approximations that have previously been used. This general amplitude has been divided into many classes of approximations and the two most interesting approximations have been systematically studied. Special attention is given to the understanding of how these approximations depend on the choice of $s_{\alpha_x\beta_x}$ and $t_{\alpha_x'\beta_x'}$. The most important result which we have obtained from our study is that for a given amplitude we know what kind of resonant structure it will give in the resonance region. More precisely, we can predict the position of the structure in photon energy K_γ and its width Γ_γ by either performing a detailed bremsstrahlung calculation or using two simple formulas which relate K_γ and Γ_γ directly to the observed resonant energy E_R and the width Γ_{el}. This important new information, which has never before been obtained, can be used to study the validity of any bremsstrahlung amplitude (or to determine which set of $s_{\alpha_x\beta_x}$ and $t_{\alpha_x'\beta_x'}$ is physically acceptable) when the predicted result is compared with the experimental data. The formulas which determine K_γ and Γ_γ in terms of E_R and Γ_{el} are very useful. An important application of these two formulas is that they can be used to determine the energy region in which both the theoretical prediction and the experimental measurement should be performed.

(ii) We have shown that there is a theoretical ambiguity which can not be avoided. (This ambiguity can not be removed by imposing the gauge invariant condition and, to the best of our knowledge, there is no other first principle which can be used to remove this ambiguity.) Mathematically, this ambiguity means that the bremsstrahlung amplitude can be evaluated at $s_{\alpha_x\beta_x}$ and $t_{\alpha_x'\beta_x'}$ where α_x, β_x, α_x', and β_x'(x=a,b,c,d) are arbitrary real numbers. Since not all of these parameters are physically acceptable and there is no other principle which can be used as a guide to select a set of correct parameters, we rely entirely on experiment to resolve the theoretical ambiguity. That is, we provide all possible results calculated from a given amplitude (or approximation) so that the validity of this amplitude (or approximation) can be determined by comparison with the experimental data.

(iii) We have shown that the one-energy one-angle approximation can not be used to describe the $p^{12}C\gamma$ data near the 1.7-MeV resonance or the 0.5-MeV resonance. This conclusion is drawn from a systematic study of the amplitude in this approximation which is evaluated at all possible values of $s_{\alpha_x\beta_x}$ and $t_{\alpha_x'\beta_x'}$. Generally speaking, the resonant structure predicted in the OEOA approximation, including the EED, is quite different from the observed one (different in either the position of the peak or the shape of the structure or both).

(iv) We have shown that the existing experimental $p^{12}C\gamma$ data (available only in the energy region K<220 keV) near the 1.7-MeV resonance can be described by the two-energy one-angle approximation

evaluated at many (infinite) different sets of parameters. We have also shown that different sets of parameters give quite different cross sections in the energy region 220<K<600 keV, but no experimental data are available in that region. Since the data in that region can be used to rule out some sets of parameters which are physically unacceptable, our study provides strong justification for doing new experiments. New experimental data will play a very important role in constructing a new theory.

(v) Although more thorough studies are needed, the results of our investigation seem to indicate that any bremsstrahlung amplitude which involves $\partial T_x^{el}/\partial s_{\alpha_x\beta_x}$ will not be valid in the energy region of a resonance. This implies that all one-energy approximations would be inadequate and hence the two-energy approximation would be required to describe the bremsstrahlung cross sections near a resonance.

(vi) We have constructed a new class of soft-photon approximation called the two-energy two-angle approximation. Various versions of the two-energy two-angle approximation have been studied and compared, and our study shows that the best choice is the simplest amplitude, which depends <u>only</u> on the elastic T-matrix, T_x^{el}, i.e., the amplitude which is free of the term involving $\partial T_x^{el}/\partial s_{\alpha_x\beta_x}$ or $\partial T_x^{el}/\partial t_{\alpha_x'\beta_x'}$. We have also compared the result of the predictions calculated in the one-energy one-angle approximation, the one-energy two-angle approximation, the two-energy one-angle approximation and the two-energy two-angle approximation; we were not able to find any approximation which can fit the $\pi^{\pm}p\gamma$ and the $p^{12}C\gamma$ data better than this simplest amplitude in the two-energy two-angle approximation.

Appendix A: The expressions for K_γ and Γ_γ

Let us assume that the elastic scattering cross section, σ_{el}, of the corresponding elastic scattering process (the A-B system) exhibits a resonance with the resonance energy E_R and the width Γ_{el} and that the bremsstrahlung spectrum, σ_γ^{OEOA}, calculated from the amplitude $M_\mu^{AB}(s_{\alpha\beta},t_{\alpha'\beta'})$ or $M_\mu^{A}(s_{\alpha\beta},t_{\alpha'\beta'})$ shows resonant structure, which is centered about a photon energy K_γ in the spectrum σ_γ^{OEOA} and has a width Γ_γ. What we try to derive here are two simple expressions which relate K_γ and Γ_γ directly to E_R and Γ_{el}, respectively. These expressions are good for the one-energy one-angle approximation, but they can be extended very easily for the other approximations.

As we know M_μ^{AB} (or M_μ^{A}) involves four different T-matrices, $T(s_{\alpha_x\beta_x},t_{\alpha_x'\beta_x'}),x=a,b,c,d$. In the OEOA approximation, we have $s_{\alpha_x\beta_x}=s_{\alpha\beta}$ and $t_{\alpha_x'\beta_x'}=t_{\alpha'\beta'}$. Thus all four T-matrices are identical and they are evaluated at the same energy $s_{\alpha\beta}$ and the same scattering angle $t_{\alpha'\beta'}$:

$$T(s_{\alpha_x\beta_x},t_{\alpha_x'\beta_x'}) = T(s_{\alpha\beta},t_{\alpha'\beta'}) .$$

If we use the following expressions for s_i and s_f (see Eq.(5))

$$s_i=(m+M)^2+2ME_i$$

$$s_f=(m+M)^2+2M(E_i-K/N) ,$$

we can write $s_{\alpha\beta}$ as a function of K in the form

$$s_{\alpha\beta}(K)=(m+M)^2+2M\{E_i-\frac{\beta}{\alpha+\beta}K/N\} . \qquad (A1)$$

Now, suppose the elastic scattering cross section σ_{el} shows a resonance at the resonance energy E_R. In terms of E_R, we can define s_R as

$$s_R=(m+M)^2+2ME_R . \qquad (A2)$$

If $\beta\neq 0$ and $s_{\alpha\beta}(0)$ is much greater than s_R (i.e., $E_i>>E_R$ and far away from any resonance), then a typical bremsstrahlung spectrum with a

characteristic 1/K dependence will be predicted because the effect of the resonance will be very small. As K increases, $s_{\alpha\beta}(K)$ approaches s_R and the resonance effects become significant. In the energy region of the resonance, i.e., when

$$s_{\alpha\beta}(K_\gamma)=s_R, \tag{A3}$$

we expect a resonant peak (structure) to appear in the bremsstrahlung spectrum at $K=K_\gamma$. Substituting Eqs.(A1) and (A2) into Eq.(A3) and solving the equation for K_γ, we obtain

$$K_\gamma=K_o(\alpha+\beta)/\beta \quad , \quad \beta\neq 0 \ , \tag{A4}$$

where

$$K_o=(E_i-E_R)N \ . \tag{A5}$$

To derive the expression for the width Γ_γ, we write $s_{\alpha\beta}(K)$ in the form

$$s_{\alpha\beta}(K)=(m+M)^2+2ME_{\alpha\beta}(K) \ , \tag{A6}$$

where

$$E_{\alpha\beta}(K)=E_i-\frac{\beta}{\alpha+\beta}K/N \ . \tag{A7}$$

From Eq.(A7), for a given E_i and θ_γ, $\Delta E_{\alpha\beta}$ (the change in $E_{\alpha\beta}$) can be written in terms of ΔK (the change in K) as

$$\Delta E_{\alpha\beta}=-\frac{\beta}{\alpha+\beta}\Delta K/N \ . \tag{A8}$$

This equation is very useful. For example, if we choose $\Delta E_{\alpha\beta}$ to be the energy difference between the beginning point and the ending point of the resonant structure observed in σ_{el}, then ΔK will be the energy difference between the ending point and the beginning point of the resonant structure predicted in σ_γ^{OEOA}. Thus, we can define $\Gamma_{el}=|\Delta E_{\alpha\beta}|$ to be the width of the resonance observed in σ_{el} and $\Gamma_\gamma=|\Delta K|$ to be the width of the resonant structure predicted in σ_γ^{OEOA}, and write the

expression for Γ_γ in terms of Γ_{el} as

$$\Gamma_\gamma=[(\alpha+\beta)/\beta]N\Gamma_{el} \quad , \ \beta\neq 0 \quad . \tag{A9}$$

It should be pointed out that the values of K_γ and Γ_γ obtained from the actual bremsstrahlung calculation (not from Eqs.(A4) and (A9)) may depend upon which amplitude, M_μ^A or $M_\mu^{AB}=M_\mu^A+B_\mu$, is used in the calculation of σ_γ^{OEOA}. This is because σ_γ^{OEOA} can be dominated either by M_μ^A, the leading term of the amplitude, or B_μ, the second term of the amplitude, in the energy region of a resonance. As we have already mentioned, M_μ^A depends only upon $T^{el}=T(s_{\alpha\beta},t_{\alpha'\beta'})$ while B_μ depends upon $\partial T^{el}/\partial s_{\alpha\beta}$ and/or $\partial T^{el}/\partial t_{\alpha'\beta'}$. Therefore, in the case when the contribution from B_μ is negligible, σ_γ^{OEOA} calculated from either M_μ^A or M_μ^{AB} will be about the same and it will be roughly proportional to σ_{el}/K (or σ_{el}/K plus a constant). In this case, the values of K_γ and Γ_γ calculated from Eqs.(A4) and (A9), respectively, will be in very good agreement with those obtained from the exact bremsstrahlung calculation. On the other hand, if $B_\mu>>M_\mu^A$ in the resonance region, then σ_γ^{OEOA} calculated from M_μ^{AB} will be much greater than that calculated from M_μ^A. Consequently, the width of the resonance Γ_γ predicted by the amplitude M_μ^{AB} will be much wider than that predicted by the amplitude M_μ^A and the position of the resonant peak K_γ predicted by these two amplitudes may be different. (σ_γ^{OEOA} calculated from M_μ^A is still roughly proportional to σ_{el}/K but σ_γ^{OEOA} calculated from M_μ^{AB} will be approximately proportional to $|(s_i-s_{\alpha\beta})\partial T^{el}/\partial s_{\alpha\beta}|^2$. The contribution from the term involving $\partial T^{el}/\partial s_{\alpha\beta}$ is much more important than that from the term involving $\partial T^{el}/\partial t_{\alpha'\beta'}$ in the resonance region.) In this case, K_γ calculated from Eq.(A4) can be different from that obtained from the

actual bremsstrahlung calculation using the amplitude M_{μ}^{AB}. To get the same value of K_{γ}, E_R in Eq.(A4) has to be replaced by $E_R'=E_R-C$, where C is a constant energy, if the expression for K_{γ} given by Eq.(A4) remains unchanged. However, Eq.(A9) for Γ_{γ} must be slightly modified to take into account the variation of $\partial T^{el}/\partial s_{\alpha\beta}$ in the resonance region. Details of the modification will not be discussed here because the result of our study seems to indicate that any amplitude which involves $\partial T^{el}/\partial s_{\alpha\beta}$ can not be used to describe the bremsstrahlung spectra in the energy region of a resonance.

Appendix B: The Locations of detectors in $\pi^{\pm}p\gamma$ experiment

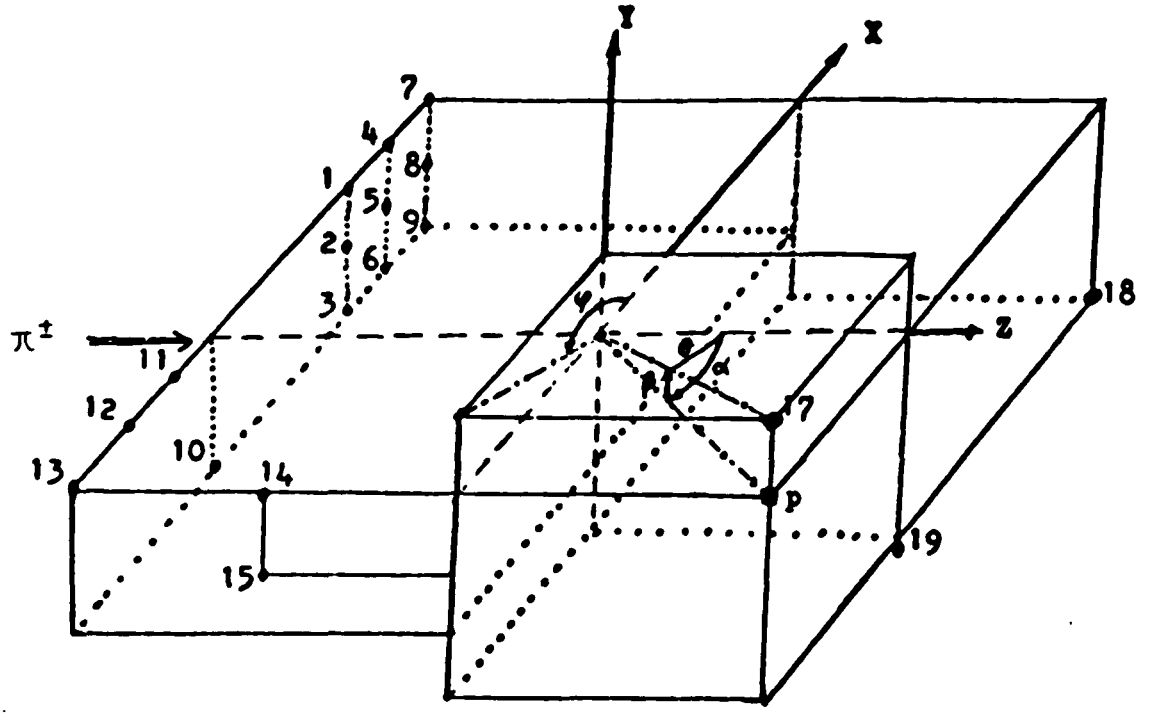

Fig. 1 The coordinate system and relative locations of the photon counters G1-G19 used in the UCLA $\pi^{\pm}p\gamma$ experiment.

Counter	α (deg)	β (deg)	θ (deg)	ϕ (deg)	d (cm) (to target)
G1	200.	0.	160.	0.	61.1
G2	200.	-18.	153.34	316.47	56.
G3	200.	-36.	139.48	295.11	56.
G4	220.	0.	140.	0.	56.
G5	220.	-18.	136.77	333.16	56.
G6	220.	-36.	128.30	311.50	56.
G7	240.	0.	120.	0.	56.
G8	240.	-18.	116.39	339.43	56.
G9	240.	-36.	113.86	320.01	56.
G10	180.	-36.	144.	270.	56.
G11	160.	0.	160.	180.	63.
G12	140.	0.	140.	180.	63.
G13	120.	0.	120.	180.	63.
G14	103.	0.	103.	180.	63.
G15	103.	-20.	102.20	200.48	63.
G17	50.	4.	50.12	174.78	300.
G18	320.	-56.	64.64	293.44	63.
G19	0.	-59.	59.	270.	63.
pion	50.5±7.	-10±24	50.5	180.	73.8[a]
proton	323±27	-26±26	0. (upper limit)	0. (upper limit)	92.1[b]

α = horizontal projection of the angle measured clockwise from the beam line.

β = the angle of elevation measured upwords from the horizontal plane.

[a] distance to first pion spark chamber.

[b] distance to first plane of counters.

Appendix C: The EED Approximation

In this appendix, we try to explain why the $\pi^{\pm}P\gamma$ spectrum, $\sigma^{EED}_{\pi p\gamma}$, calculated in the EED approximation shows a typical bremsstrahlung spectrum with 1/K dependence without any resonant structure for most of the photon counters G_i (i=1,2...,19), in good agreement with the experiment.

Nefkens and Sober have calculated $\sigma^{EED}_{\pi p\gamma}$ from the following formula:

$$\sigma^{EED}_{\pi p\gamma} = GKD^{\mu}D_{\mu}[d\sigma_{\pi p}(s,t)/d\Omega] \quad , \qquad (C1)$$

where

$$D^{\mu}=\mp\frac{q_{i\mu}}{q_i\cdot K}-\frac{p_{i\mu}}{p_i\cdot K}\pm\frac{q_{f\mu}}{q_f\cdot K}+\frac{p_{f\mu}}{p_f\cdot K} \qquad (C2)$$

$$G=[e^2/16\pi^3]s^{\frac{1}{2}}q_f^{\,3}/\{q_i[q_f^{\,2}(s^{\frac{1}{2}}-K)+E_q(\vec{q}_f\cdot\vec{K})]\} \quad .$$

and $d\sigma_{\pi p}(s,t)/d\Omega$ is the $\pi^{\pm}P$ elastic scattering cross section evaluated at s and t. In the published EED calculations, $d\sigma_{\pi p}/d\Omega$ was evaluated at (i)s_o and t_o and (ii)$\bar{s}$ and $\bar{t}$. Here $s_o=s_i=\lim_{k\to o}s_f$, $t_o=\lim_{k\to o}t_p=\lim_{k\to o}t_q$, $\bar{s}=\frac{1}{2}(s_i+s_f)$ and $\bar{t}=\frac{1}{2}(t_p+t_q)$. The amplitude used in the case (i) is identical to our amplitude $M^{A}_{\mu}(s_o,t_o)$ given by Eq.(16b) with $Z_B=1$, $Z_A=\pm1$ for $\pi^{\pm}$ and the T-matrix evaluated at $\lim_{k\to o}s_{\alpha\beta}=s_o$ and $\lim_{k\to o}t_{\alpha'\beta'}=t_o$, which can be obtained by choosing $\beta/\alpha=0$ and $\alpha'/\beta'=-(q_f-q_i-\frac{1}{2}R_q)\cdot R_q/(p_f-p_i-\frac{1}{2}R_p)\cdot R_p$. The amplitude used in the case (ii) is the same as that used in the case (i) except that the T-matrix in this case is evaluated at s and t, which can be obtained by choosing $\alpha=\beta=1$ ($s_{\alpha\beta}=\bar{s}$) and $\alpha'=\beta'=1$ ($t_{\alpha'\beta'}=\bar{t}$). In order to obtain Eq.(B1), Nefkens and Sober have made another approximation. They have ignored the contribution from the proton anomalous magnetic moment λ and they have

used the elastic projection operator, $\Lambda(\bar{p}_f) = \lim_{k\to o}\Lambda(p_f) = \lim_{k\to o}(\not{p}_f+M)/2M$ in their calculation. This elastic projection operator, combined together with the amplitude M^A_μ, enable them to write $\sigma^{EED}_{\pi p\gamma}$ in terms of $d\sigma_{\pi p}/d\Omega$ as shown in Eq.(B1).

Now let us explain why $\sigma^{EED}_{\pi p\gamma}$ shows no resonant structure for the $\pi^{\pm}p\gamma$ case and gives a typical bremsstrahlung spectrum with 1/K dependence for most of the photon counters G_i (i=1,2,.....19), in good agreement with the experiment. In the case (i), $d\sigma_{\pi p}/d\Omega$ is evaluated at s_o and t_o. Since s_o and t_o are independent of K, $d\sigma_{\pi p}/d\Omega$ will not vary with K. Therefore, if $\sigma^{EED}_{\pi p\gamma}$ is plotted as a function of K, its shape will be determined mainly by the factor $KD^\mu D_\mu$, which is roughly proportional to 1/K. This is why $\sigma^{EED}_{\pi p\gamma}$ decreases monotonically with increasing K. To support this argument, we have calculated $\sigma^{EED}_{\pi p\gamma}$ and we have obtained all spectra which are smooth curves with 1/K dependence. Some of these calculations are shown in Figs.6,7, and 8 (the dot-dashed curves). As for the case (ii), $d\sigma_{\pi p}/d\Omega$ is evaluated at $\bar{s}$ and $\bar{t}$. Since $\bar{s}$ and $\bar{t}$ are functions of K, $d\sigma_{\pi p}/d\Omega$ is no longer independent of K. This means that $\sigma^{EED}_{\pi p\gamma}$ will depend on both the factor $KD^\mu D_\mu \sim 1/K$ and $d\sigma_{\pi p}(\bar{s},\bar{t})/d\Omega$ when $\sigma^{EED}_{\pi p\gamma}$ is plotted as a function of K. The fact that $\bar{t}$ depends upon K implies that the scattering angle will change with K. More precisely, as K increases the scattering angle used in the calculation of $d\sigma_{\pi p}(\bar{s},\bar{t})/d\Omega$ will be shifted from one angle to another. The change in the scattering angle is not small for the $\pi^{\pm}p\gamma$ case at 298 MeV. For G14, for example, the scattering angle is changed from 69^o at K=15 MeV to 100^o at 140 MeV. This change will cause $d\sigma_{\pi p}(\bar{s},\bar{t})/d\Omega$ to change slowly and smoothly with increasing K. There is another important

factor which is directly related to $\bar{s}$. As we know, when K increases, $\bar{s}$ will reach the resonant energy s_R at a photon energy K_γ : $\bar{s}(K_\gamma)=s_R$. In other words, the predicted resonant peak, if any, is expected to appear at the photon energy K_γ in the bremsstrahlung spectrum. Our calculation shows that K_γ is about 110~140 MeV, depending on the photon counters and the incident energy, for this $\pi^\pm p\gamma$ case. Since 110~140 MeV is close to the maximum kinematically allowed photon energy K_{max} and the measured photon spectrum is extended to about 120 MeV, no resonant structure can be expected from $d\sigma_{\pi p}(\bar{s},\bar{t})/d\Omega$ for most of the photon counters. (If $K_\gamma<K_{max}$ and the photon spectrum is extended to K' with $K_{max}>K'>K_\gamma$, then $d\sigma_{\pi p}(\bar{s},\bar{t})/d\Omega$ will show resonant structure in the energy region $0<K<K'$.) All these factors combined together cause $d\sigma_{\pi p}(\bar{s},\bar{t})/d\Omega$ to vary slowly and smoothly with increasing K (see Figs.7 and 8) for most of the photon counters. Without any resonant structure from the elastic scattering cross section $d\sigma_{\pi p}(\bar{s},\bar{t})/d\Omega$, the shape of $\sigma^{EED}_{\pi p\gamma}$ will be determined mainly by the factor $KD^\mu D_\mu$. This is the the main reason why most of the calculated $\sigma^{EED}_{\pi p\gamma}(\bar{s},\bar{t})$ decrease smoothly with increasing K. Some of these calculations are also shown in Figs.6,7 and 8 (the solid curves).It should be pointed out that if $\bar{t}$ is replaced by t_o, which is independent of K (i.e., the scattering angle is fixed), then the calculated cross section $\sigma^{EED}_{\pi p\gamma}(\bar{s},t_o)$ will show resonant structure, just as we have pointed out in section IV. Some of these calculations are shown in Fig.6 (the dashed curves).

Although the EED approximation predicts $\pi^\pm p\gamma$ cross sections which are in good agreement with the UCLA data, it gives very poor results for the $p^{12}C\gamma$ cross sections. (see section IV.) There is no contradiction

between these two predictions because the predicted cross section depends on the incident bombarding energy, $s_{\alpha\beta}$ and $t_{\alpha'\beta'}$. Different values of $s_{\alpha\beta}$, $t_{\alpha'\beta'}$ and the incident energy would give quite different cross sections in the resonant region. This is exactly the point we try to emphasize in this work. In Fig.9, the $p^{12}C\gamma$ cross sections $\sigma^{EED}_{pc\gamma}(s,t)$ are calculated in the EED approximation using Eq.(B1). Here again, $d\sigma_{pc}(s,t)/d\Omega$ is evaluated at (i)s_o and t_o and (ii)$\bar{s}$ and $\bar{t}$. If $d\sigma_{pc}/d\Omega$ is evaluated at s_o and t_o, then the predicted $\sigma^{EED}_{pc\gamma}$ shows no resonant structure as expected for the reason we have already discussed. (See the dashed curve in Fig.9(c).) If $d\sigma_{pc}/d\Omega$ is evaluated at $\bar{s}$ and $\bar{t}$, on the other hand, then the predicted spectrum shows resonant structure with a peak which appears at $K_\gamma=2K_o\sim270$ keV (since $(\alpha+\beta)/\beta=2$). (See the solid curve in Fig.9(c).) Since the observed peak appears at $K_o=135$ keV, the predicted spectrum is therefore in total disagreement with the experiment. This kind of result is exactly what we have found in our one-energy one-angle case. To be more precise, the curve for $\sigma^{EED}_{pc\gamma}$ with $d\sigma_{pc}/d\Omega$ evaluated at $\bar{s}$ and $\bar{t}$ is very similar to the spectrum calculated from the amplitude $M^A_\mu(s,t_o)$. This is because $\bar{t}$ changes slightly with K in the energy region $10<K<400$ keV (The change in the scattering angle is less than 1.0^o), i.e., $\bar{t}\sim t_o$ and $\sigma^{EED}_{pc\gamma}(\bar{s},\bar{t}) \sim \sigma^{EED}_{pc\gamma}(\bar{s},t_o)$. We have also found that $K_\gamma<<K_{max}$ for this low energy $p^{12}C\gamma$ case. This fact, together with the fact that $\bar{t}\sim t_o$, can be used to explain why the resonant structure is predicted in the $p^{12}C\gamma$ case.

Finally, we should emphasize that the EED approximation of Nefkens and Sober has not only neglected the second term B_μ of the

bremsstrahlung amplitude but also ignored the contribution from the proton anomalous magnetic moment λ. The contribution from these terms is not negligible for the $\pi^{\pm}p\gamma$ processes near the $\Delta(1232)$ resonance. As we have already mentioned in section IV, the contribution from the B_{μ} terms causes the calculated $\pi^{\pm}p\gamma$ cross section to rise steeply with increasing K above 80 MeV. And our study shows that the contribution from λ does change substantially the magnitude of the $\pi^{\pm}p\gamma$ cross sections for some photon counters. For some cases, the agreement between the predicted cross sections and the UCLA data becomes very poor.

Appendix D: $\pi^{\pm}p\gamma$ Amplitude in Feshbach-Yennie Approximation

$$M_{\mu}^{A}(s_i,s_f,t_o) = [Z_1\frac{q_{f\mu}}{q_f\cdot K} + Z_2\frac{p_{f\mu}+R_{f\mu}}{p_f\cdot K} - (Z_1+Z_2)\frac{(q_f+p_f+R_f)_{\mu}}{(q_f+p_f)\cdot K}]T$$
$$-T'[Z_1\frac{q_{i\mu}}{q_i\cdot K} + Z_2\frac{p_{i\mu}-R_{i\mu}}{p_i\cdot K} - (Z_1+Z_2)\frac{(q_ip_i-R_i)_{\mu}}{(q_i+p)\cdot K}]$$

$$M_{\mu}^{AB}(s_i,s_f,t_o) = [Z_1\frac{q_{f\mu}}{q_f\cdot K} + Z_2\frac{p_{f\mu}+R_{f\mu}}{p_f\cdot K} - (Z_1+Z_2)-\frac{(q_f+p_f+R_f)_{\mu}}{(q_f+p_f)\cdot K}]T$$
$$-T'[Z_1\frac{q_{i\mu}}{q_i\cdot K} + Z_2\frac{p_{i\mu}-R_{i\mu}}{p_i\cdot K} - (Z_1+Z_2)-\frac{(q_ip_i-R_i)_{\mu}}{(q_i+p)\cdot K}]$$
$$+[Z_1\frac{q_{f\mu}}{q_f\cdot K}(t_p-t)+Z_2\frac{p_{f\mu}}{p_f\cdot K}(t_q-t)-(Z_1X_{\mu}^{p}+Z_2X_{\mu}^{q})]-\frac{\partial T}{\partial t}$$
$$-[Z_1\frac{q_{i\mu}}{q_i\cdot K}(t_p-t)+Z_2\frac{p_{i\mu}}{p_i\cdot K}(t_q-t)-(Z_1X_{\mu}^{p}+Z_2X_{\mu}^{q})]\frac{\partial T'}{\partial t}$$

where

$$T=T(s_i,t), \qquad T'=T(s_f,t)$$

$$t=\lim_{k\to o}t_p=\lim_{k\to o}t_q$$

$$(t_p-t)=X_{\mu}^{p}K^{\mu}, \qquad (t_q-t)=X_{\mu}^{q}K^{\mu}$$

Appendix E: Averaged $P^{12}C\gamma$ Cross Section

In $p^{12}C\gamma$ case, because of the finite size of the photon detector, the theoretical calculations are averaged over the disk-shaped photon detector. The efficiency is regarded as even all over the detector. The 16 points on which the average is made are defined in Ref. 21. The (θ,ϕ) angles in spherical system centered at the ^{12}C target can be determined as follows:

$$\cos\beta\cos\alpha = z = \cos\theta = OP_z$$

$$\sin\beta = y = \sin\theta\sin\phi = OP_y$$

$$\cos\beta\sin\alpha = x = \sin\theta\cos\phi = OP_x$$

that is,

$$\cos\theta = \cos\alpha\cos\beta$$

$$\tan\phi = \tan\beta/\sin\alpha \ ,$$

where the angle α is measured from the beam line on the Z-axis to OP_{xz} (the projection of OP on the X-Z plane) and β is the angle of elevation measured from Z-X plane (i.e., the angle between OP and OP_{xz}). See Fig. iii and Table A for details. The comparison of the averaged and unaveraged cross sections is given in Fig. iv.

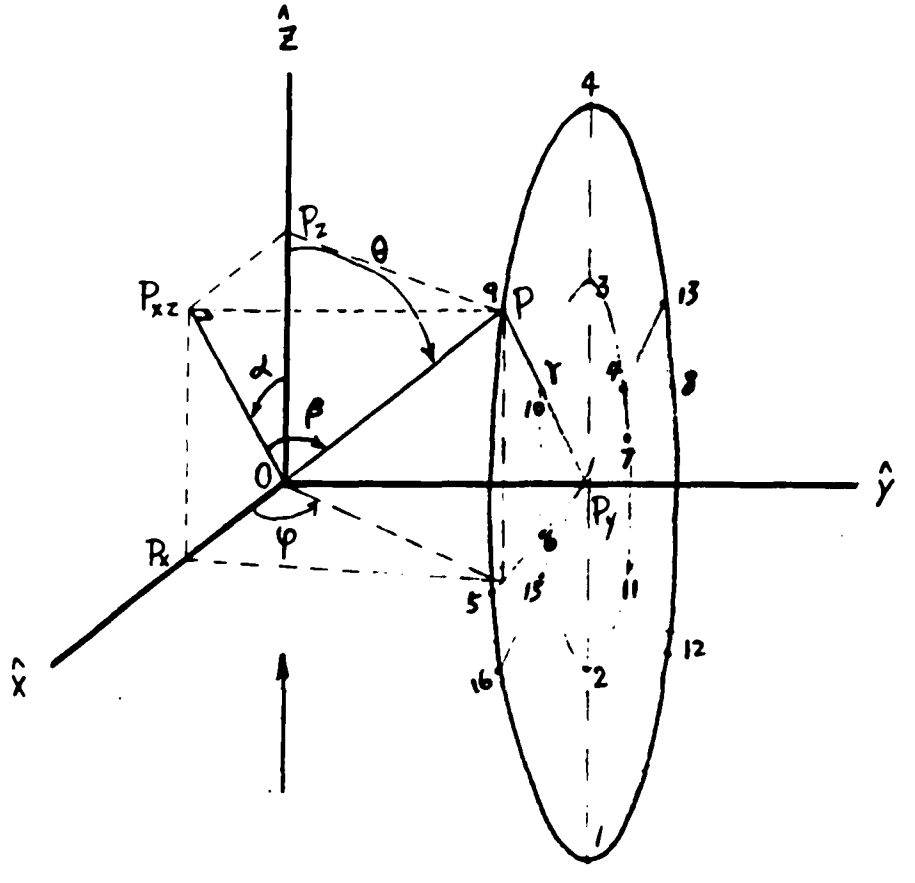

Fig. *ii* The definition of the angles α, β, θ and ϕ.

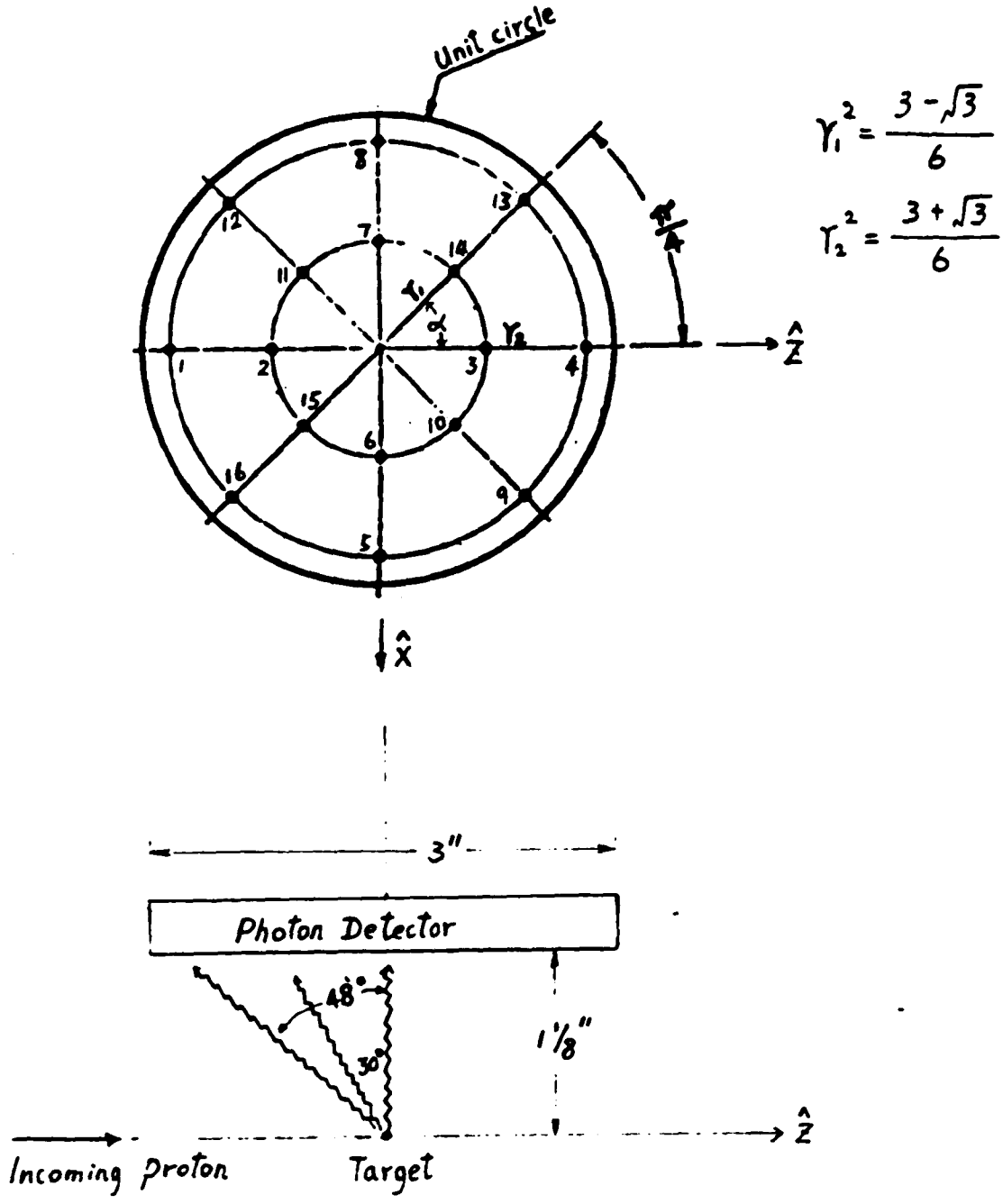

Fig. iii The diagram of the photon detector disk and its location relative to the incident beam and the target.

TABLE A : The location of the 16 points on the photon detector in spherical system: (θ, ϕ)
where

$$\cos\theta = \cos\alpha\cos\beta$$
$$\tan\phi = \tan\beta/\sin\alpha$$

Point	α	β	θ	ϕ
1	180°	42°	138°	90°
2	180°	60°	120°	90°
3	0°	60°	60°	90°
4	0°	42°	42°	90°
5	90°	42°	90°	42°
6	90°	60°	90°	60°
7	270°	60°	90°	120°
8	270°	42°	90°	138°
9	45°	42°	58°	52°
10	45°	60°	69°	68°
11	225°	60°	110°	112°
12	225°	42°	122°	128°
13	315°	42°	58°	128°
14	315°	60°	69°	112°
15	135°	60°	110°	68°
16	135°	42°	122°	52°

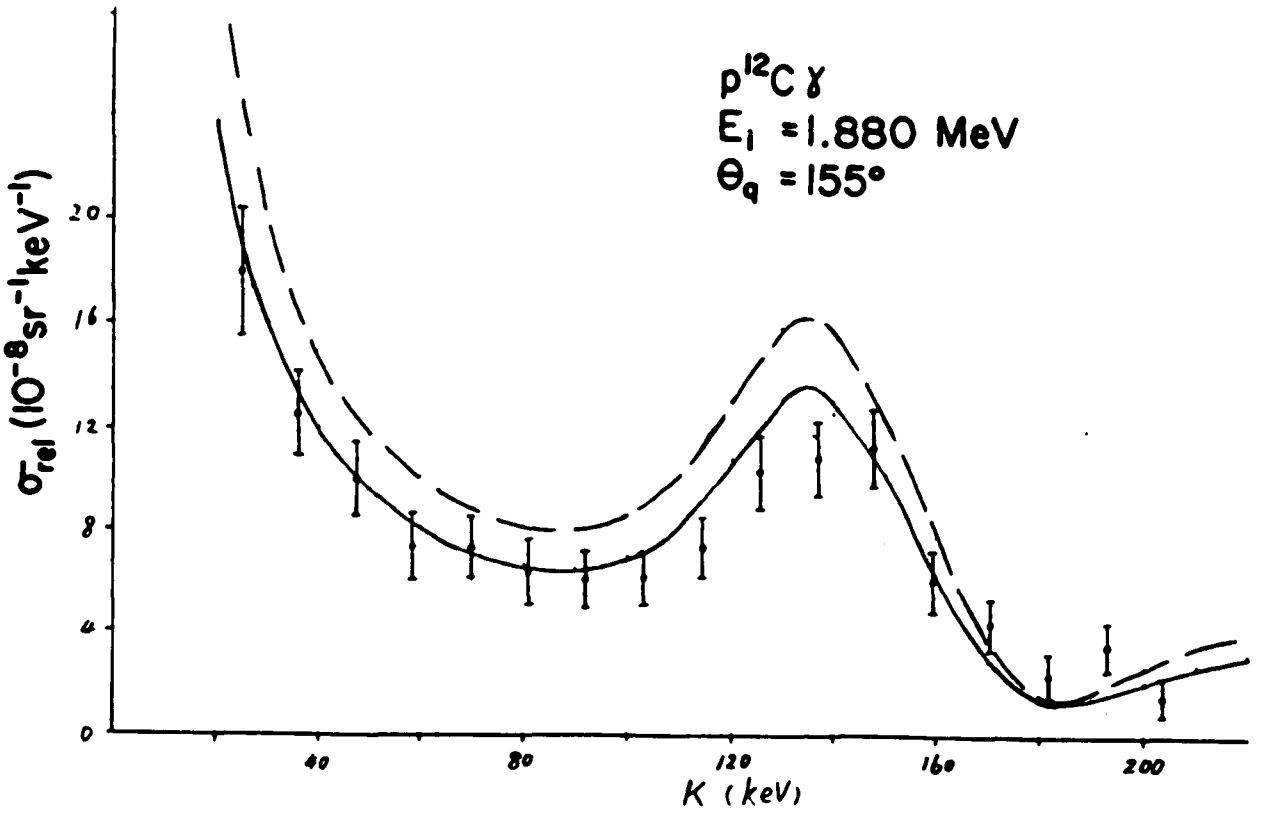

Fig. iv The relative $p^{12}C\gamma$ cross section σ_{rel} as a function of photon energy K at an incident proton energy of 1.880 MeV. The solid curve represents the averaged $p^{12}C\gamma$ and the dashed curve represents the unaveraged $p^{12}C\gamma$.

Appendix F: Variation of M_μ^A and M_μ^{AB} in TEOA from G1 to G11

In order to understand why M_μ^{AB} in TEOA fits the data for photon counter G11 but not the data for G1, we have calculated the cross sections for the photon counter located at positions II, III and IV (between G1 and G11). Their locations are shown below.

As we can see from Fig.V , when the photon counter moves from G1 to G11, the predicted spectra based on the amplitude M_μ^{AB} get better gradually, but the predicted spectra based on M_μ^A become worse and worse.

$\pi^+ p\gamma$ E_π=269 MeV					
	Photon counter				
	I(G1)	II	III	IV	V(G11)
θ	160	170	180	170	160
ϕ	0	0	0	180	180

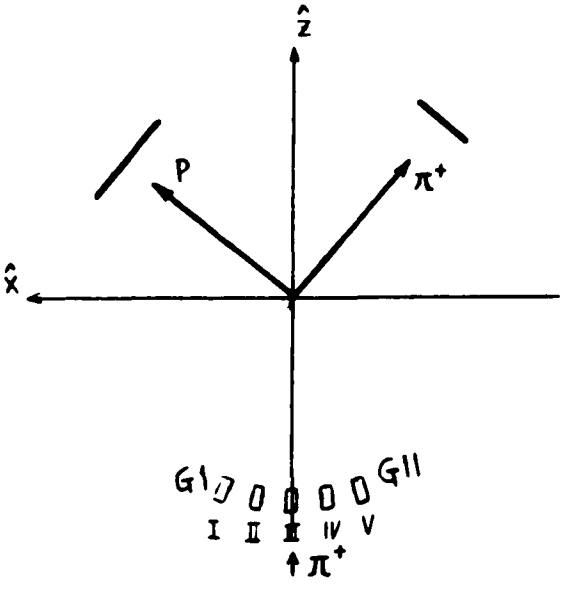

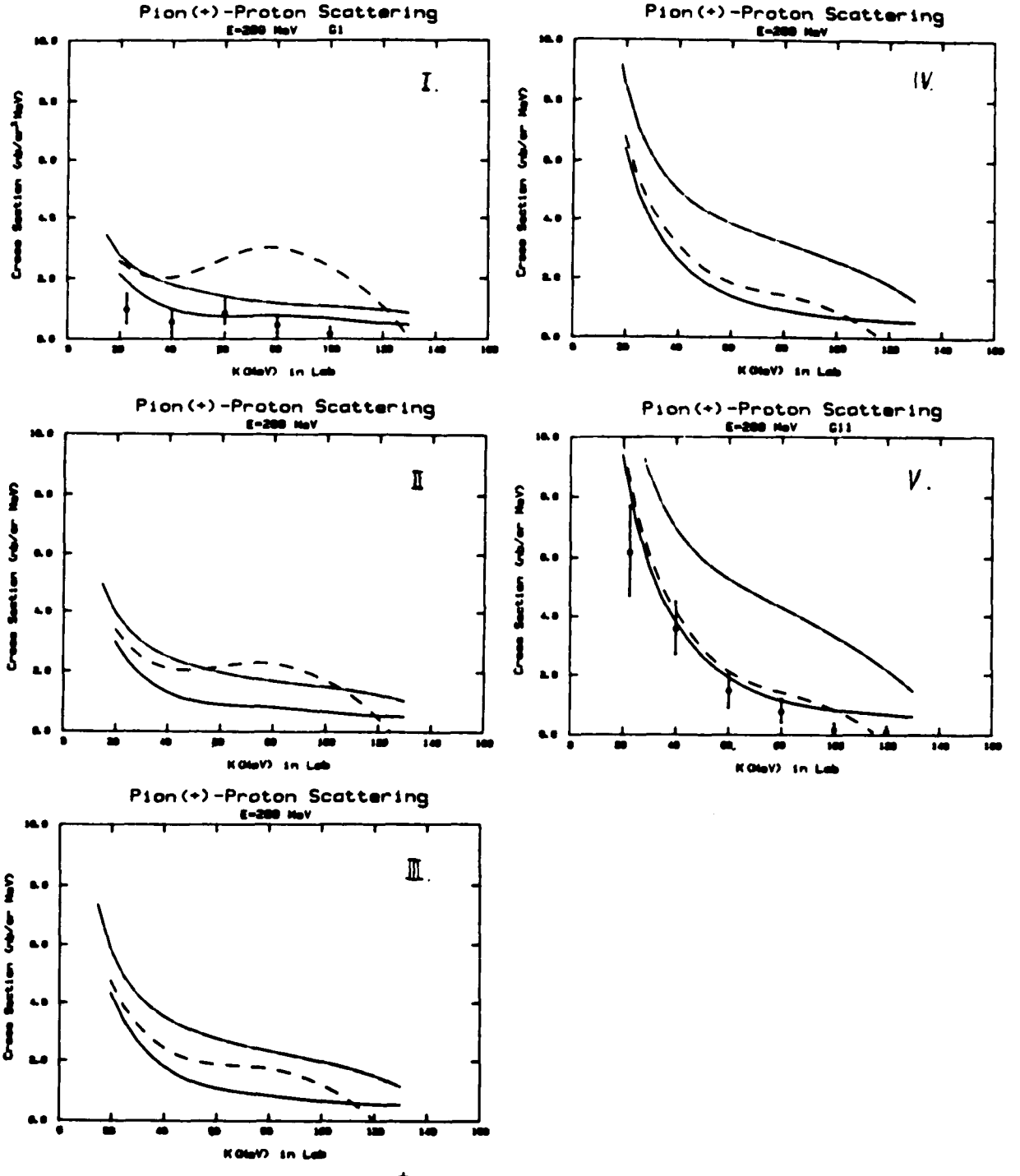

Fig. V The change of $\pi^+ p\gamma$ cross sections at 269 MeV for the photon counter moving from G1 to G11. The experimental $\pi^+ p\gamma$ data are from Ref.2.

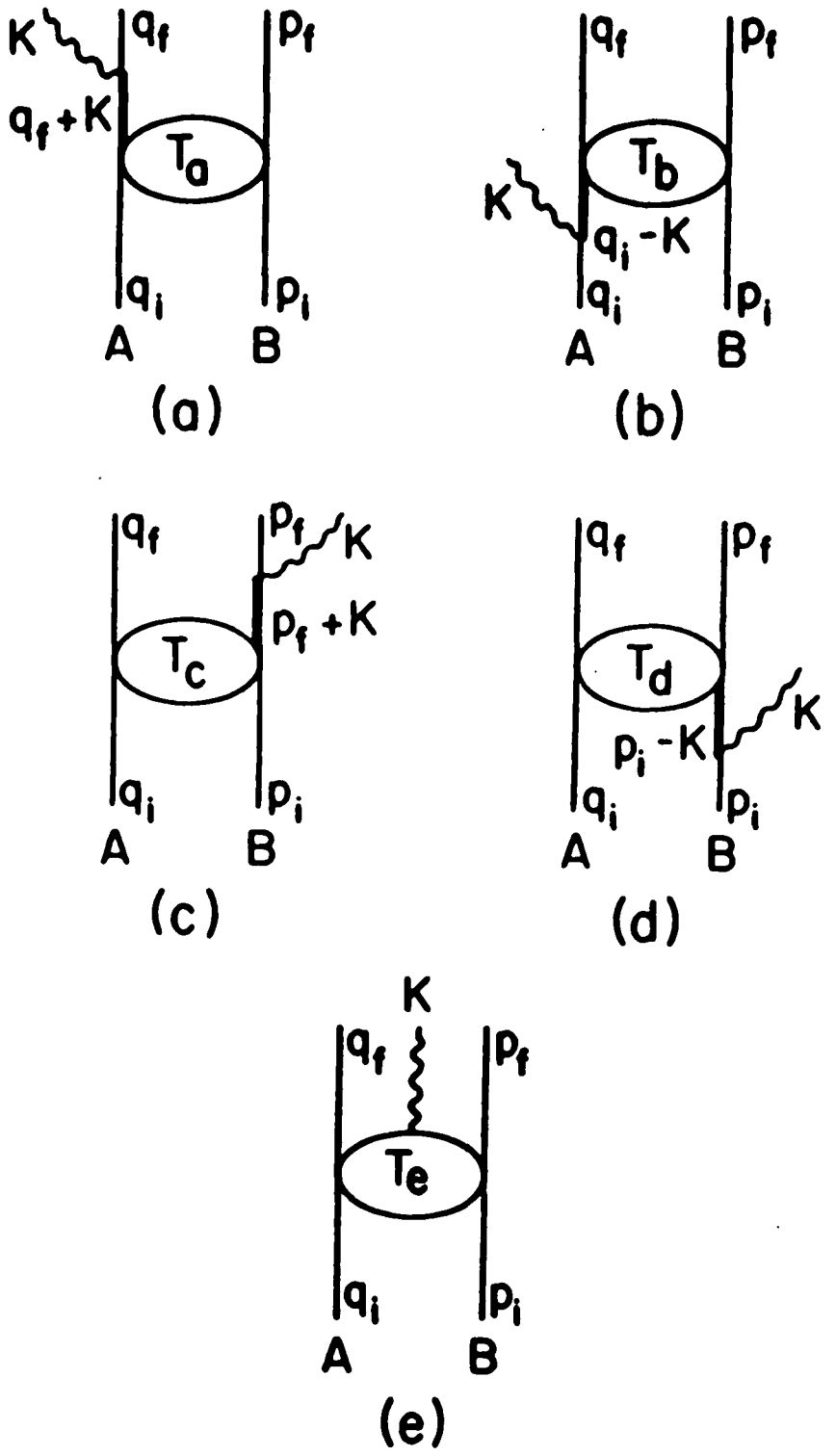

Fig.1 Feynman diagrams for bremsstrahlung:

(a)-(d) the external scattering diagrams;

(e) the internal scattering diagram.

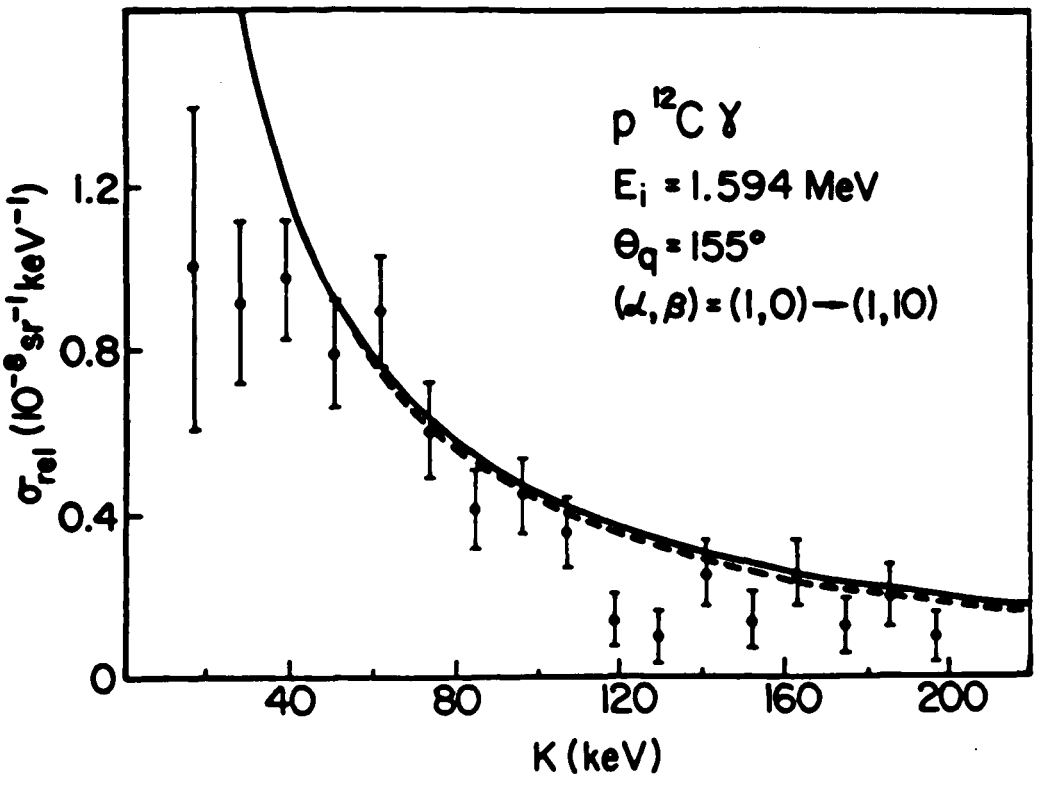

Fig.2 The relative $p^{12}C\gamma$ cross section σ_{rel} as a function of photon energy K at an incident proton energy of 1.594 MeV. The solid band represents the calculation using the amplitude $M_{\mu}^{\lambda}(s_{\alpha\beta}, t_o)$ in the OEOA approximation with (α,β) changing from (1,0) to (1,10) and the dashed band represents the calculation using the amplitude $M_{\mu}^{AB}(s_{\alpha\beta}, t_o)$ in the OEOA approximation with (α,β) changing from (1,0) to (1,10). The data are from Ref.10.

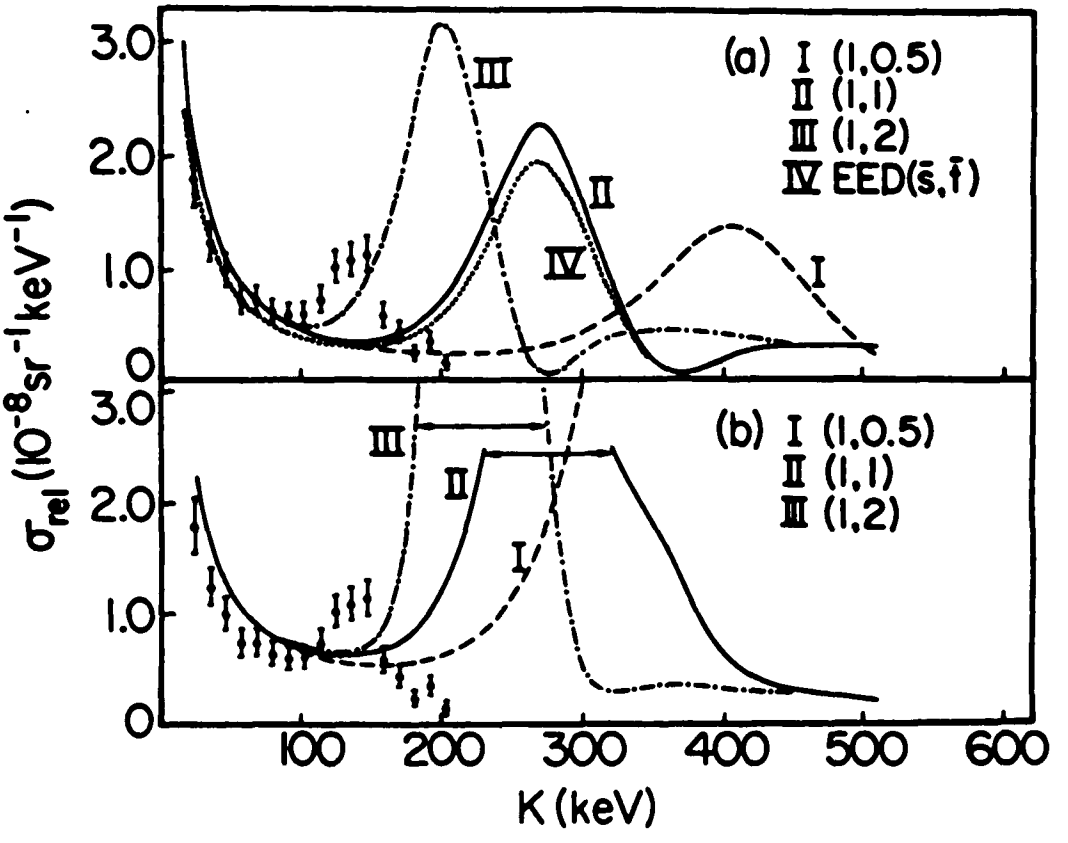

Fig.3 The relative $p^{12}C\gamma$ cross section σ_{rel} as a function of photon energy K at an incident proton energy of 1.880 MeV. Curves represent calculations using the amplitude (a) $M_{\mu}^{A}(s_{\alpha\beta},t_{o})$ in the OEOA approximation and $M_{\mu}^{A}(s,t)$ in the EED approximation and (b) $M_{\mu}^{AB}(s_{\alpha\beta},t_{o})$ in the OEOA approximation. The data are from Ref. 10.

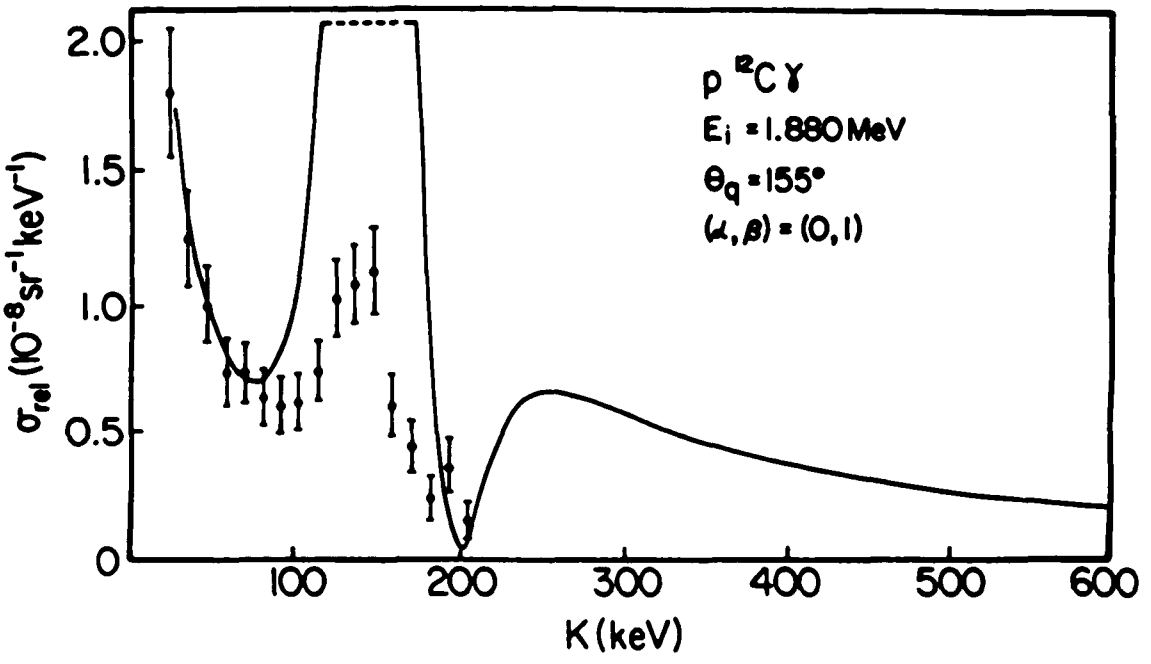

Fig.4 The relative $p^{12}C\gamma$ cross section σ_{rel} as a function of photon energy K at an incident proton energy of 1.880 MeV. The solid curve is calculated from the amplitude $M^{A}_{\mu}(s_{\alpha\beta}, t_o)$ in the OEOA approximation with $(\alpha,\beta)=(0,1)$ so that $(\alpha+\beta)/\beta=1$. The data are from Ref.*10*.

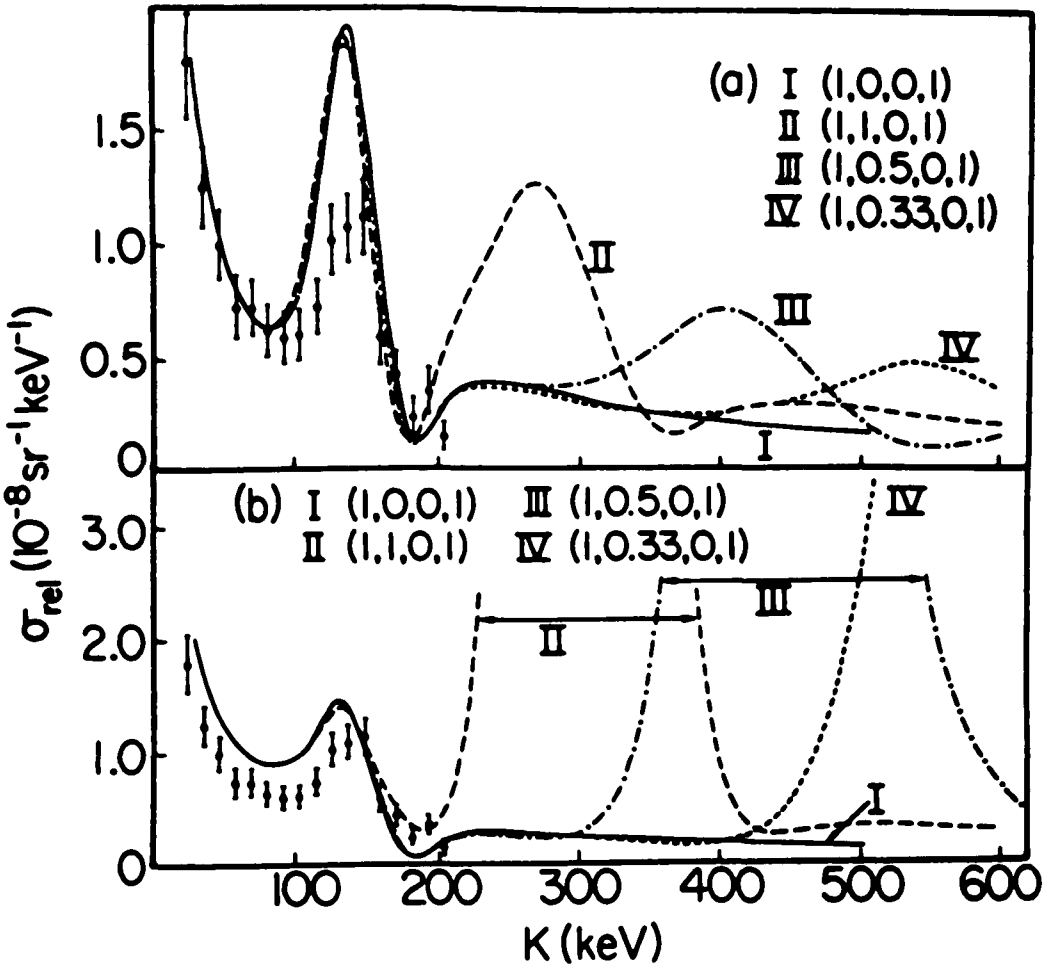

Fig.5 Relative $p^{12}C\gamma$ cross section σ_{rel} as a function of photon energy K at an incident proton energy of 1.880 MeV. Curves represent calculations using the amplitude (a) $M_{\mu}^{A}(s_{\alpha_1\beta_1}, s_{\alpha_2\beta_2}, t_o)$ in the TEOA approximation and (b) $M_{\mu}^{AB}(s_{\alpha_1\beta_1}, s_{\alpha_2\beta_2}, t_o)$ in the TEOA approximation. The data are from Ref.*10*.

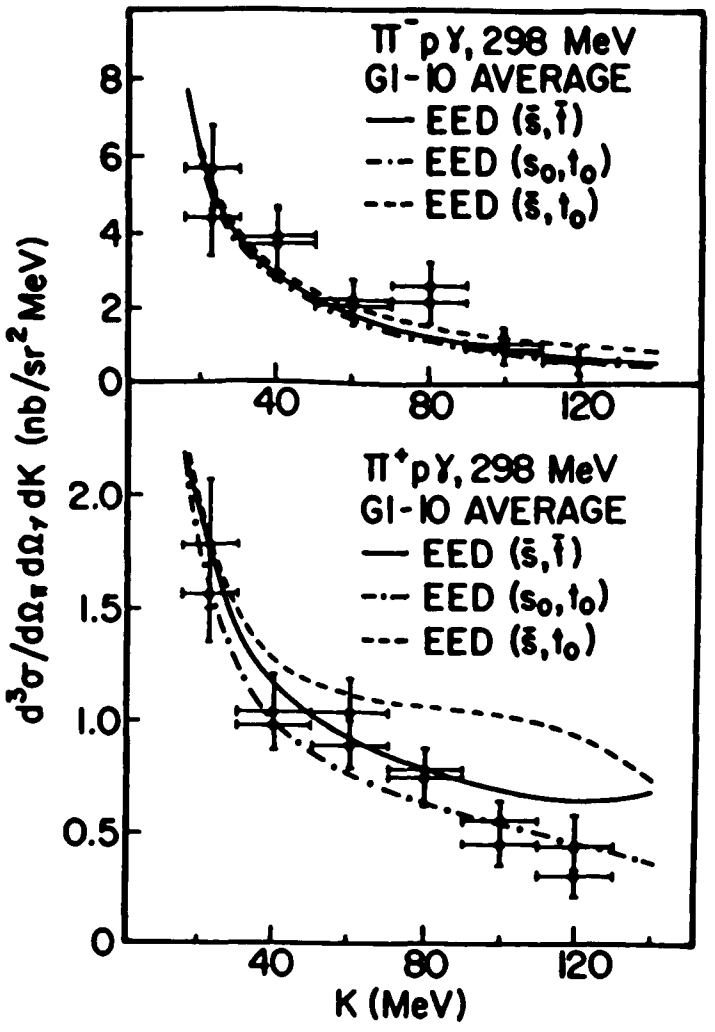

Fig.6 A comparison of EED predictions (the average cross section over the ten photon counters G1 to G10) with the $\pi^{\pm}p\gamma$ data at 298 MeV. The solid curves represent the results of calculation using Eq.(B1) with the elastic $\pi^{\pm}p$ cross section evaluated at (s,t). The dash-dotted curves and the dashed curves are also calculated from Eq.(B1) but with the elastic $\pi^{\pm}p$ cross section evaluated at (s_o,t_o) and (s,t_o), respectively. The average experimental data are from Ref.2.

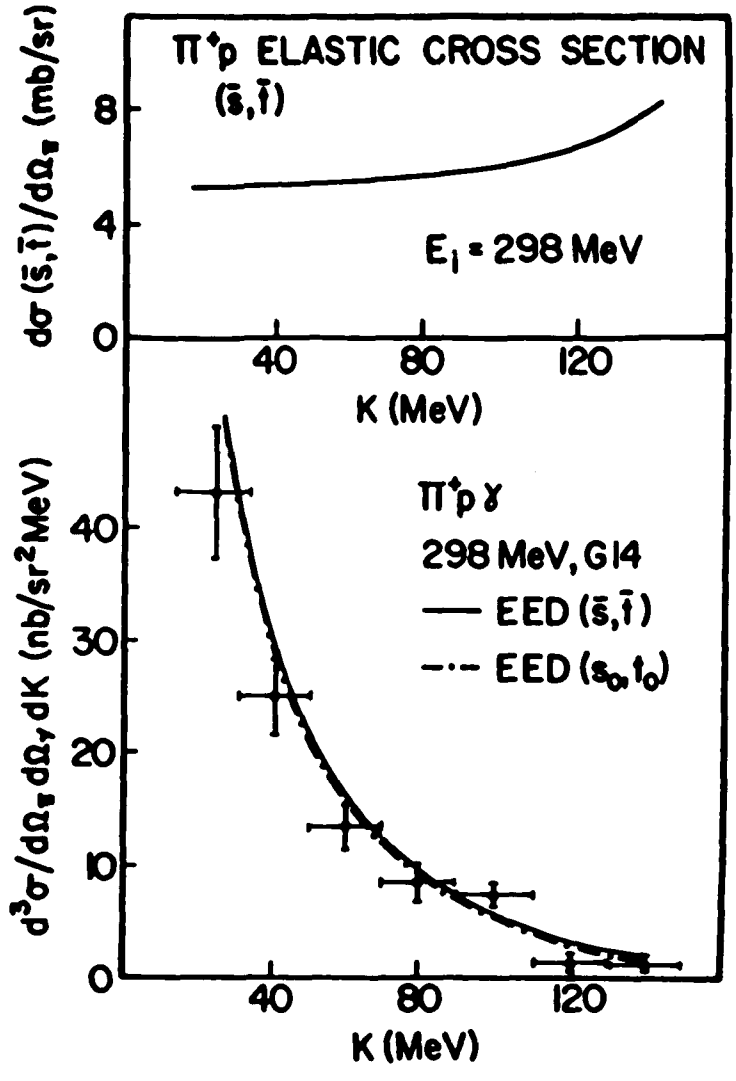

Fig.7 (Top): The π^+p elastic cross section, evaluated at $(\bar{s},\bar{t})$, as a function of photon energy K at an incident pion energy of 298 MeV. (Bottom): The $\pi^+p\gamma$ cross section as a function of photon energy K at 298 MeV for the photon counter G14. The solid curve represents the result of EED calculation using Eq.(B1) with the elastic π^+p cross section evaluated at $(\bar{s},\bar{t})$. (This elastic cross section is shown in the top figure.) The dash-dotted curve represents the same calculation but with the elastic π^+p cross section evaluated at (s_o,t_o). The experimental $\pi^+p\gamma$ data are from Ref.2.

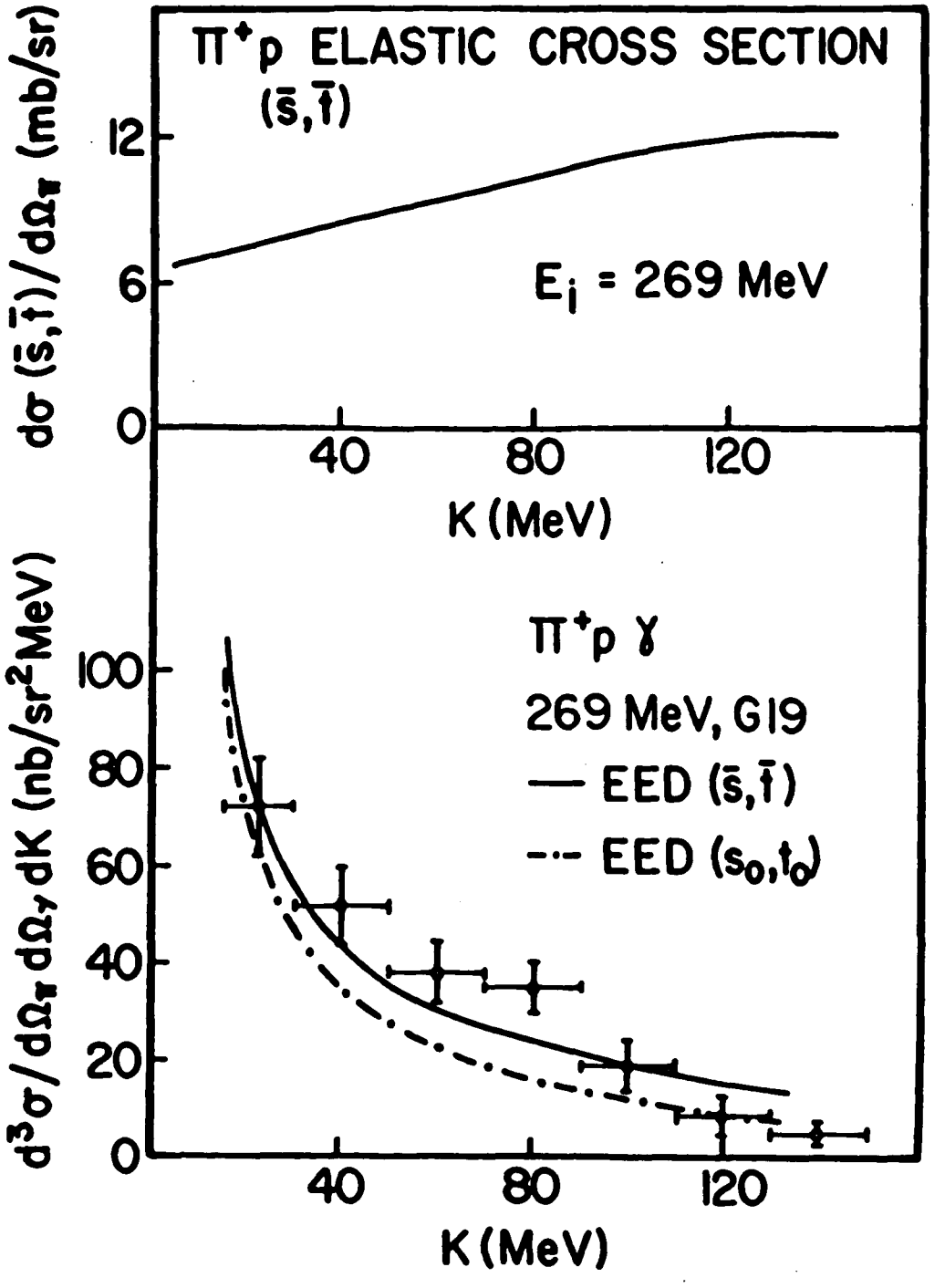

Fig.8 Same as Fig.7 but at 269 MeV for G19.

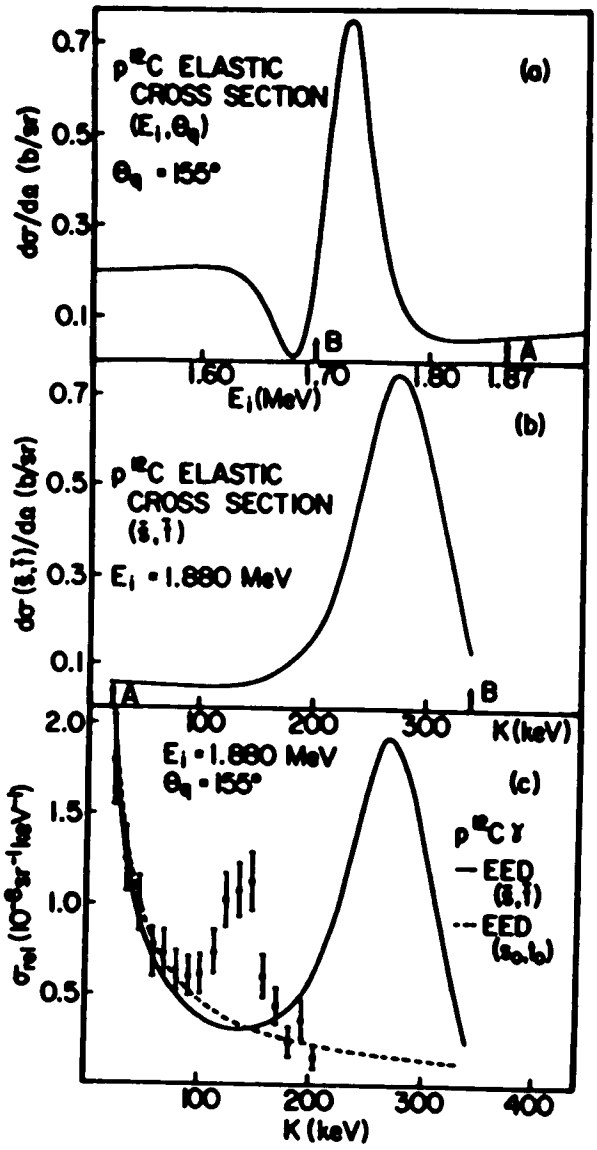

Fig.9 (a) The $p^{12}C$ elastic cross section as a function of incident proton energy E_i for $\theta_q = 155^\circ$

(b) The $p^{12}C$ elastic scattering cross section, evaluated at (s,t), as a function of photon energy K at an incident proton energy of 1.880 MeV. Every point between the arrows A and B on this curve (cross section) corresponds to a point between A and B on the curve shown in (a). Note that the cross section in (a) is plotted as a function of E_i while the cross section in (b) is plotted as a function of K (since s is a function of K).

(c) A comparison of EED predictions with the $p^{12}C\gamma$ data at 1.880 MeV for $\theta_q = 155^\circ$. The solid curve represents the result of EED calculation using Eq.(B1) with the elastic $p^{12}C$ cross section evaluated at (s,t). (This elastic $p^{12}C$ cross section is shown in (b).) The dashed curve represents the same calculation but with the elastic $p^{12}C$ cross section evaluated at (s_o, t_o). The experimental data are from Ref.10.

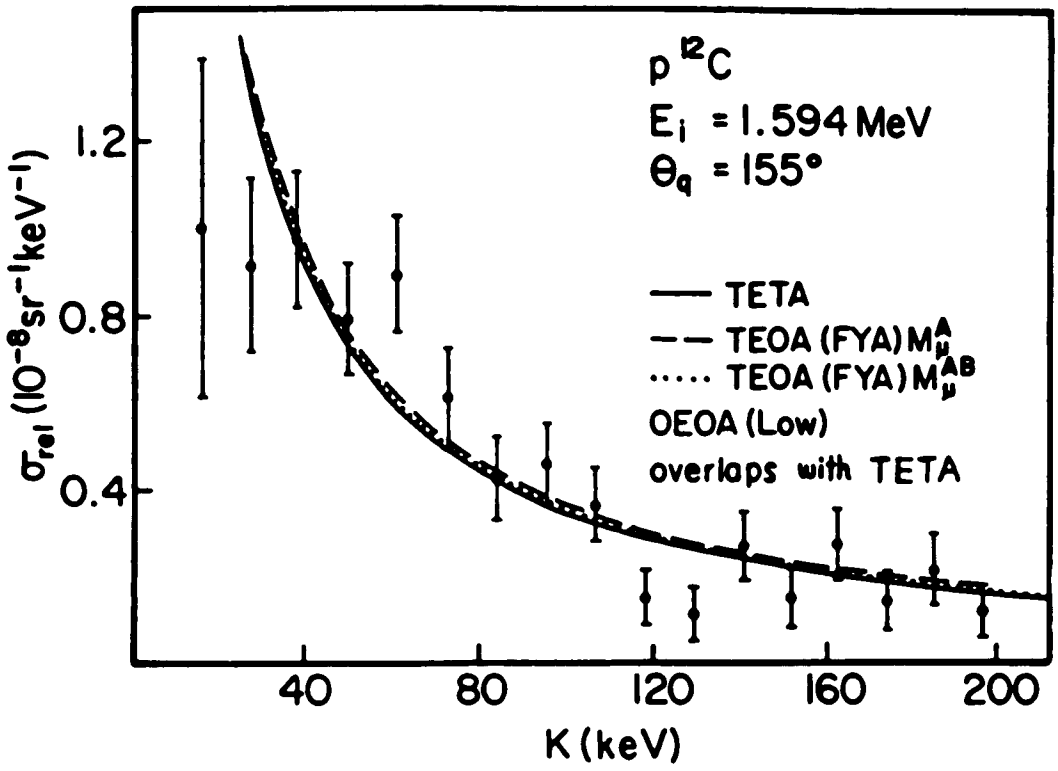

Fig.10 The relative $p^{12}C\gamma$ cross section σ_{rel} as a function of photon energy K at an incident proton energy of 1.594 MeV. The solid curve represents the calculation using TETA, The dashed curve represents the calculation using the amplitude $M_{\mu}^{A}(s_i, s_f, t_o)$ in the TEOA appaoximation and the dotted curve represents the calculation using the amplitude $M_{\mu}^{AB}(s_i, s_f, t_o)$ in the TEOA approximation. The curve calculated in Low's original OEOA overlaps with the solid curve. The data are from Ref.*10*.

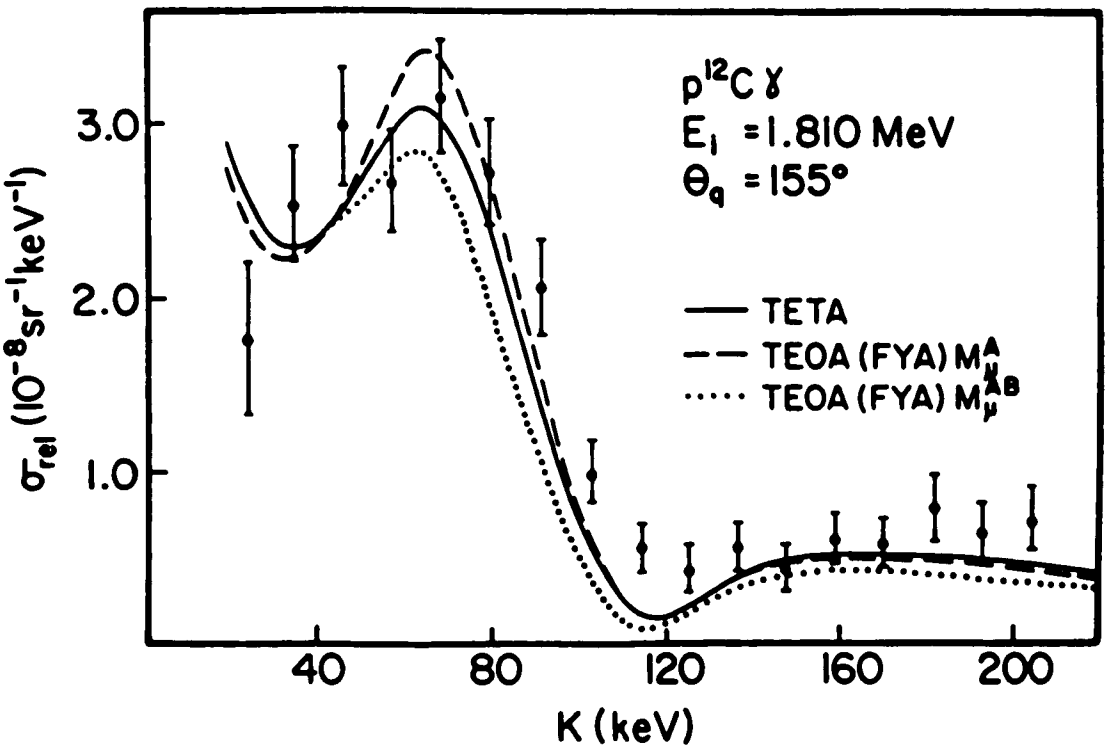

Fig.11 The relative $p^{12}C\gamma$ cross section σ_{rel} as a function of photon energy K at an incident proton energy of 1.810 MeV. Curves represent calculations using the amplitude $M_\mu^A(s_i,s_f,t_p,t_q)$ given by Eq.(39) in TETA, $M_\mu^A(s_i,s_f,t_o)$ in TEOA and $M_\mu^{AB}(s_i,s_f,t_o)$ in TEOA. The data are from Ref.*10*.

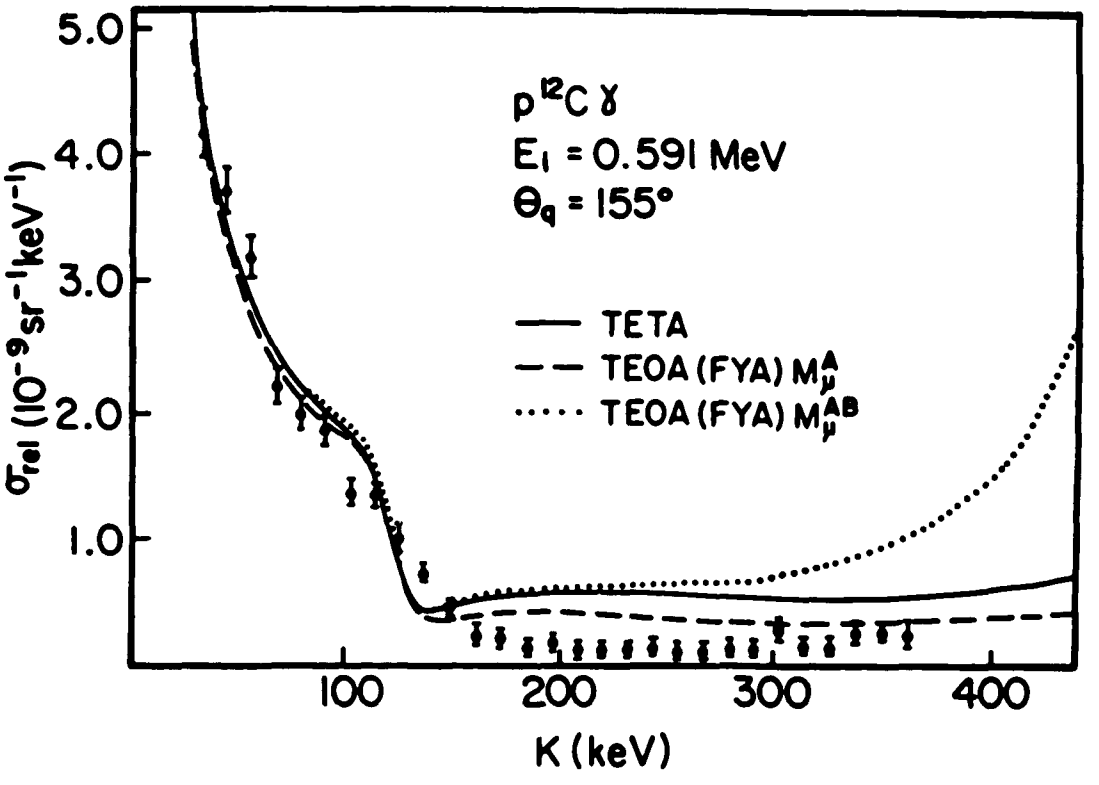

Fig.12 Same as Fig.11 but at an incident proton energy of 0.591 MeV.

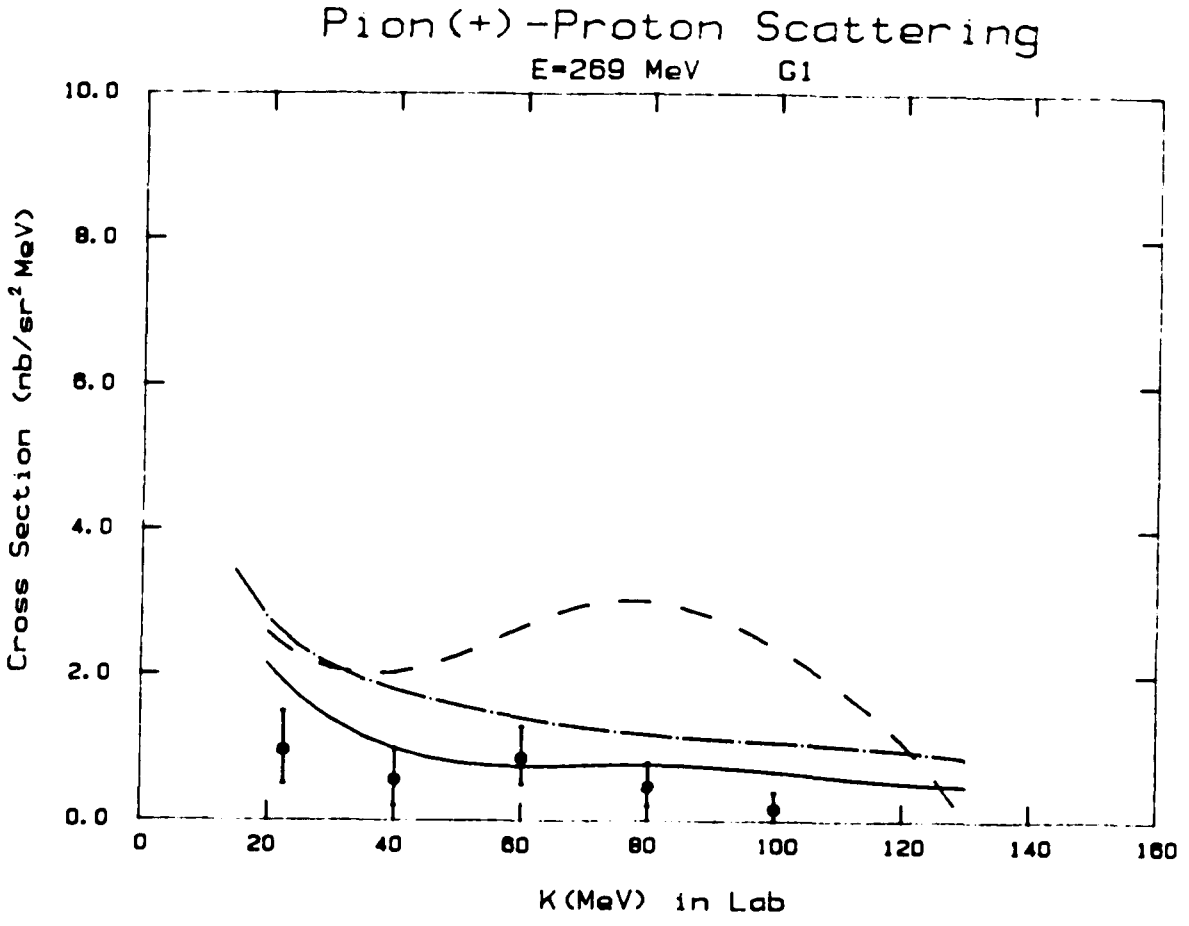

Fig.13 The $\pi^+ p\gamma$ cross section as a function of photon energy K at 269 MeV for the photon counter G1. The solid curve represents the result of calculation using the TETA amplitude given by Eq.(38). The dash-dotted curve represents the result of calculation using the amplitude $M_\mu^A(s_i, s_f, t_o)$ in TEOA and the dashed curve represents the result of calculation using the amplitude $M_\mu^{AB}(s_i, s_f, t_o)$ in TEOA. The experimental $\pi^+ p\gamma$ data are from Ref.2.

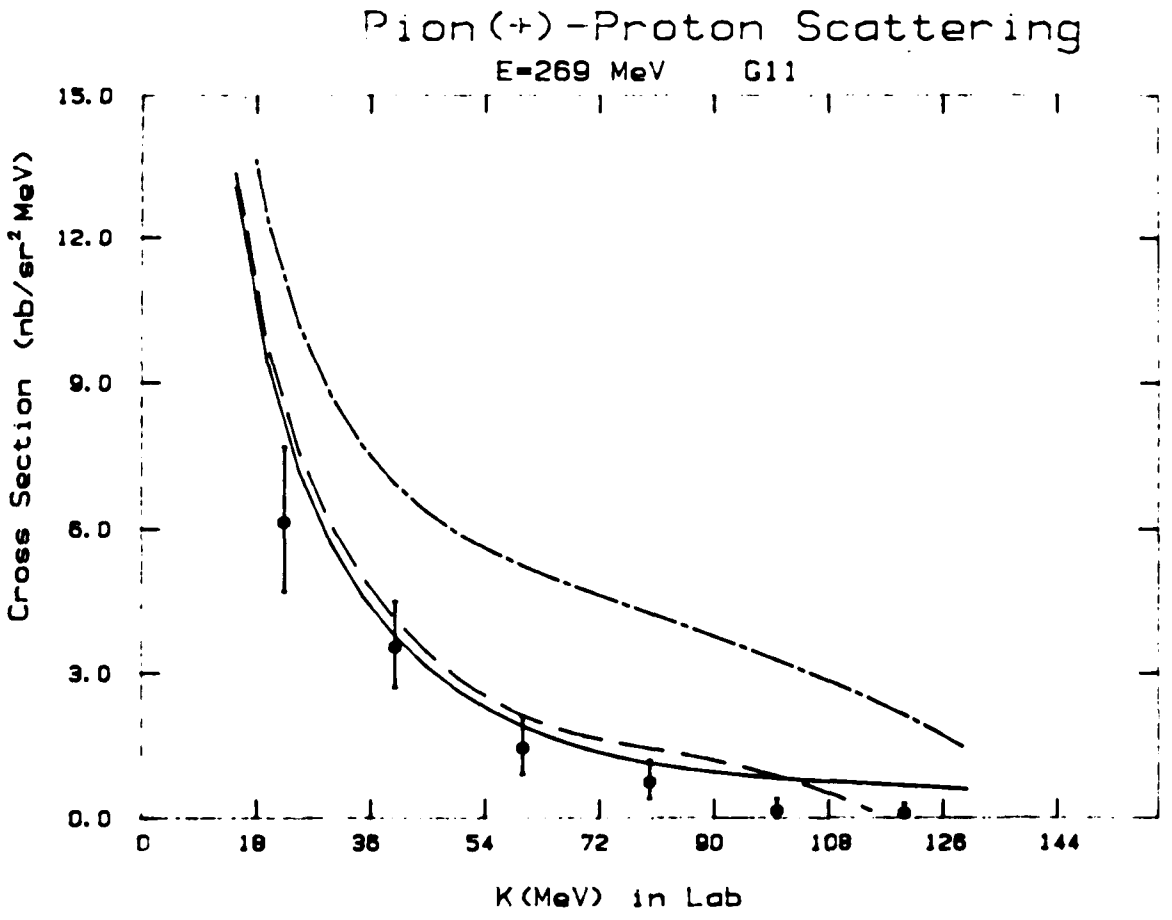

Fig.14 Same as Fig.13 but for the photon counter G11.

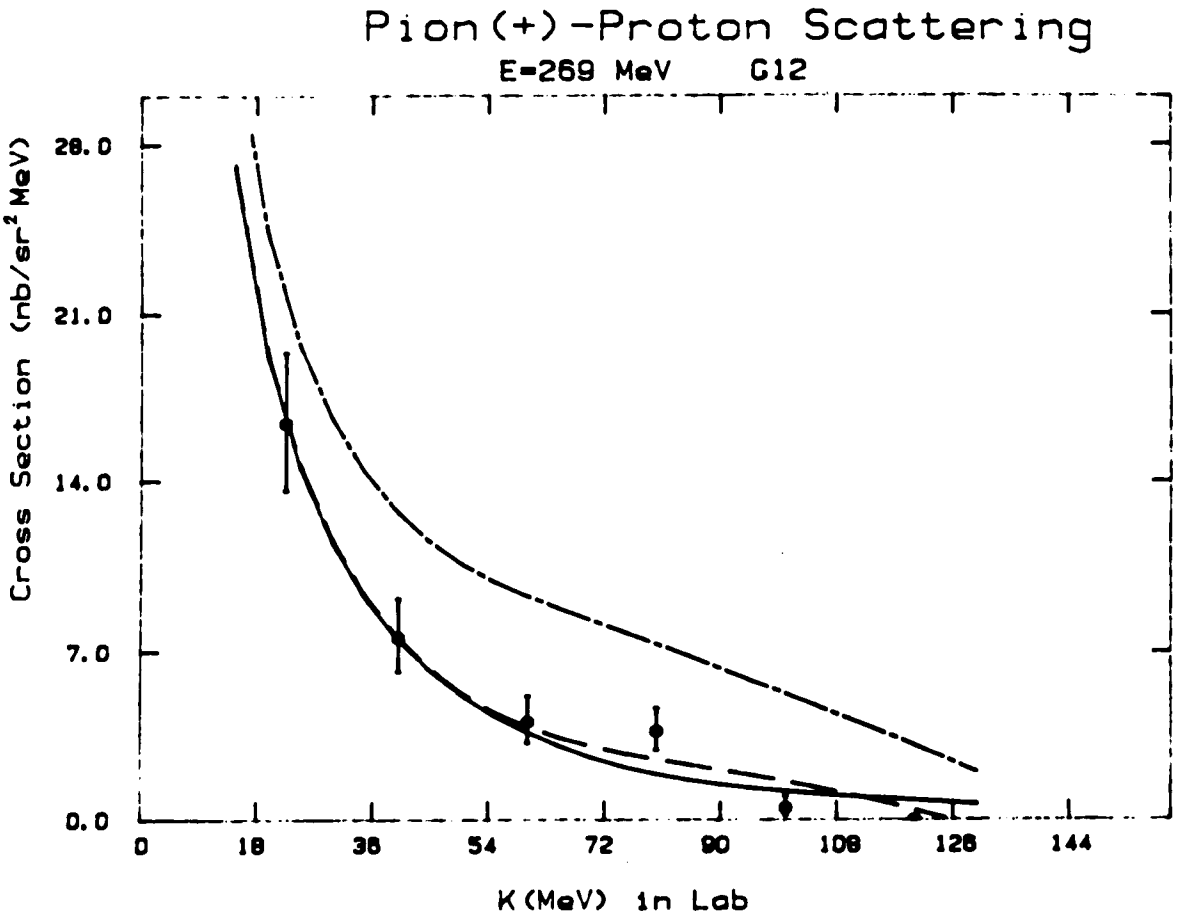

Fig.15 Same as Fig.13 but for the photon counter G12.

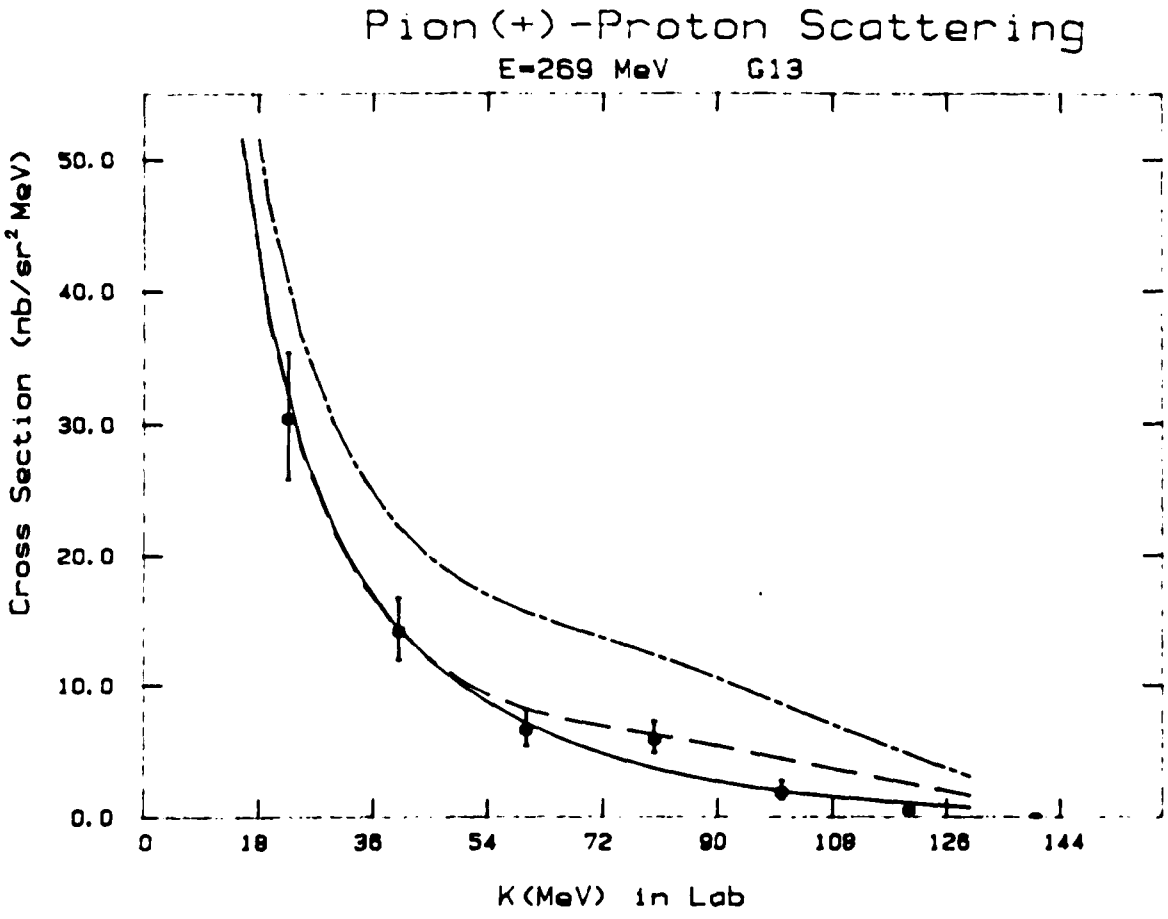

Fig.16 Same as Fig.13 but for the photon counter G13.

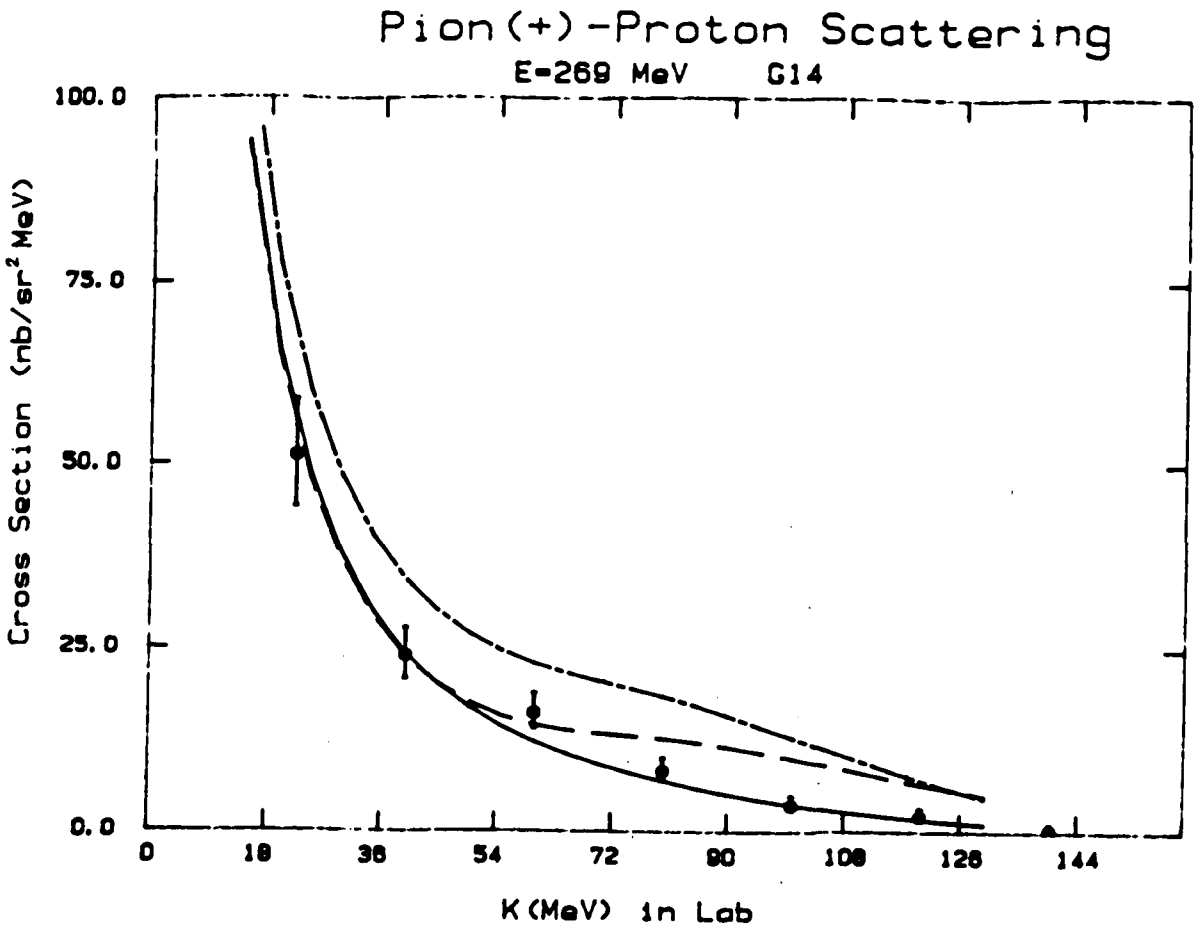

Fig.17 Same as Fig.13 but for the photon counter G14.

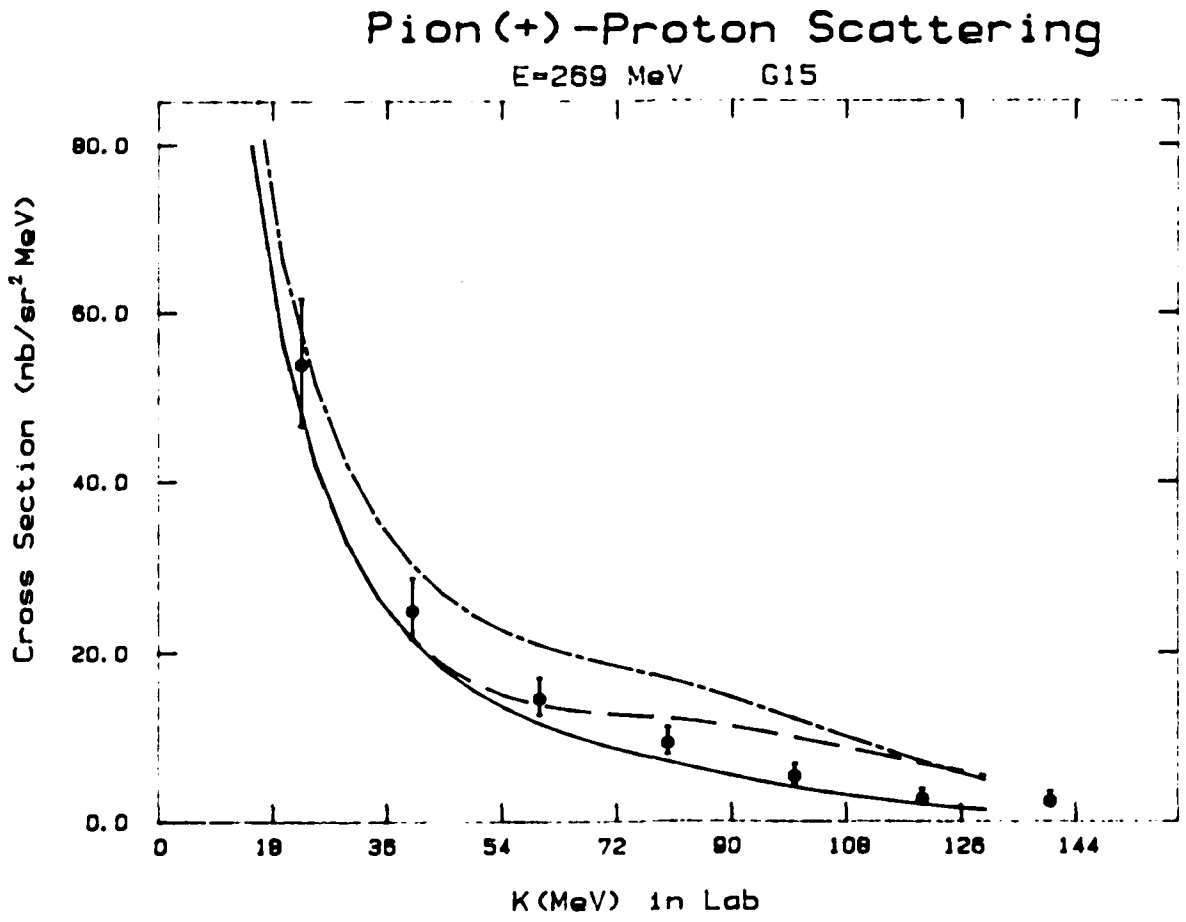

Fig.18 Same as Fig.13 but for the photon counter G15.

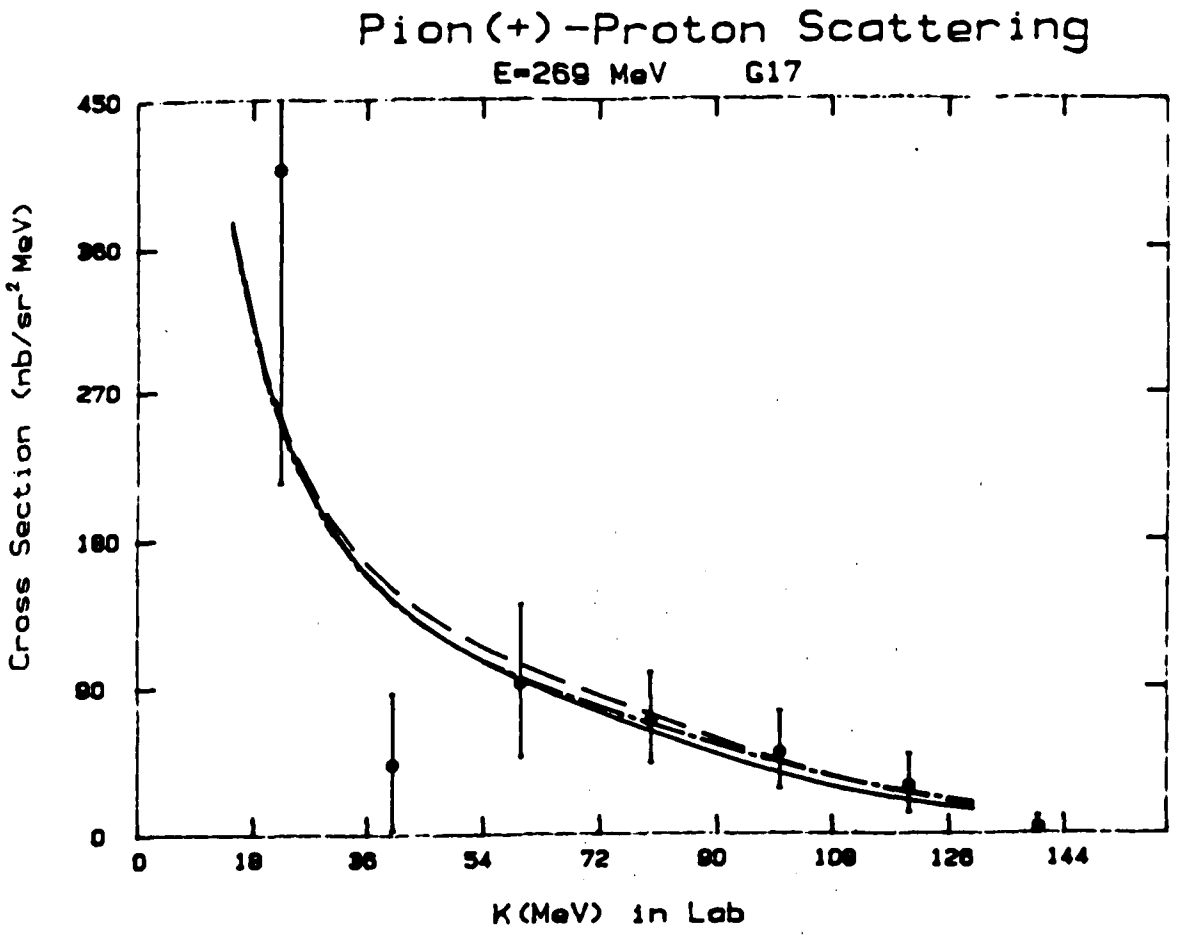

Fig.19 Same as Fig.13 but for the photon counter G17.

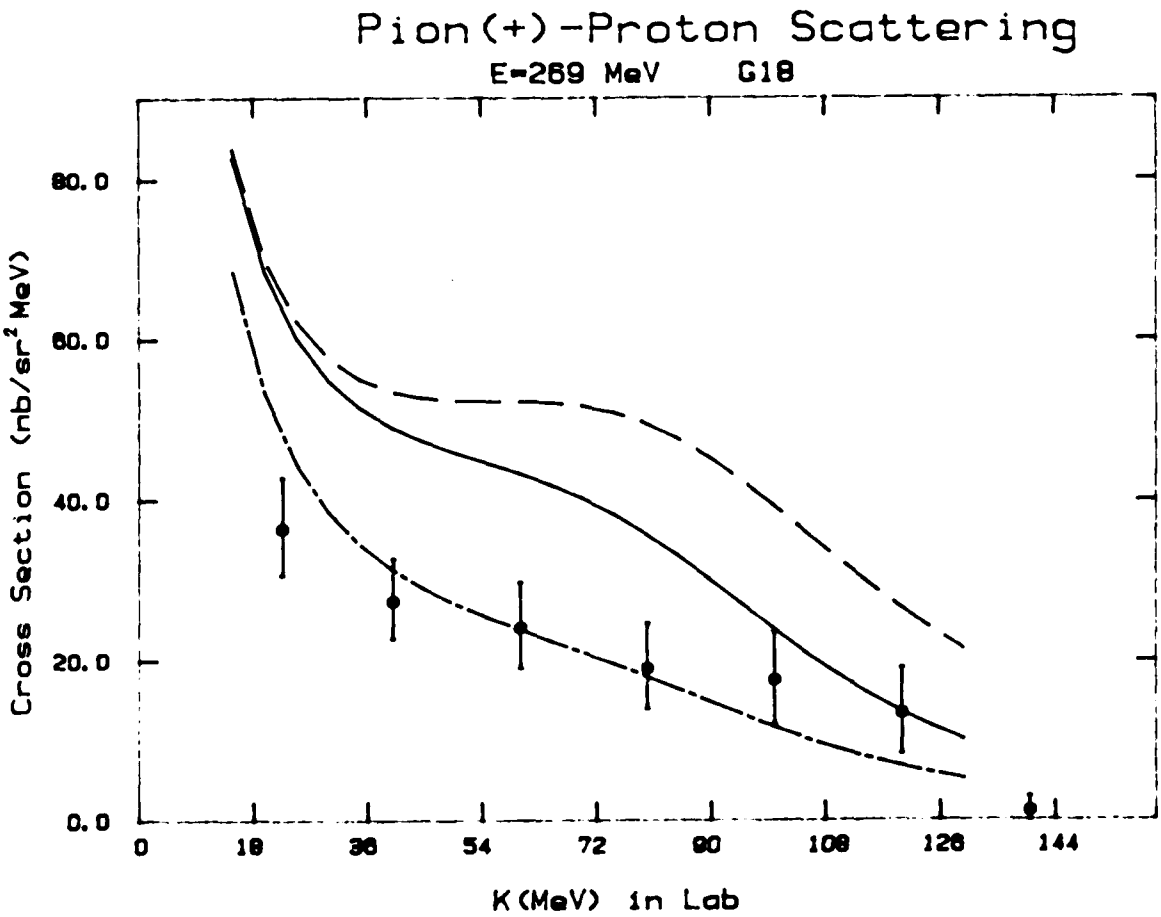

Fig.20 Same as Fig.13 but for the photon counter G18.

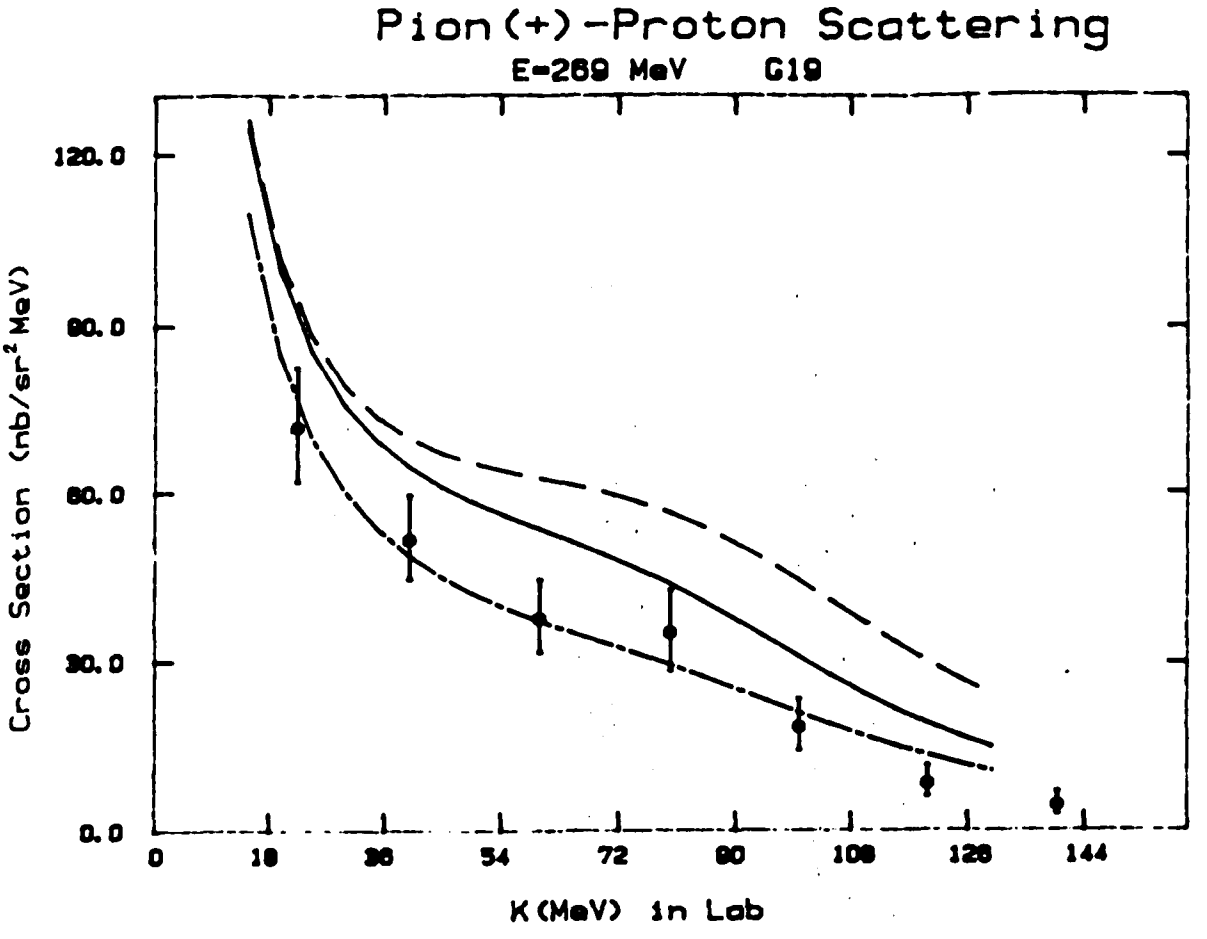

Fig.21 Same as Fig.13 but for the photon counter G19.

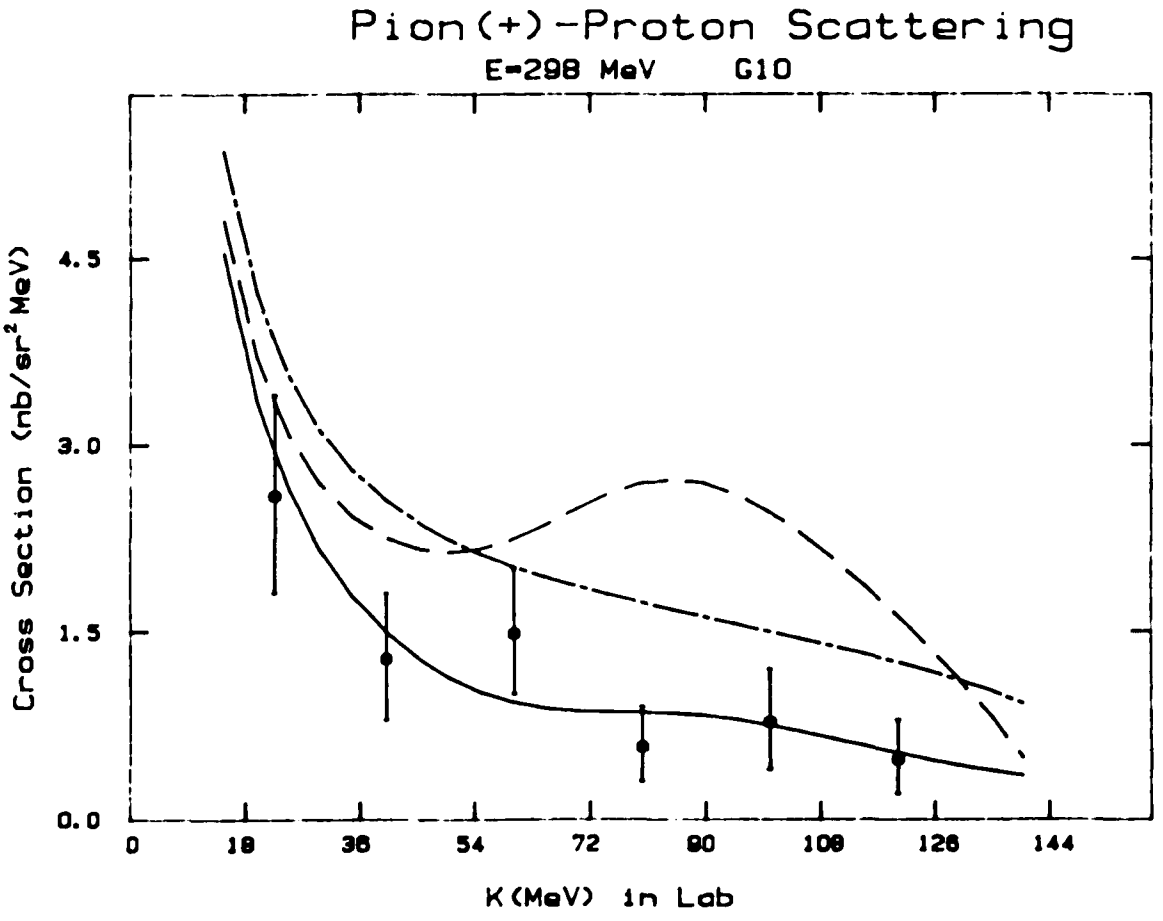

Fig.22 Same as Fig.13 but at 298 MeV for the photon counter G10.

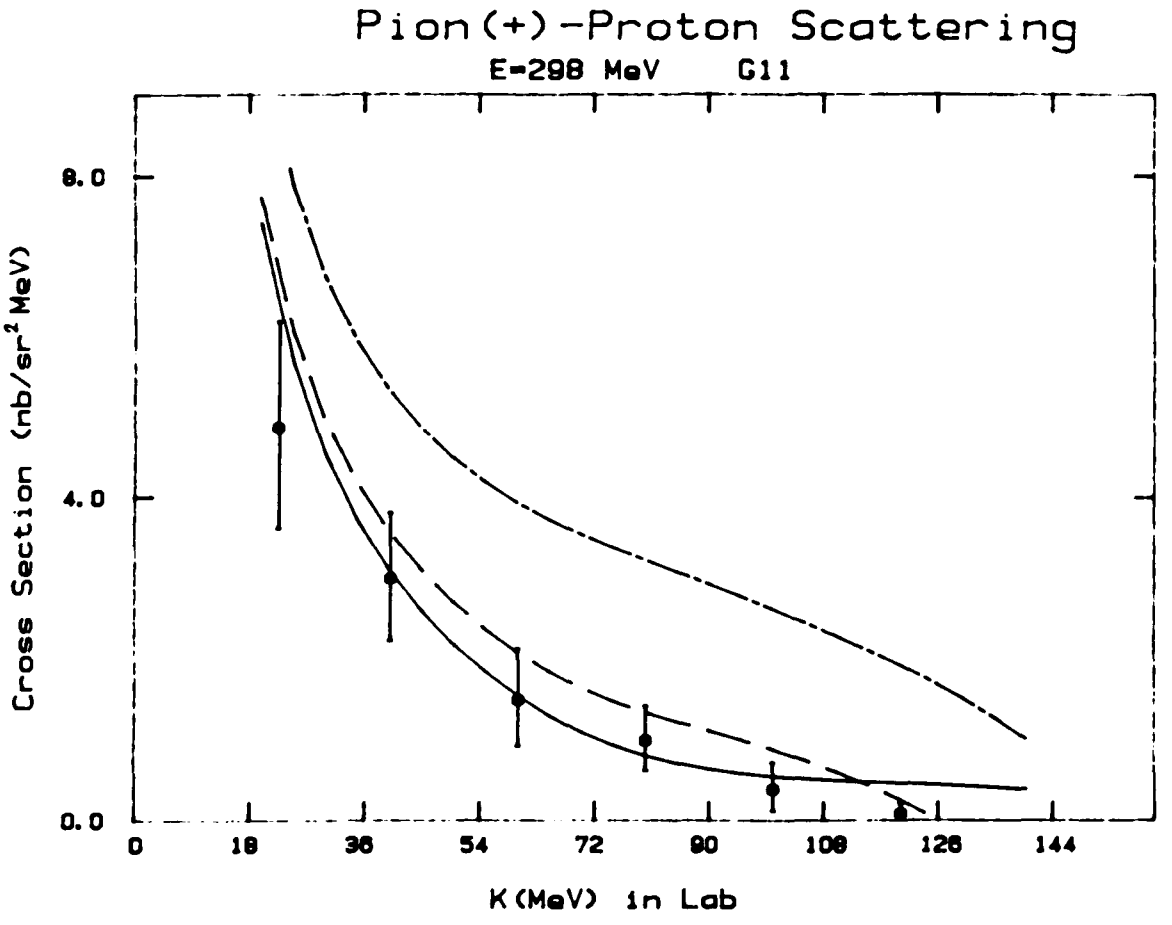

Fig.23 Same as Fig.13 but at 298 MeV for the photon counter G11.

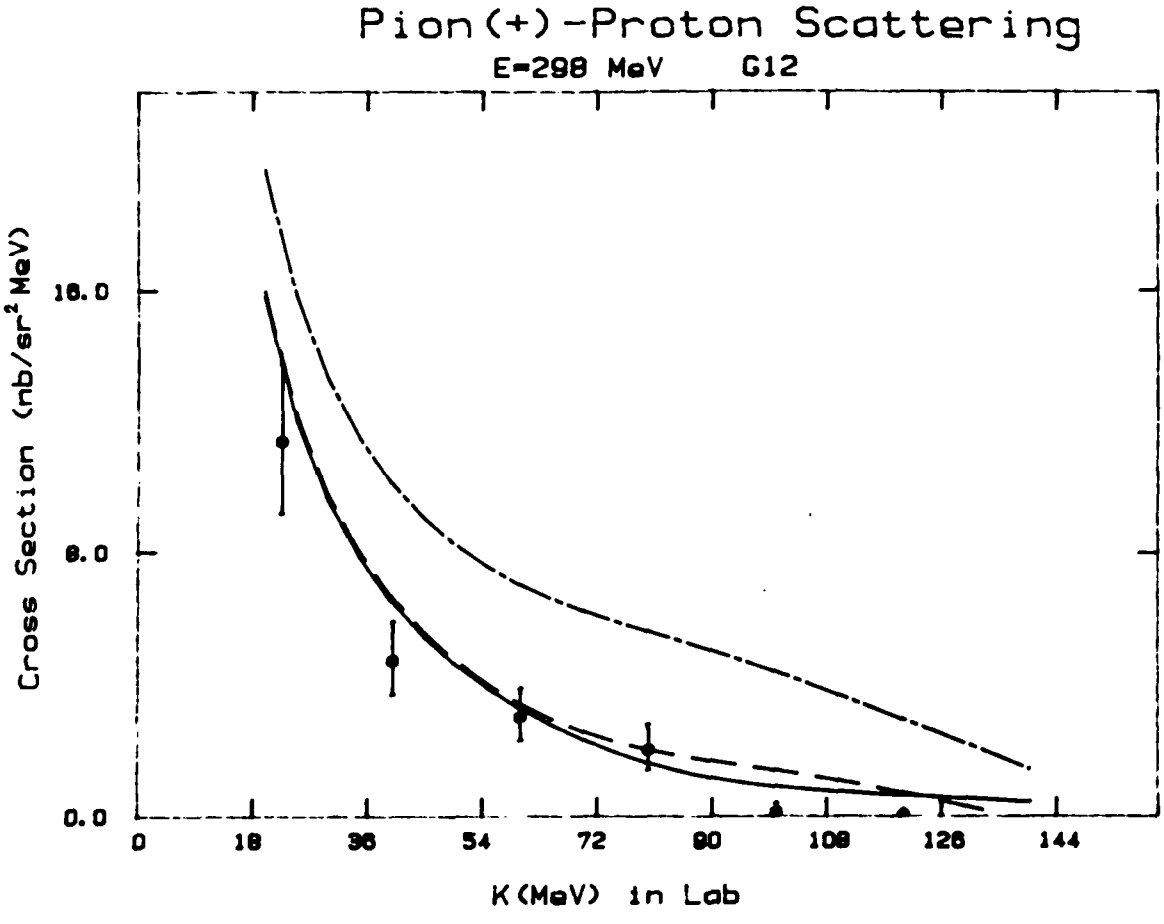

Fig.24 Same as Fig.13 but at 298 MeV for the photon counter G12.

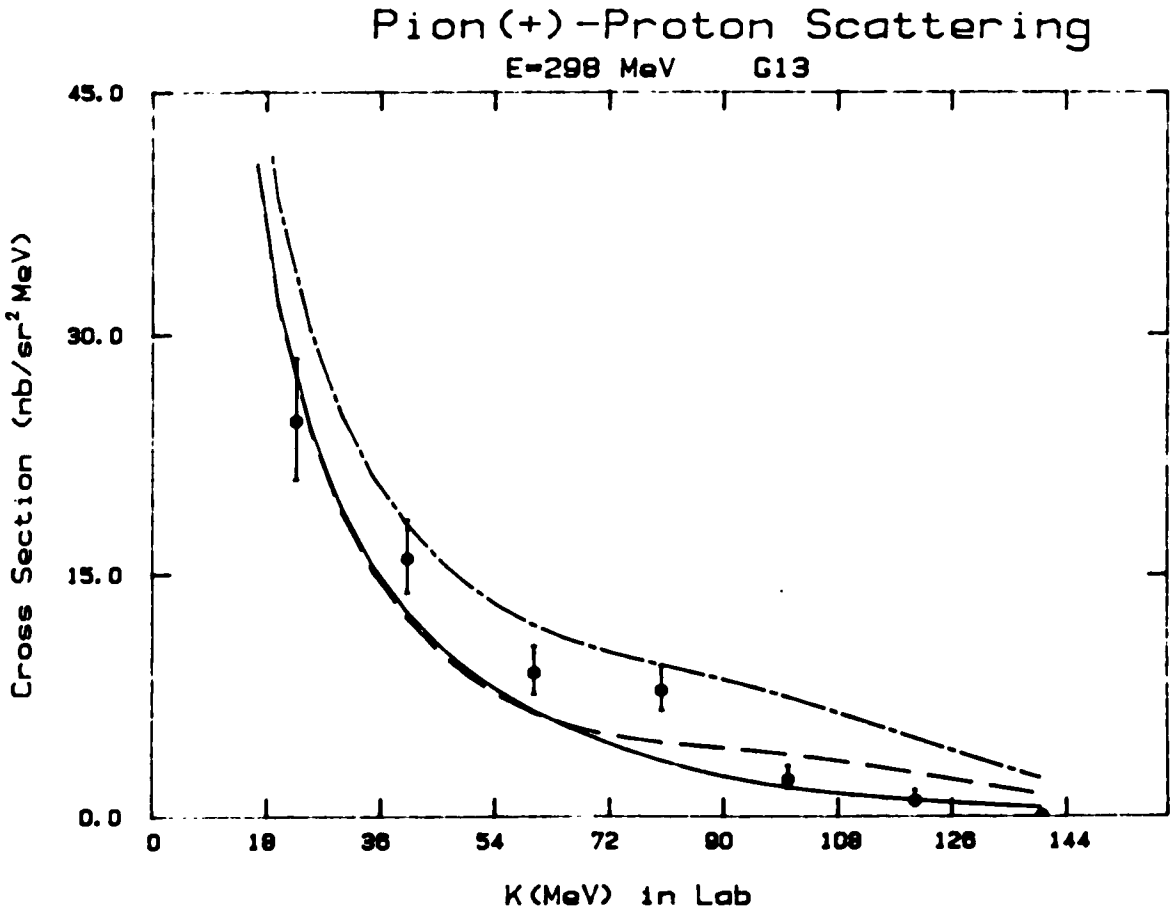

Fig.25 Same as Fig.13 but at 298 MeV for the photon counter G13.

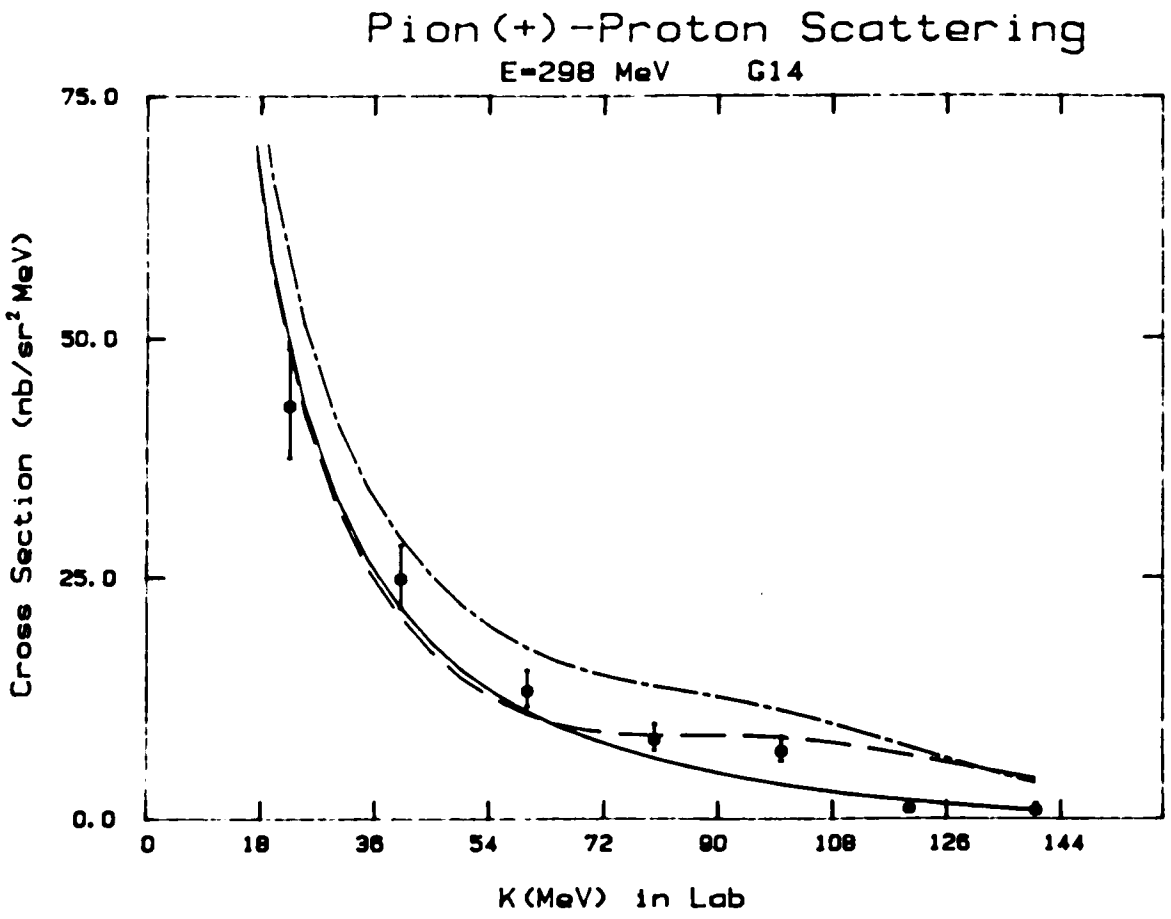

Fig.26 Same as Fig.13 but at 298 MeV for the photon counter G14.

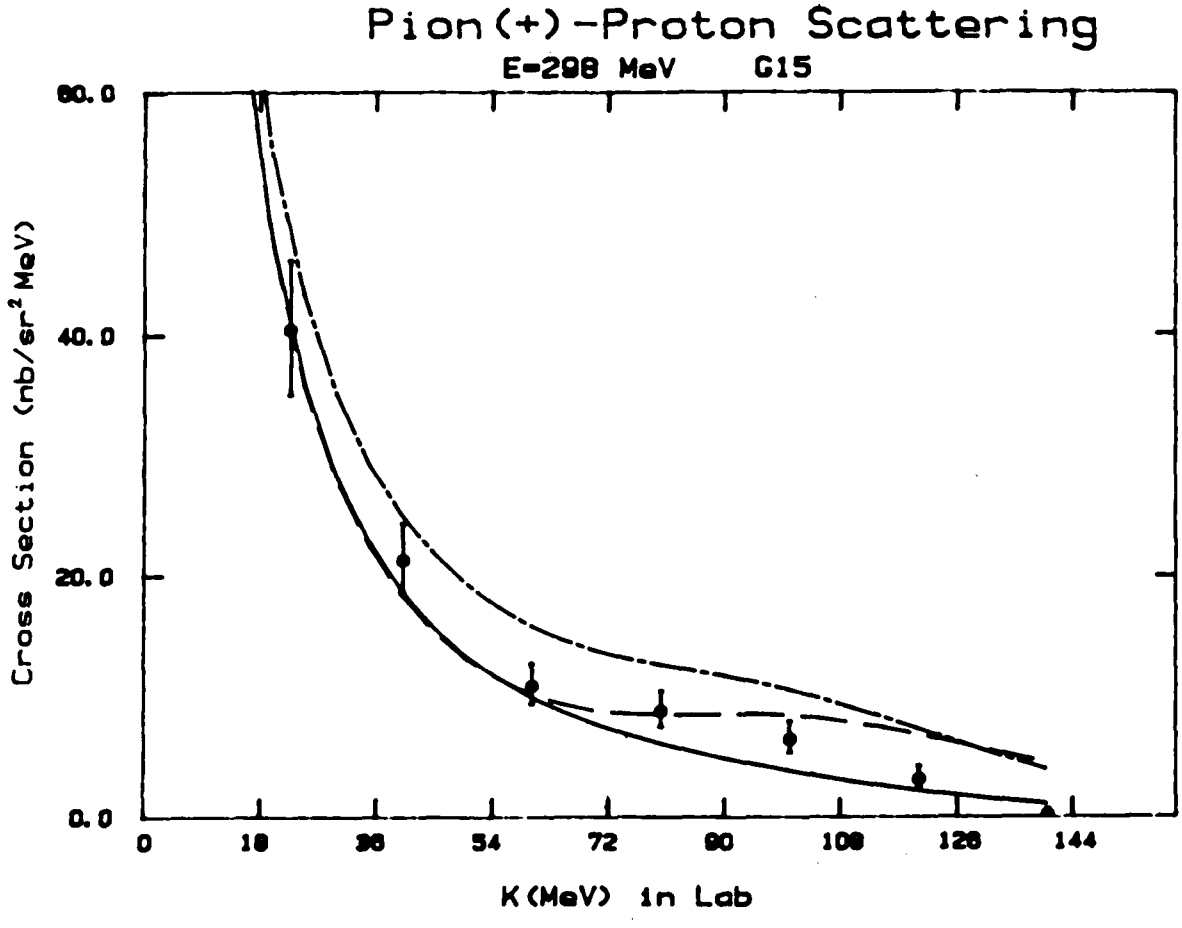

Fig.27 Same as Fig.13 but at 298 MeV for the photon counter G15.

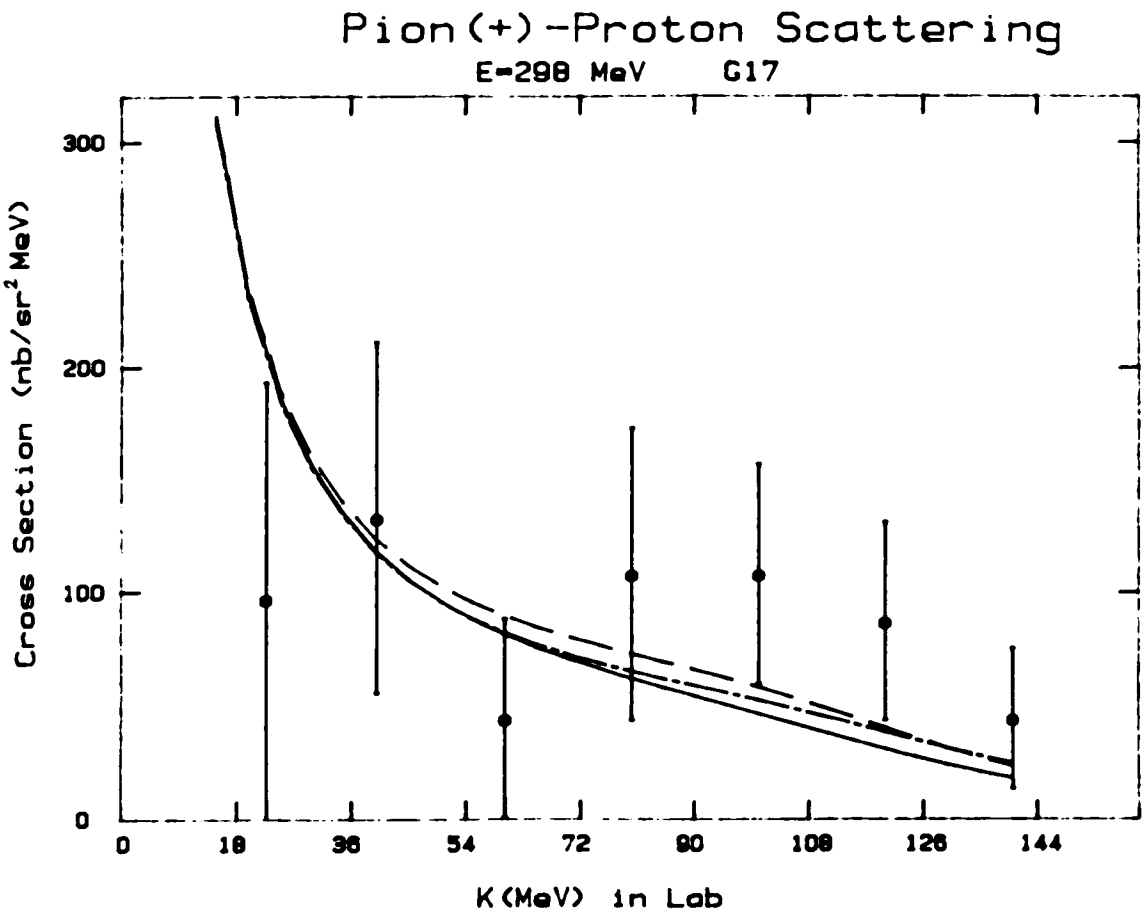

Fig.28 Same as Fig.13 but at 298 MeV for the photon counter G17.

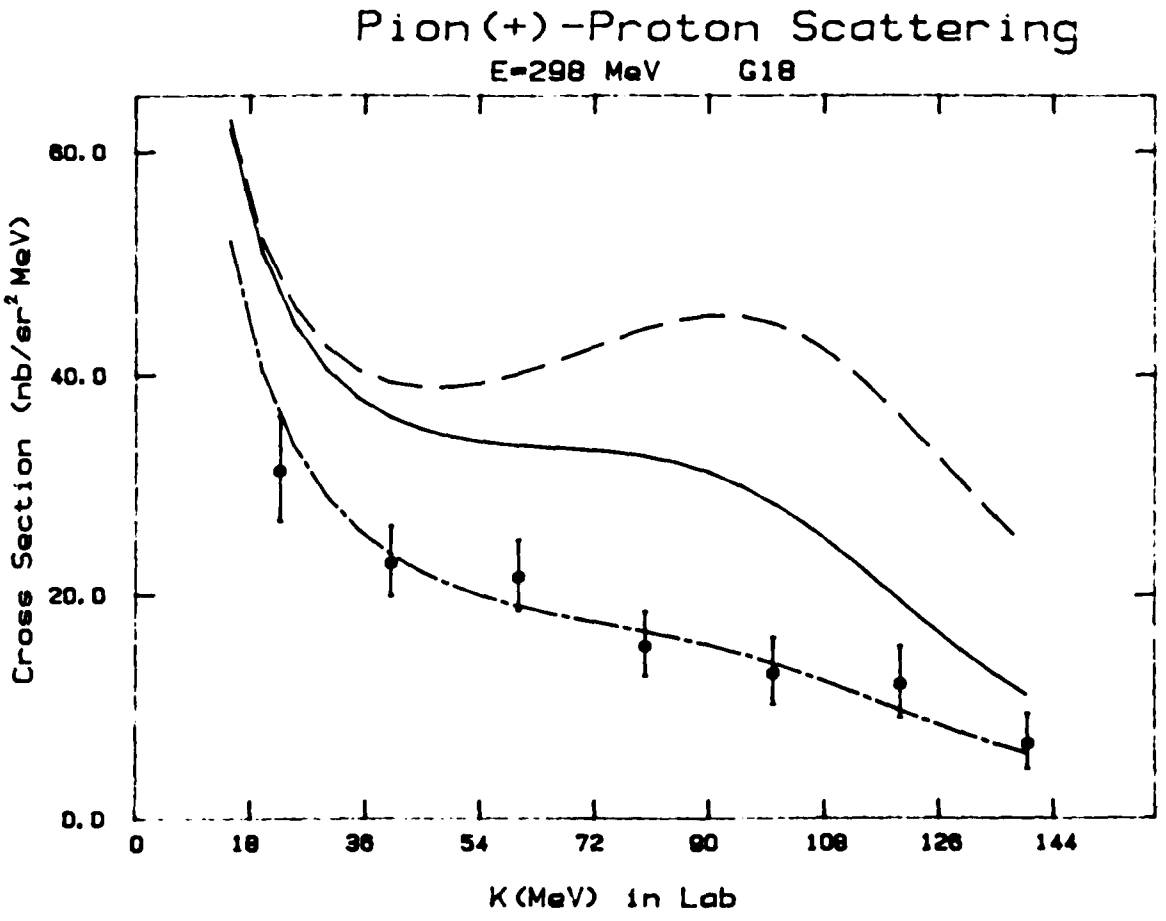

Fig.29 Same as Fig.13 but at 298 MeV for the photon counter G18.

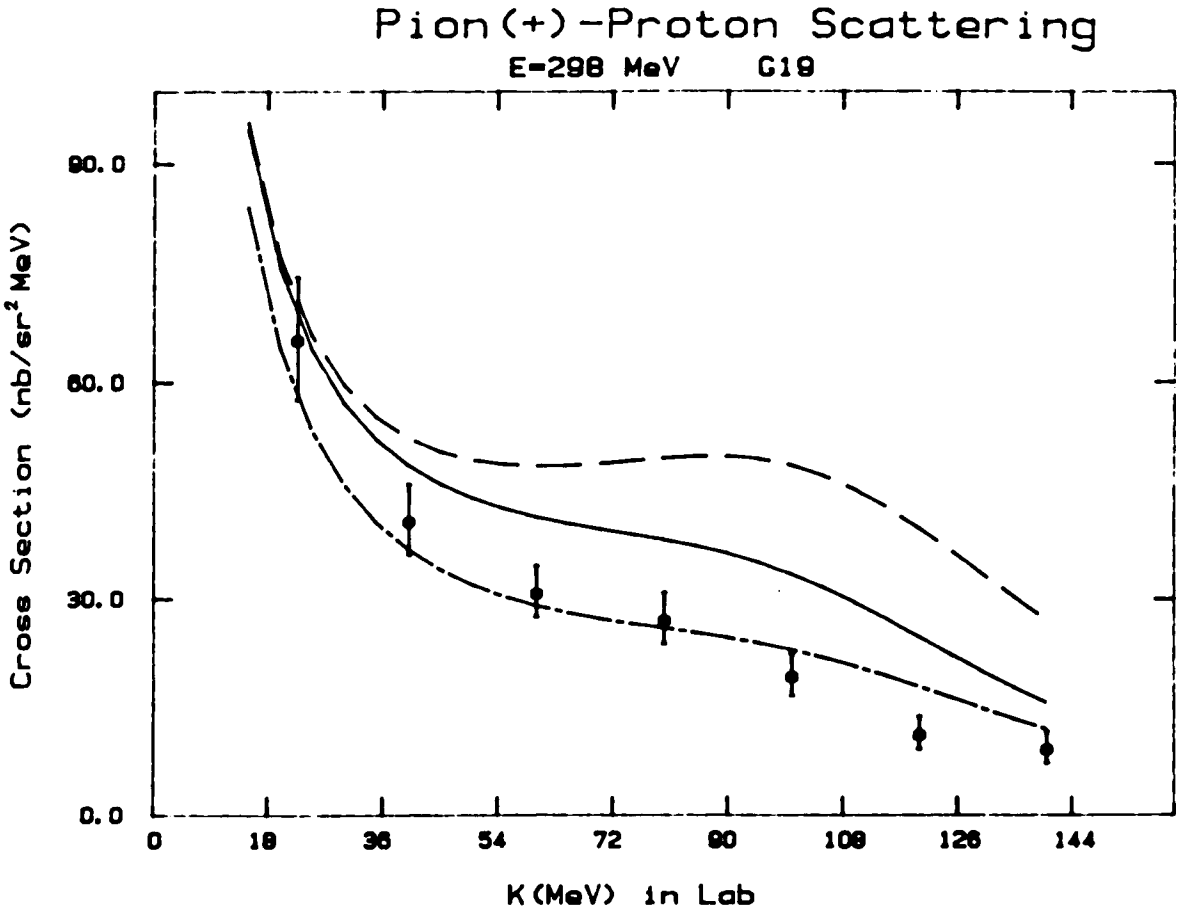

Fig.30 Same as Fig.13 but at 298 MeV for the photon counter G19.

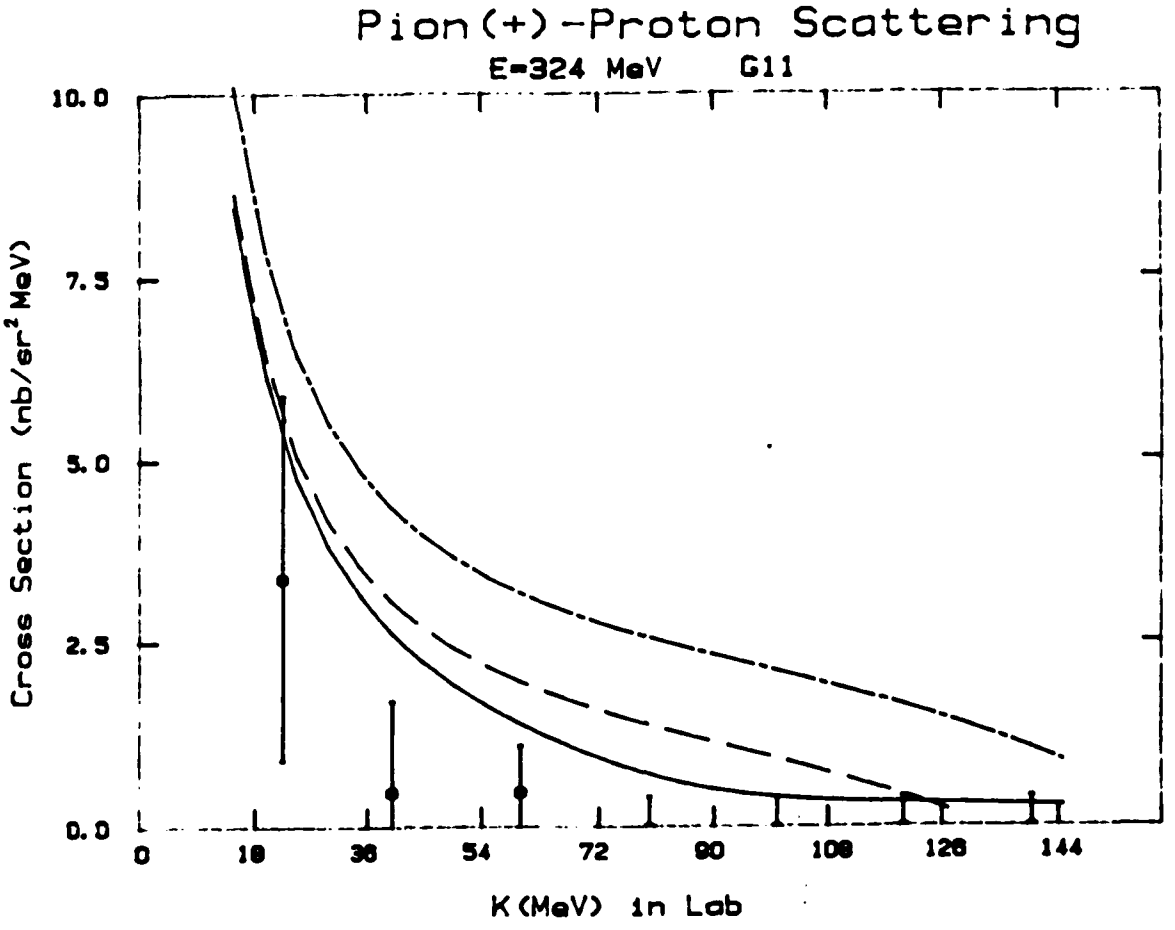

Fig.31 Same as Fig.13 but at 324 MeV for the photon counter G11.

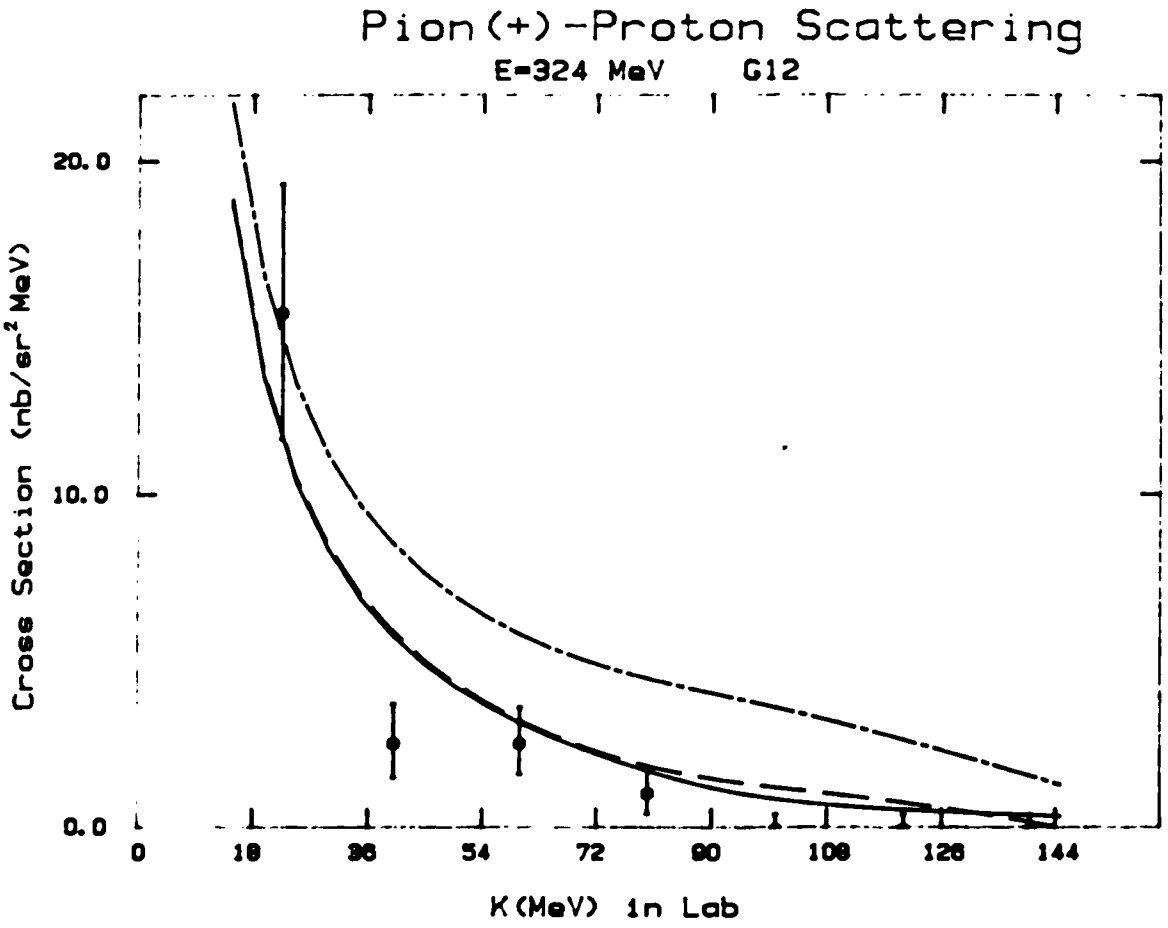

Fig.32 Same as Fig.13 but at 324 MeV for the photon counter G12.

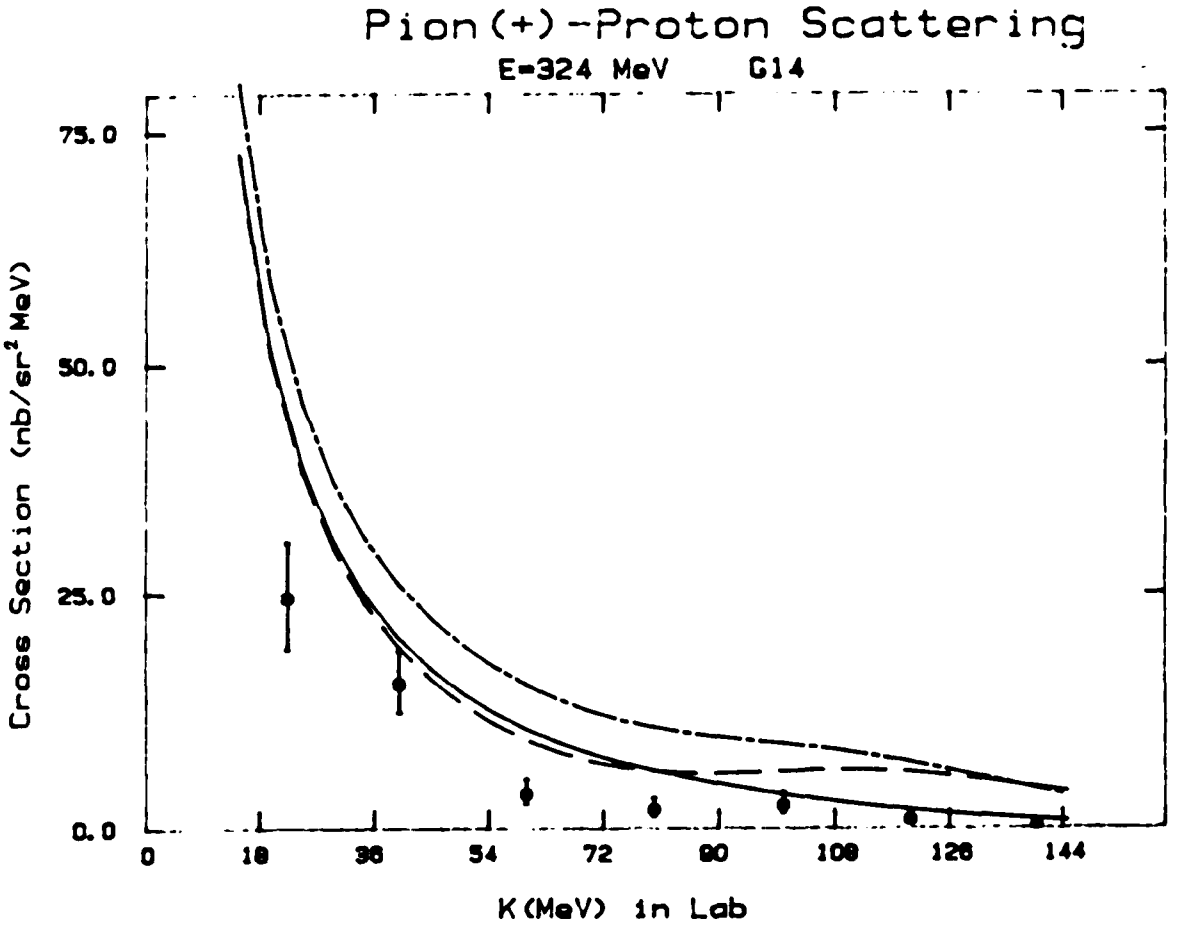

Fig.33 Same as Fig.13 but at 324 MeV for the photon counter G14.

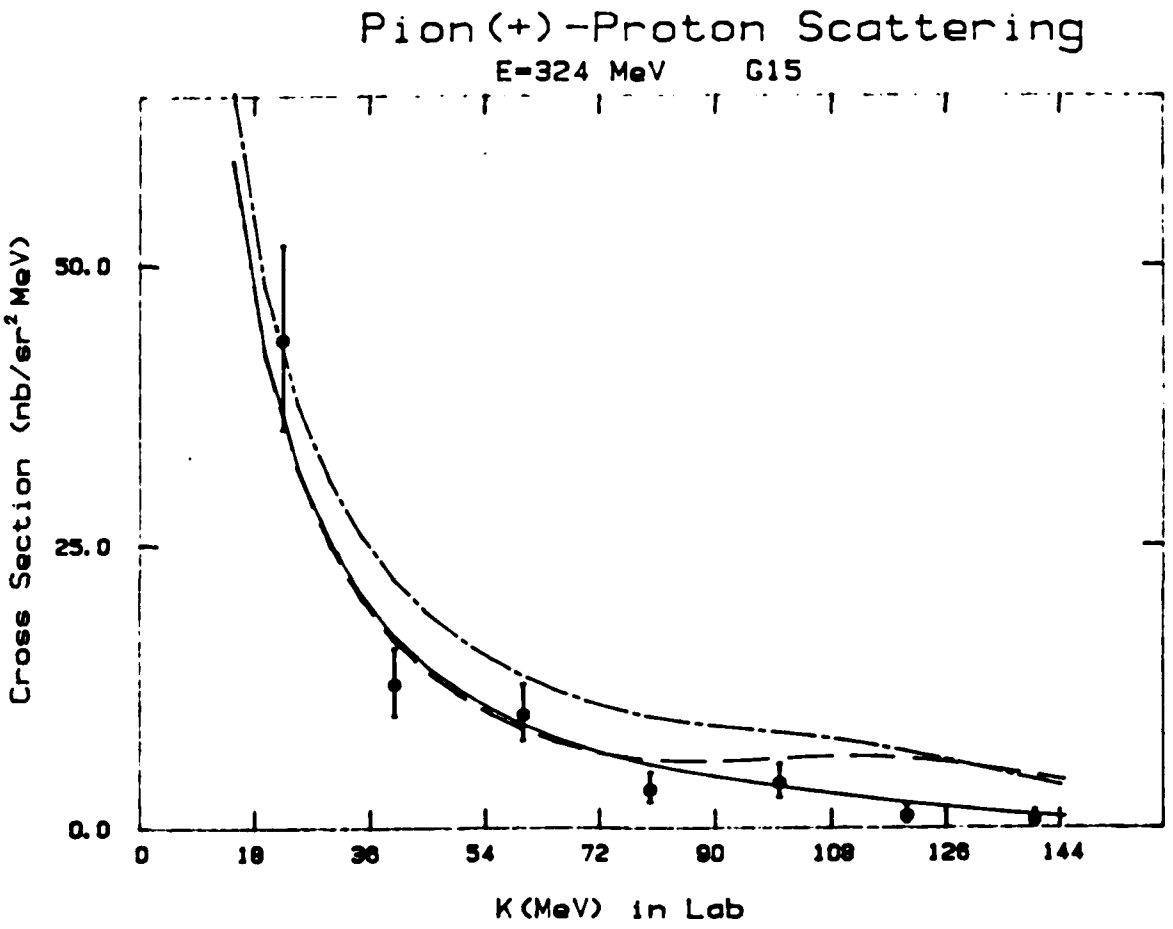

Fig.34 Same as Fig.13 but at 324 MeV for the photon counter G15.

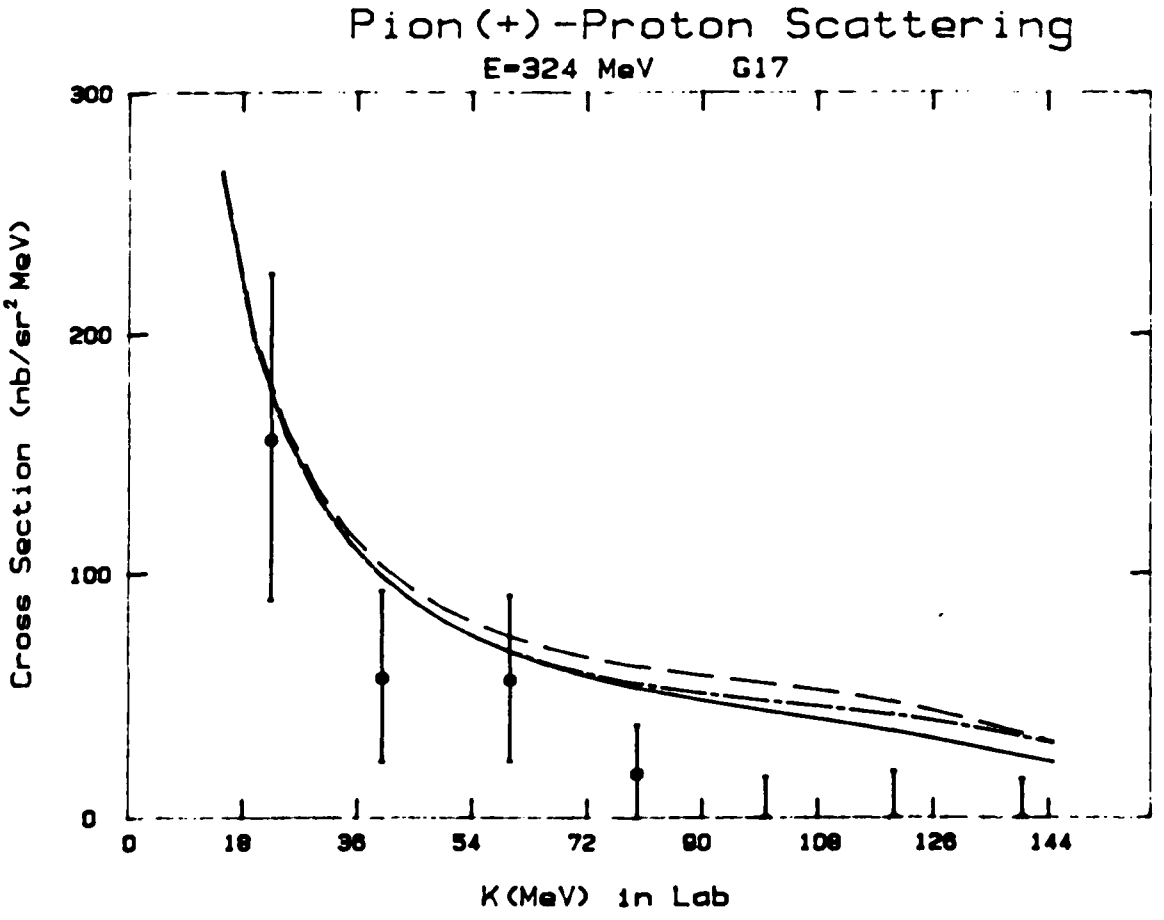

Fig.35 Same as Fig.13 but at 324 MeV for the photon counter G17.

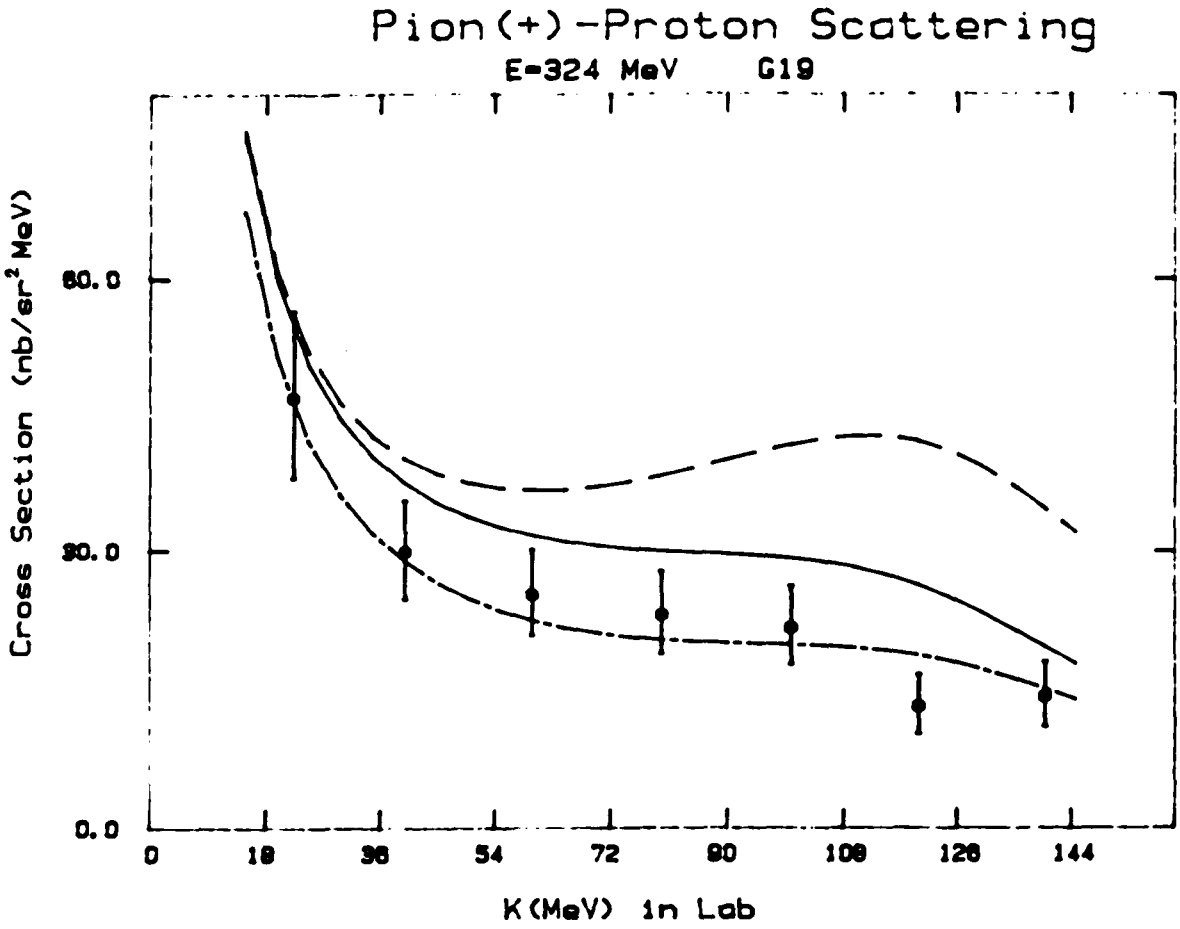

Fig.36 Same as Fig.13 but at 324 MeV for the photon counter G19.

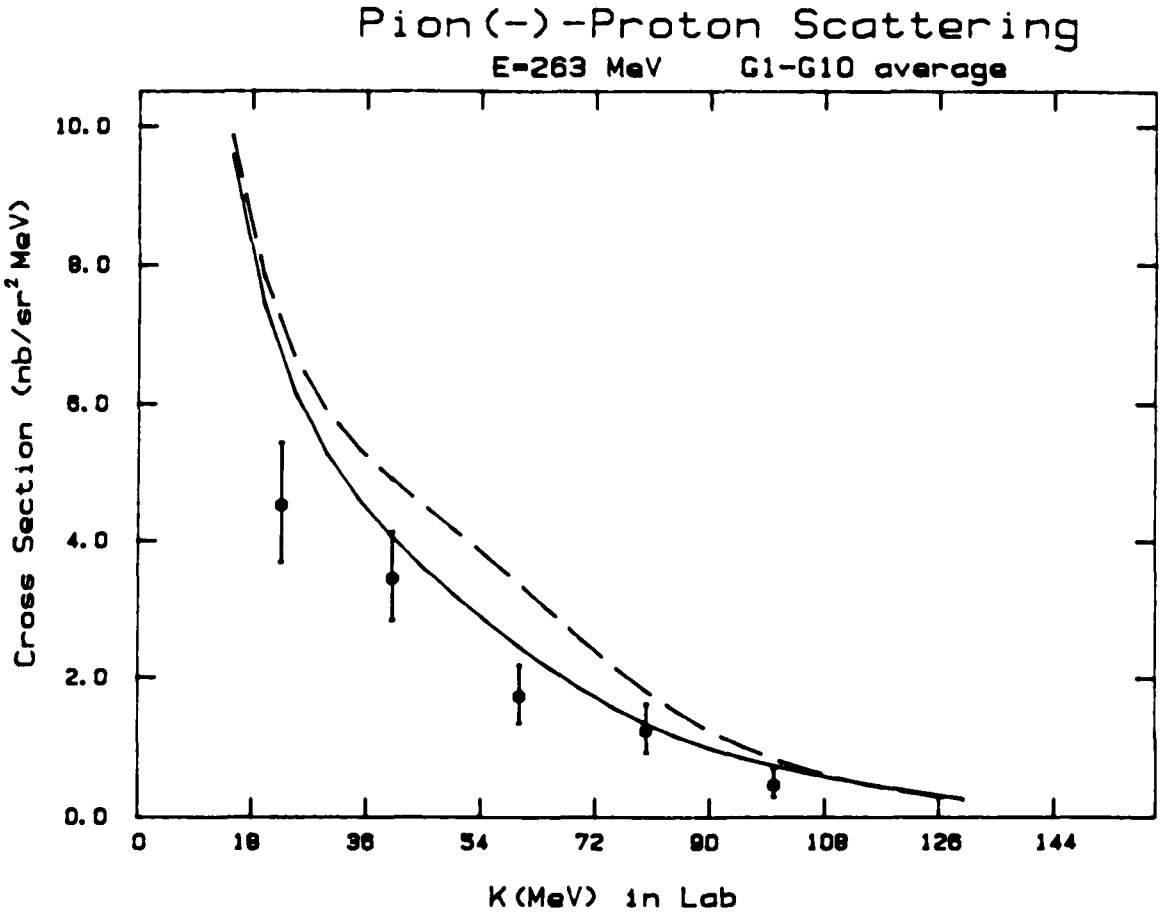

Fig.37 The $\pi^- p\gamma$ cross section as a function of photon energy K at 263 MeV for the photon counter G1-G10(averaged). The solid curve represents the result of calculation using the TETA amplitude given by Eq.(38) and the dashed curve represents the result of calculation using the amplitude $M_{\mu}^{AB}(s_i, s_f, t_o)$ in TEOA. The experimental $\pi^- p\gamma$ data are from Ref.2.

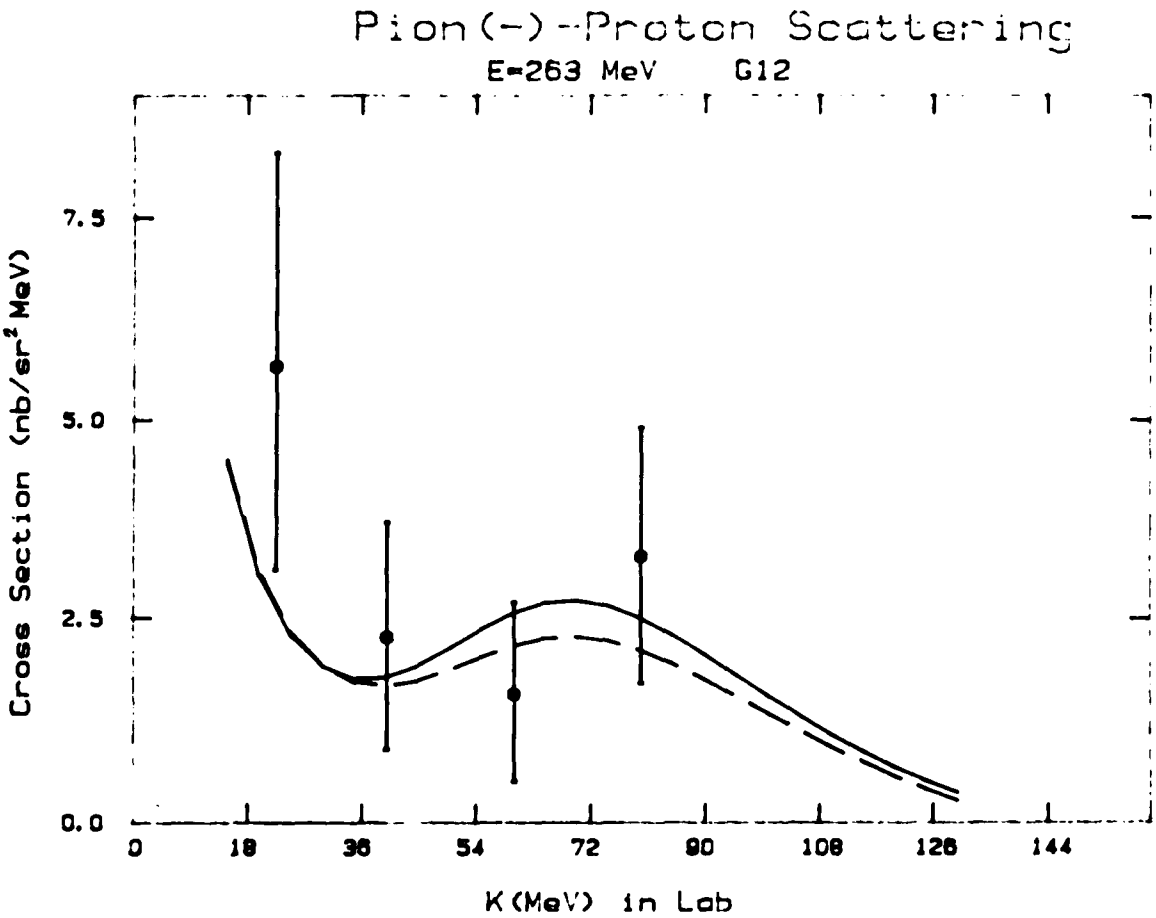

Fig.38 Same as Fig.38 but for the photon counter G12.

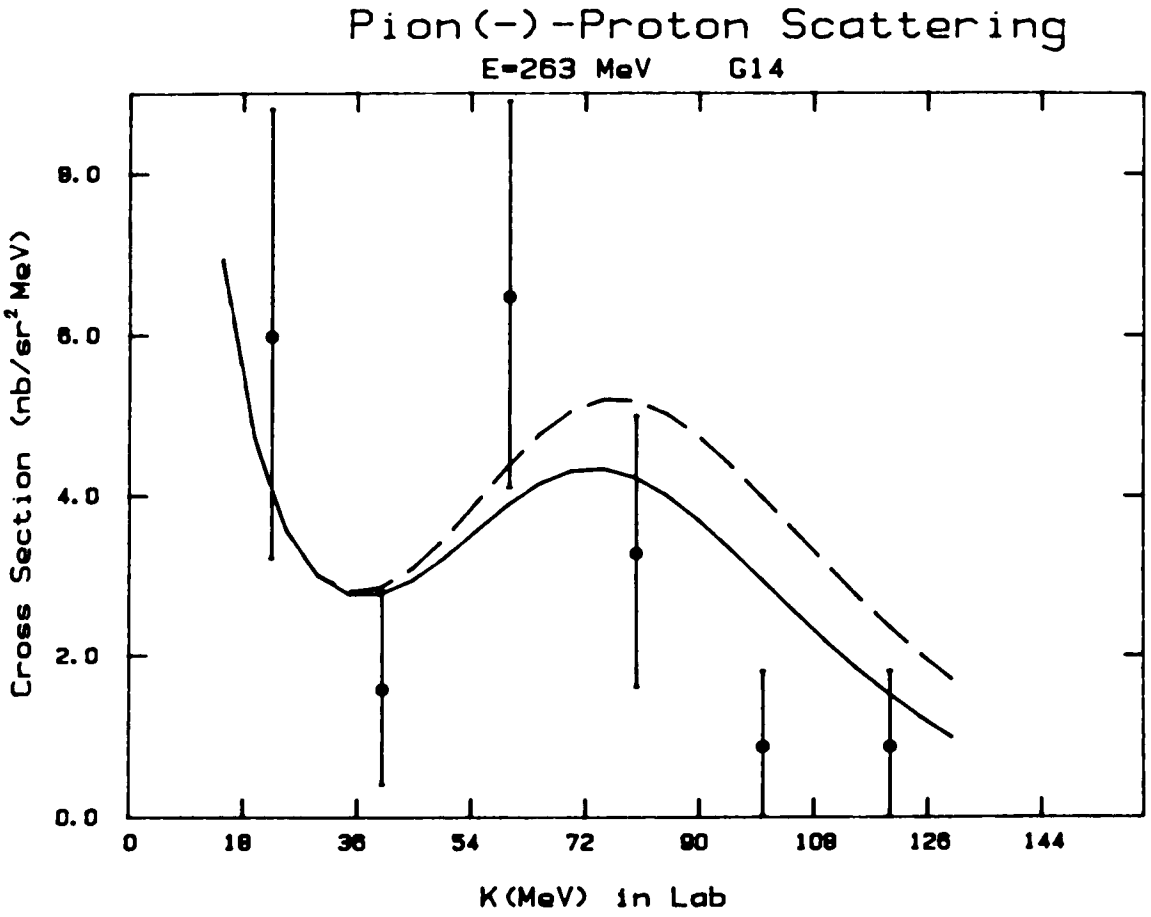

Fig.39 Same as Fig.38 but for the photon counter G14.

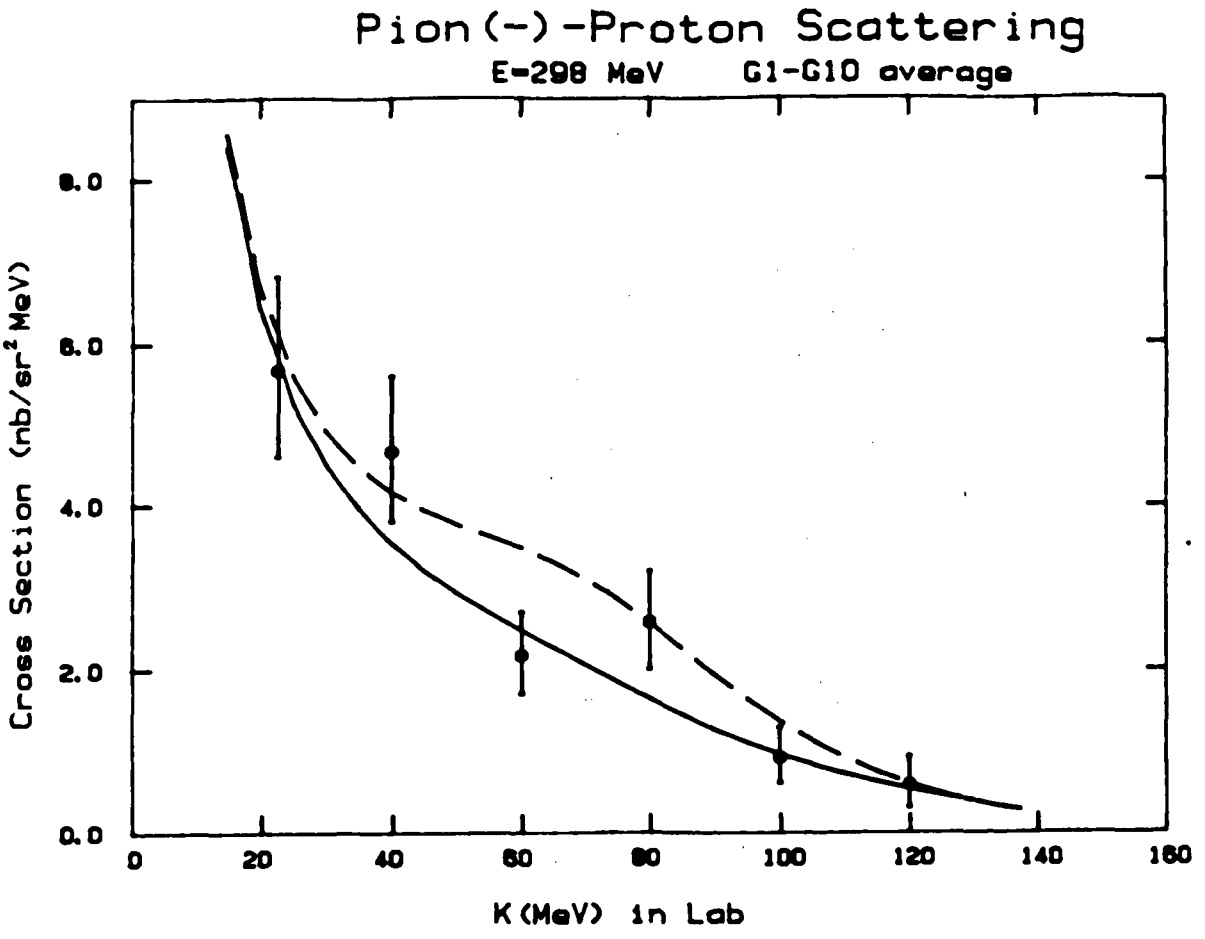

Fig.40 Same as Fig.38 but at 298 MeV for the photon counter G1-G10(average).

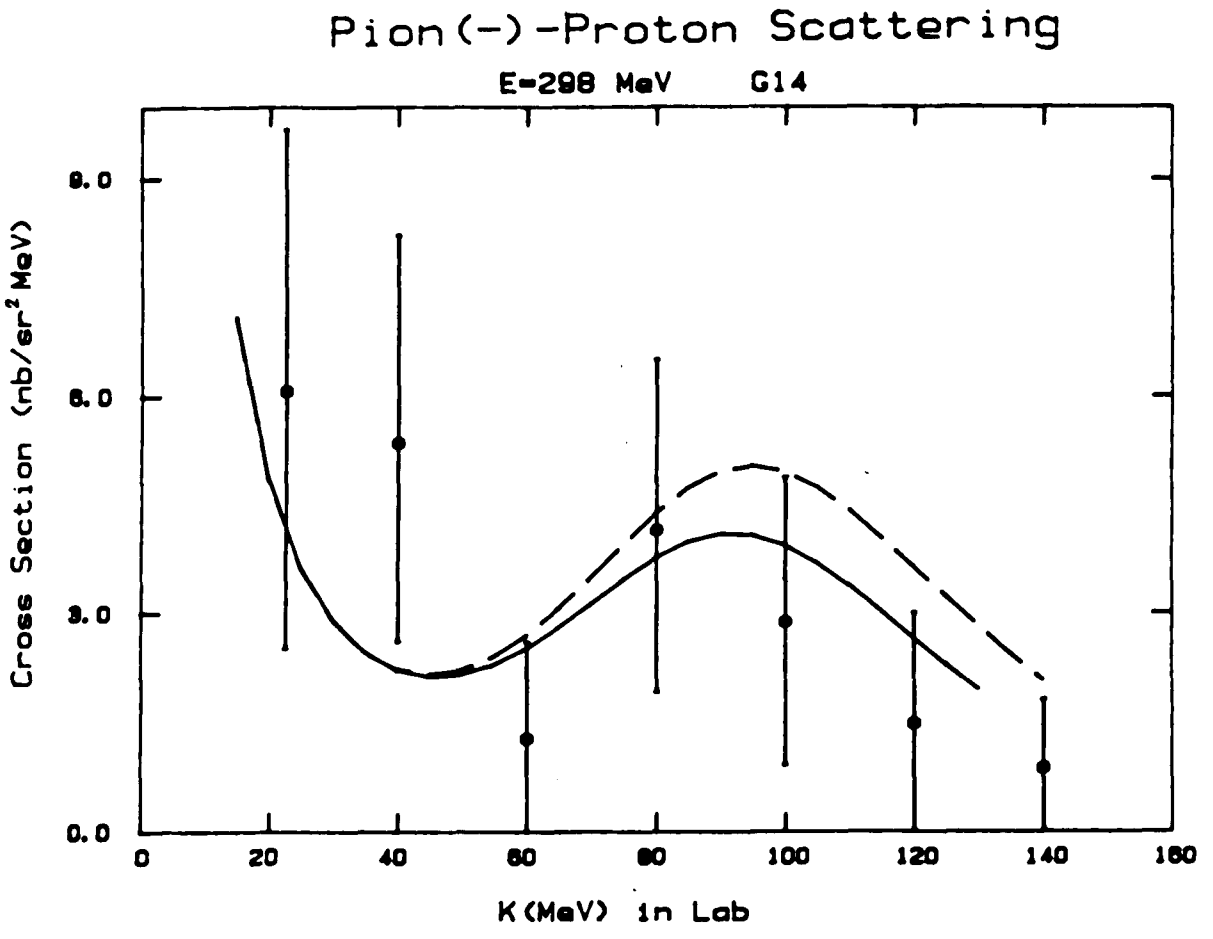

Fig.41 Same as Fig.38 but at 298 MeV for the photon counter G14.

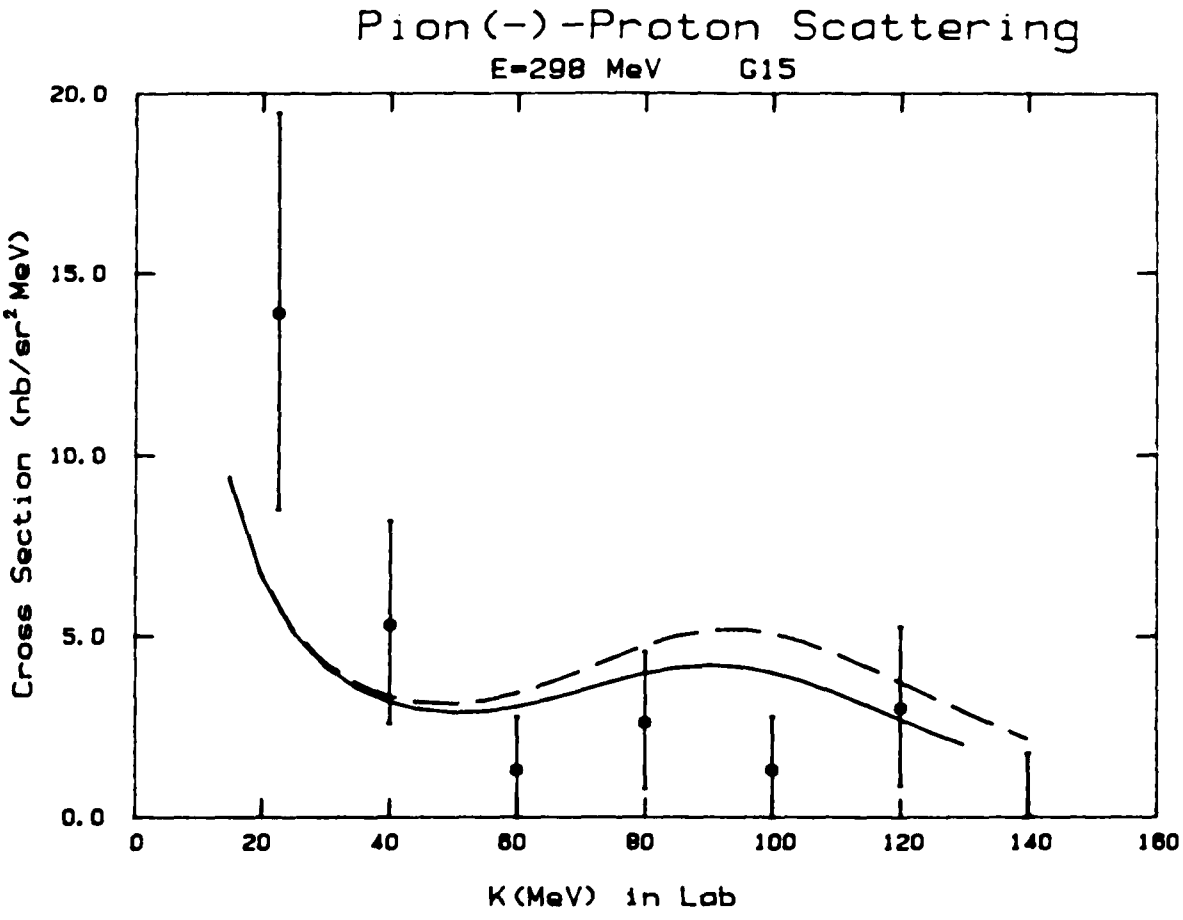

Fig.42 Same as Fig.38 but at 298 MeV for the photon counter G15.

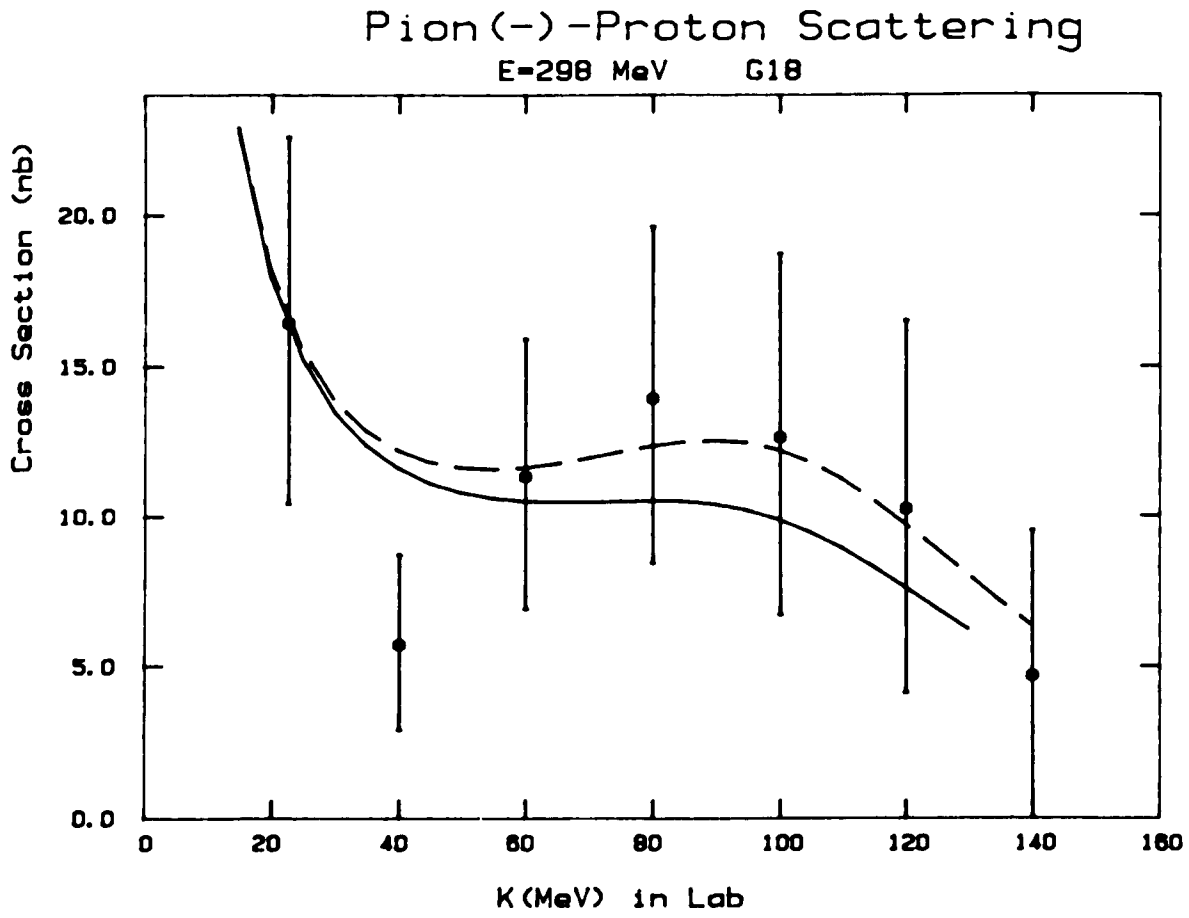

Fig.43 Same as Fig.38 but at 298 MeV for the photon counter G18.

References

1. M.I.Sobel and A.H.Cromer, Phys. Rev. 132, 2698(1963); An extensive list of references can be obtained from the following review articles: (i) M.L.Halbert, Proceedings of Gull Lake Symposium on the Two-body Force in Nuclei, (Plenum Press, New York, 1972). (ii) M.J.Moravcsik, Reports on Progress in Physics, 35 587(1972). (iii) E.M.Nyman, Physics Reports, 9, 179(1974). (iv) M.K.Liou, Proceedings of the International Conference on Few Body Problems in Nuclear and Particle Physics, Quebec, Canada. Edited by R.J.Slobodrian et al., Les Presses De L'Universite Leval, Quebec, (1975). (v) J.V.Jovanovich, Nucleon-Nucleon Interactions - 1977 (Vancouver) AIP Conference Proceedings No. 41, edited by H.Fearing, D.Measday and S.Strathdee).
2. B.M.K.Nefkens et al., Phys. Rev. D18, 3911(1978) and references therein.
3. R.M.Eisberg, D.R.Yennie and D.H.wilkinson, Nucl. Phys. 18, 338(1960)
4. H.Feshbach and D.R.Yennie, Nucl. Phys. 37, 150(1962).
5. F.Janouch and R.Mach, Nucl. Phys. A158, 193(1970); A.M.Green, Proceedings of the International Conference on Few-body Problems in Nuclear and Particle Physics, (Les Presses De L'Universite Leval, Quebec, 1975)
6. C.Maroni, I.Massa, and G.Vannini, Nucl. Phys. A273, 429(1976).

7. C.C.Trail et al., Phys. Rev. C21, 2131(1980). D18, 3911(1978) and references therein.

8. P.M.S.Lesser, C.C.Trail, C.C.Perng, and M.K.Liou, Phys. Rev. Lett. 48, 308(1982).

9. H.Taketani, M.Adachi, N.Endo and T.Suzuki, Phys. Lett. 113B, 11(1982); H.Taketani et al., Nucl. Inst. Methods, 196, 283(1982).

10. C.C.Perng, M.K.Liou, Z.M.Ding, P.M.S.Lesser, and C.C.Trail, Phys. Rev. C29, 518(1984).

11. C.C.Perng, Ph.D Thesis, City University of New York.

12. F.E.Low, Phys. Rev. 110, 974(1958).

13. S.L.Adler and Y.Dothan, Phys. Rev. 151, 1267(1966). T.H.Burnett and N.M.Kroll, Phys. Rev. Lett. 20, 86(1968).

14. B.M.K.Nefkens and D.I.Sober, Phys. Rev. D14, 2434(1976) and Ref.2.

15. M.K.Liou and W.T.Nutt, Phys. Rev. D16, 2176(1977); Nuovo Cimento 46A, 365(1978), and M.K.Liou and C.K.Liu, Phys. Rev. D26, 1635(1982).

16. M.K.Liou, C.K.Liu, P.M.S.Lesser, and C.C.Trail, Phys. Rev. C21, 518(1980). C.K.Liu, M.K.Liou, C.C.Trail and P.M.S.Lesser, Phys. Rev. C26, 723(1982).

17. M.K.Liou, and Z.M.Ding, Preprint; More references can be found in Refs.2 and 15.

18. M.K.Liou, Phys. Rev. D18, 3390(1978).

19. D.I. Sober et. al., Phys. Rev. D11, 1017(1975).

20. We must point out here that although the amplitude used by the UCLA group is not valid in the energy region of the Δ-resonance, it will be a good amplitude in the energy region very far from the Δ-resonance. The work of Smith et al. (D.E.A.Smith et al., Phys. Rev. D21, 1715(1980)) provides further evidence in support of this argument. It is on the radiative π^+p scattering below the (1232) resonance.

21. J. Soc. Indust. Appl. Math. Vol.5, No.2, June 1957.